Electronic Supplementary Information

Efficient hydrogenation of ketones and aldehydes catalysed by a well-defined PNNP-rhenium complex

Contents

I. General information

Unless otherwise stated, all operations were performed under a dry Ar or N_2 atmosphere by using glovebox techniques and standard Schlenk manipulations. Organic solvents including1,4-dioxane, toluene, *n*-hexane, and tetrahydrofuran were dried by refluxing with sodium-potassium alloys under N_2 atmosphere prior to use. Isopropanol, *n*-propanol, ethanol, and methanol were distilled with CaH_2 and stored in glovebox for use. The aminophosphine ligands were synthesized according to the literature reports[1-2]. $Re(CO)_5Cl$ and carbonyl derivatives were purchased from J&K or aladdin Chemical Co. and used as received. ^1H (400 MHz), $^{13}C\{^1H\}$ (100 MHz), and $^{31}P\{^1H\}$ (160 MHz) NMR spectra were measured on a Bruker AVIII-400 spectrometer. Infrared (IR) spectra were recorded using a Nicolet FT-IR 330 spectrometer. Elemental analysis was performed on a Thermo Quest Italia SPA EA 1110 instrument. Crystallographic data for complexes **1**, **2**, and **4** were collected at 120 K on a Rigaku XtaLAB Synergy R - HyPix or Stoe Stadivari diffractometer.

II. X-ray crystallographic analysis

Single crystal of rhenium complex **1** was collected at on a Rigaku XtaLAB Synergy R - HyPix diffractometer. Single crystals of rhenium complexes **2** and **4** were collected at on a Stoe Stadivari diffractometer. The crystal was kept at 120.00 K during data collection under nitrogen flow. Using Olex2[3], the structure was solved with the ShelXT[4] structure solution program using Intrinsic Phasing and refined with the ShelXL[5] refinement package using least-squares minimization. All the non-hydrogen atoms were found directly. All the on-hydrogen atoms were refined anisotropically. All the hydrogen atoms were set in geometrically calculated positions and refined isotropically using a riding model.

The unidentified diffuse electron densities resulting from the residual solvent molecules were removed by the Mask tool of Olex2 and refined further using the data generated. For the complex **1**, a solvent mask was calculated and 26 electrons were found in a volume of 161\%A^3^ in 2 voids per unit cell. This is consistent with the presence of 0.25[C_2H_6O] per Asymmetric Unit which account for 26 electrons per unit cell. For the complex **2**, A solvent mask was calculated and 492 electrons were found in a volume of 1652\%A^3^ in 1 void per unit cell. This is consistent with the presence of 1.5[CH_2Cl_2] per Asymmetric Unit which account for 504 electrons per unit cell.

The PLAT971 and PLAT972 alerts were caused by the min/max residual electron density near the heavy atom for crystallographic data of complexes **1** and **2**.

Table S1 Crystal data and structure refinement for complex **1**

CCDC number	2442979
Empirical formula	$C_{45.5}H_{48.5}ClN_2O_{3.75}P_2Re$
Formula weight	966.95
Temperature/K	120.00(10)
Crystal system	triclinic
Space group	P-1
a/Å	12.5495(2)
b/Å	15.2226(3)
c/Å	24.5566(2)
α/°	75.1370(10)
β/°	81.8350(10)
γ/°	67.072(2)
Volume/Å^3	4171.34(13)
Z	4
ρ_{calc}g/cm^3	1.540
μ/mm^{-1}	7.365
F(000)	1950.0
Crystal size/mm^3	0.15 × 0.1 × 0.08
Radiation	Cu Kα (λ = 1.54184)
2Θ range for data collection/°	6.464 to 156.752
Index ranges	-15 ≤ h ≤ 15, -19 ≤ k ≤ 18, -31 ≤ l ≤ 23
Reflections collected	54583
Independent reflections	17199 [R_{int} = 0.0655, R_{sigma} = 0.0465]
Data/restraints/parameters	17199/1027/988
Goodness-of-fit on F^2	1.082
Final R indexes [I>=2σ (I)]	R_1 = 0.0505, wR_2 = 0.1441
Final R indexes [all data]	R_1 = 0.0531, wR_2 = 0.1465
Largest diff. peak/hole / e Å^{-3}	2.70/-3.08

Table S2 Crystal data and structure refinement for complex **2**

CCDC number	2442980
Empirical formula	$C_{47.5}H_{47}Cl_4N_2O_2P_2Re$
Formula weight	1067.81
Temperature/K	120
Crystal system	orthorhombic
Space group	Pbcn
a/Å	13.0948(2)
b/Å	20.8238(5)
c/Å	32.3858(6)
α/°	90
β/°	90
γ/°	90
Volume/Å^3	8831.1(3)
Z	8
ρ_{calc}g/cm^3	1.606
μ/mm^{-1}	8.622
F(000)	4280.0
Crystal size/mm^3	0.15 × 0.1 × 0.1
Radiation	Cu Kα (λ = 1.54186)
2Θ range for data collection/°	7.976 to 139.49
Index ranges	-15 ≤ h ≤ 10, -18 ≤ k ≤ 24, -15 ≤ l ≤ 38
Reflections collected	21094
Independent reflections	8018 [R_{int} = 0.0420, R_{sigma} = 0.0380]
Data/restraints/parameters	8018/0/487
Goodness-of-fit on F^2	1.036
Final R indexes [I>=2σ (I)]	R_1 = 0.0543, wR_2 = 0.1579
Final R indexes [all data]	R_1 = 0.0615, wR_2 = 0.1694
Largest diff. peak/hole / e Å^{-3}	3.28/-1.85

Table S3 Crystal data and structure refinement for complex **4**

CCDC number	2457551
Empirical formula	$C_{53}H_{51}N_2O_2P_2Re$
Formula weight	996.10
Temperature/K	120
Crystal system	triclinic
Space group	P-1
a/Å	12.7975(4)
b/Å	13.4519(4)
c/Å	13.8667(4)
α/°	82.494(2)
β/°	88.151(2)
γ/°	67.487(2)
Volume/Å^3	2185.94(12)
Z	2
ρ_{calc}g/cm^3	1.513
μ/mm^{-1}	6.470
F(000)	1008.0
Crystal size/mm^3	0.12 × 0.1 × 0.07
Radiation	Cu Kα (λ = 1.54186)
2Θ range for data collection/°	6.43 to 138.968
Index ranges	-15 ≤ h ≤ 6, -16 ≤ k ≤ 13, -16 ≤ l ≤ 15
Reflections collected	19590
Independent reflections	7837 [R_{int} = 0.0232, R_{sigma} = 0.0297]
Data/restraints/parameters	7837/0/542
Goodness-of-fit on F^2	1.133
Final R indexes [I>=2σ (I)]	R_1 = 0.0301, wR_2 = 0.0833
Final R indexes [all data]	R_1 = 0.0341, wR_2 = 0.0904
Largest diff. peak/hole / e Å^{-3}	1.32/-0.90

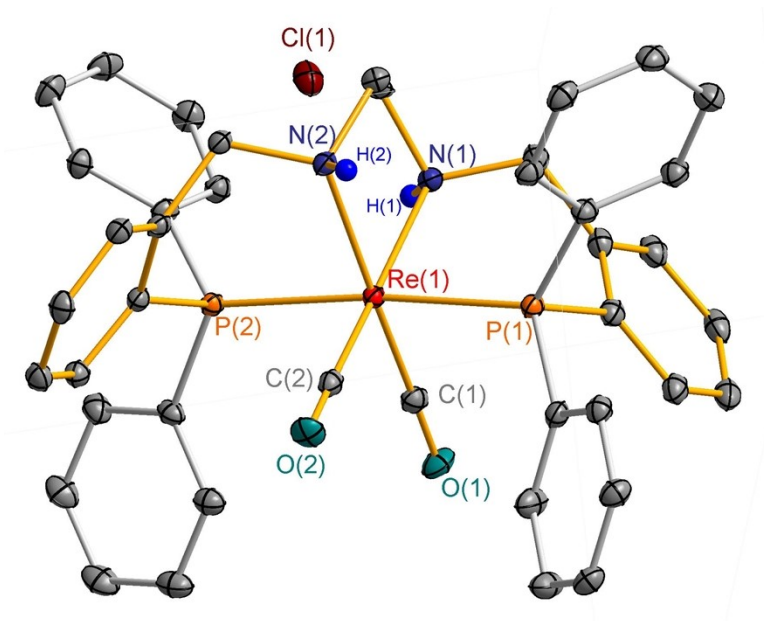

Fig. S1 X-ray crystal structure of complex **1** with thermal ellipsoids drawn at 30% probability level. Most hydrogen atoms have been omitted for clarity. Selected bond lengths (Å) and angles (°): Re(1)-P(1) 2.4364(9), Re(1)-P(2) 2.4009(9), Re(1)-N(1) 2.254(3), Re(1)-N(2) 2.272(3), Re(1)-C(1) 1.911(4), Re(1)-C(2) 1.913(4), P(1)-Re(1)-P(2) 174.33(3), N(2)-Re(1)-P(1) 86.13(8), N(2)-Re(1)-P(2) 98.23(8), N(1)-Re(1)-P(1) 98.26(8), N(1)-Re(1)-P(2) 86.23(8), N(1)-Re(1)-N(2) 78.19(11), C(2)-Re(1)-P(1) 86.42(11), C(2)-Re(1)-P(2) 89.60(11), C(2)-Re(1)-N(2) 94.59(14), C(2)-Re(1)-N(1) 171.03(13), C(1)-Re(1)-P(1) 91.83(12), C(1)-Re(1)-P(2) 84.24(12), C(1)-Re(1)-N(2) 173.34(14), C(1)-Re(1)-N(1) 95.86(15), C(1)-Re(1)-C(2) 91.61(17).

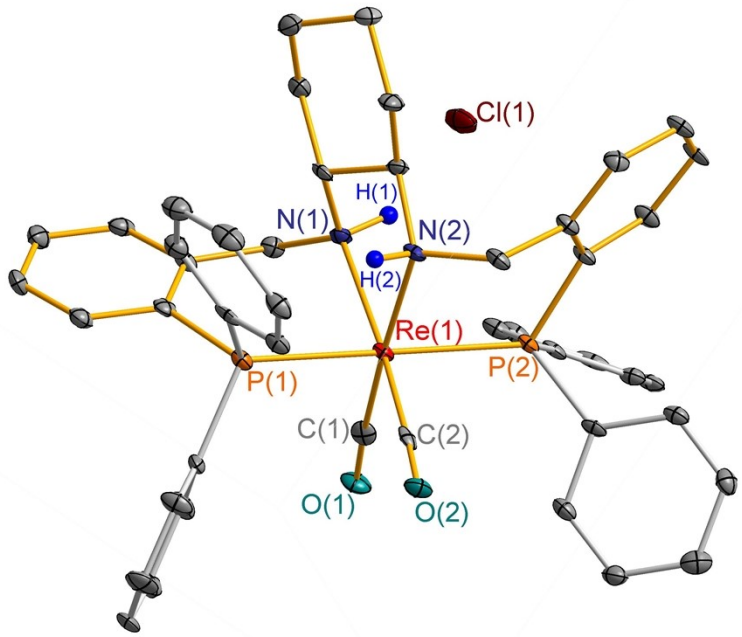

Fig. S2 X-ray crystal structure of complex **2** with thermal ellipsoids drawn at 30% probability level. Most hydrogen atoms have been omitted for clarity. Selected bond lengths (Å) and angles (°): Re(1)-P(1) 2.3919(13), Re(1)-P(2) 2.4328(13), Re(1)-N(1) 2.246(4), Re(1)-N(2) 2.239(5), Re(1)-C(1) 1.901(6), Re(1)-C(2) 1.889(5), P(1)-Re(1)-P(2) 178.24(4), N(2)-Re(1)-P(2) 85.58(12), N(2)-Re(1)-P(1) 93.11(12), N(1)-Re(1)-P(2) 97.18(12), N(1)-Re(1)-P(1) 83.65(12), N(1)-Re(1)-N(2) 76.76(16), C(2)-Re(1)-P(2) 90.66(15), C(2)-Re(1)-P(1) 88.24(15), C(2)-Re(1)-N(2) 92.95(19), C(2)-Re(1)-N(1) 166.48(19), C(2)-Re(1)-C(1) 89.7(2), C(1)-Re(1)-P(2) 90.33(16), C(1)-Re(1)-P(1) 91.04(17), C(1)-Re(1)-N(2) 175.2(2), C(1)-Re(1)-N(1) 101.26(19).

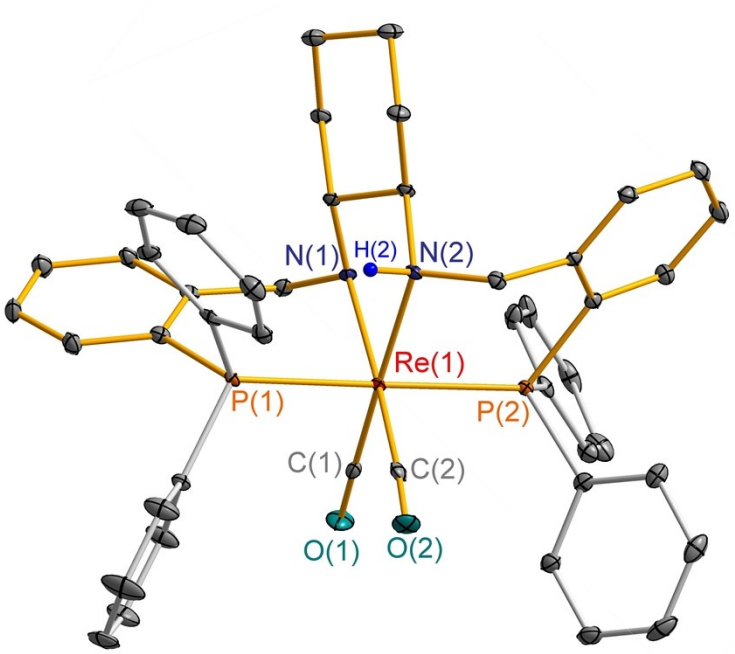

Fig. S3 X-ray crystal structure of complex **4** with thermal ellipsoids drawn at 30% probability level. Most hydrogen atoms have been omitted for clarity. Selected bond lengths (Å) and angles (°): Re(1)-P(1) 2.3737(8), Re(1)-P(2) 2.3984(8), Re(1)-N(1) 2.178(3), Re(1)-N(2) 2.242(3), Re(1)-C(1) 1.898(4), Re(1)-C(2) 1.921(4), P(1)-Re(1)-P(2) 178.54(3), N(2)-Re(1)-P(2) 86.39(7), N(2)-Re(1)-P(1) 93.78(7), N(1)-Re(1)-P(2) 94.07(7), N(1)-Re(1)-P(1) 84.57(7), N(1)-Re(1)-N(2) 76.06(10), C(2)-Re(1)-P(2) 90.99(10), C(2)-Re(1)-P(1) 90.43(10), C(2)-Re(1)-N(2) 97.52(12), C(2)-Re(1)-N(1) 171.53(13), C(2)-Re(1)-C(1) 89.65(15), C(1)-Re(1)-P(2) 89.59(10), C(1)-Re(1)-P(1) 90.06(10), C(1)-Re(1)-N(2) 171.83(12), C(1)-Re(1)-N(1) 97.17(13).

III. Activity tests

Table S4 Catalytic hydrogenation of acetophenone into 1-phenylethanol by **2** and base

Entry	Base	Conv. (%)[a]	Yield (%)[a]
1	KOMe	68	68
2	KOEt	90	90
3	*t*BuOK	45	45
4	NaOMe	98	98
5	NaOEt	99	99
6	*t*BuONa	48	48
7	KOH	34	34
8	NaOH	55	55
9	K_2CO_3	11	11
10	$K_2C_2O_4$	-	-

General conditions: 2.0 mmol acetophenone (0.5 mmol/mL *i*PrOH solution), 0.1 mol% **2**, 10 mol% base, 20 bar H_2, 100 °C, 1 h. [a] Analyzed by GC.

Table S5 Catalytic hydrogenation of acetophenone into 1-phenylethanol by **2** in different solvent

Entry	Solvent	Conv. (%)[a]	Yield (%)[a]
1	*i*PrOH	99	99
2	*n*PrOH	18	18
3	EtOH	4	4
4	MeOH	7	7
5	Toluene	3	3
6	THF	6	6
7	1,4-Dioxane	3	3

General conditions: 2.0 mmol acetophenone (0.5 mmol/mL solution), 0.1 mol% **2**, 10 mol% NaOEt, 20 bar H_2, 100 °C, 1 h. [a] Analyzed by GC.

IV. NMR spectra

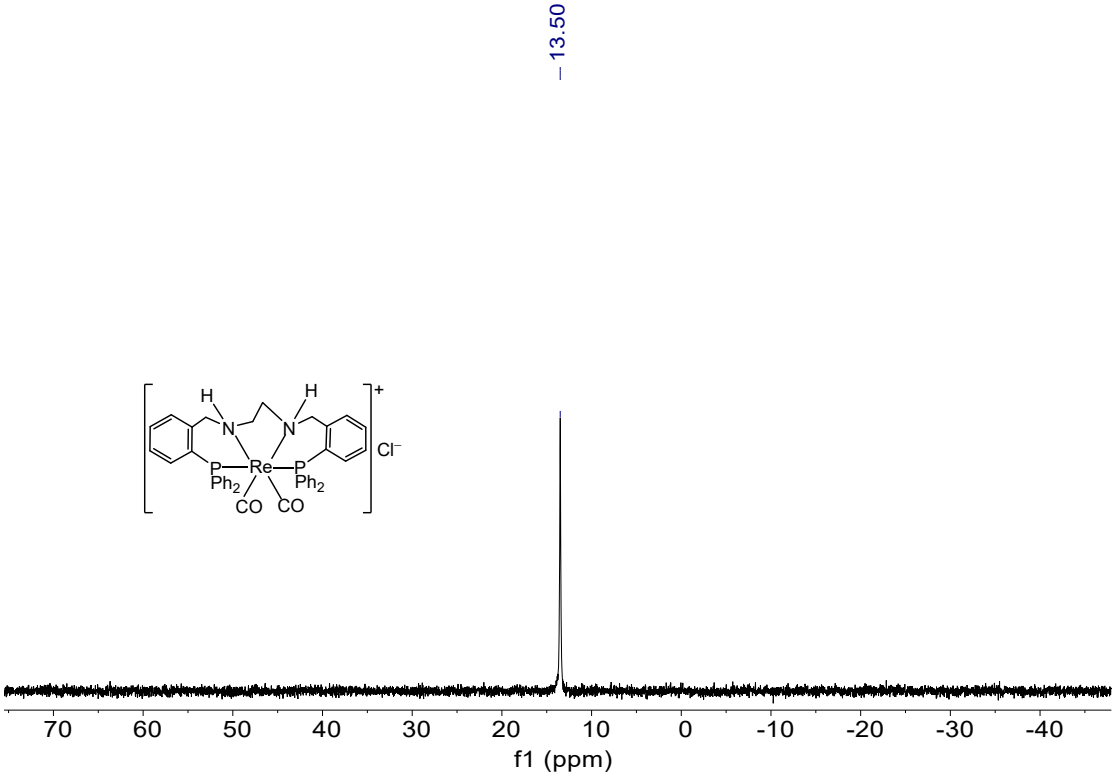

Fig. S4 $^{31}P\{^{1}H\}$ NMR spectrum of **1** measured in $CDCl_3$.

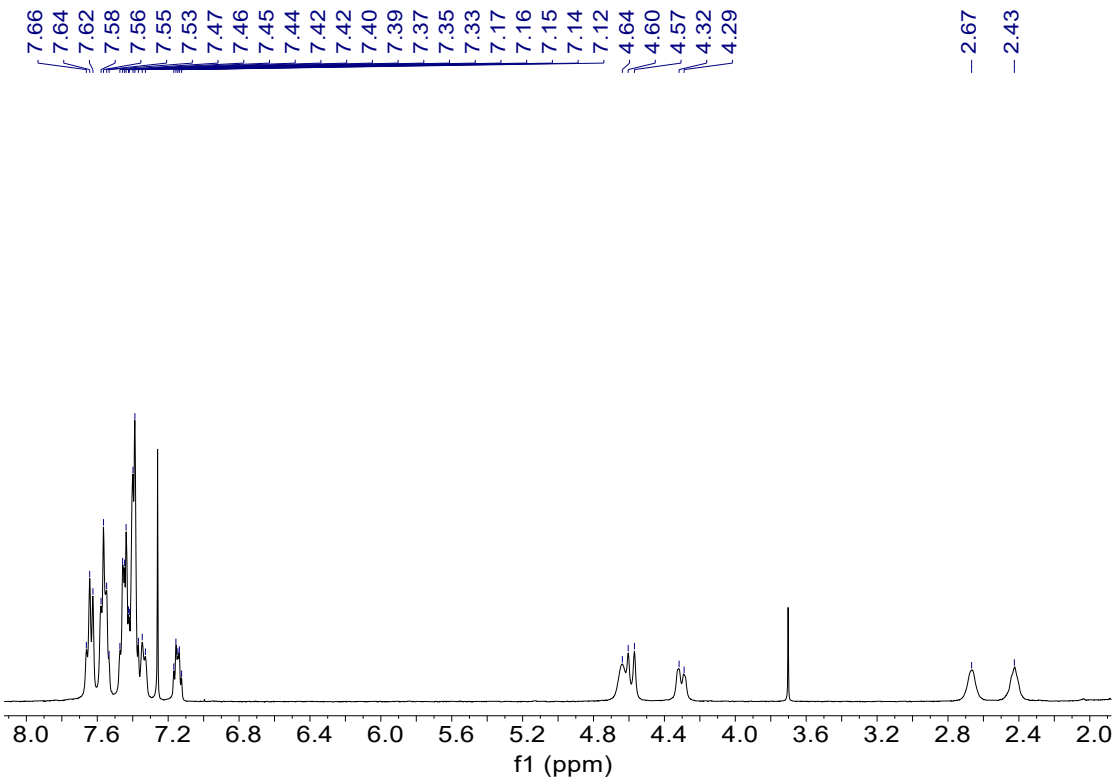

Fig. S5 ^{1}H NMR spectrum of **1** measured in $CDCl_3$.

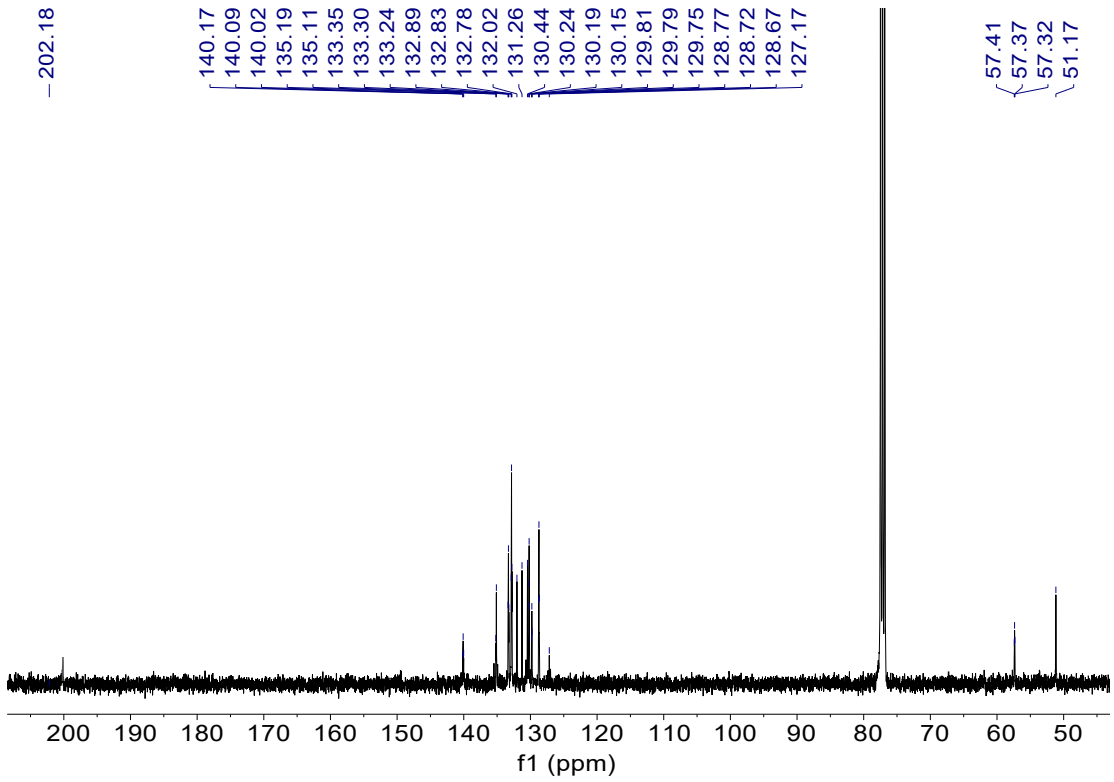

Fig. S6 $^{13}C\{^{1}H\}$ NMR spectrum of **1** measured in $CDCl_3$.

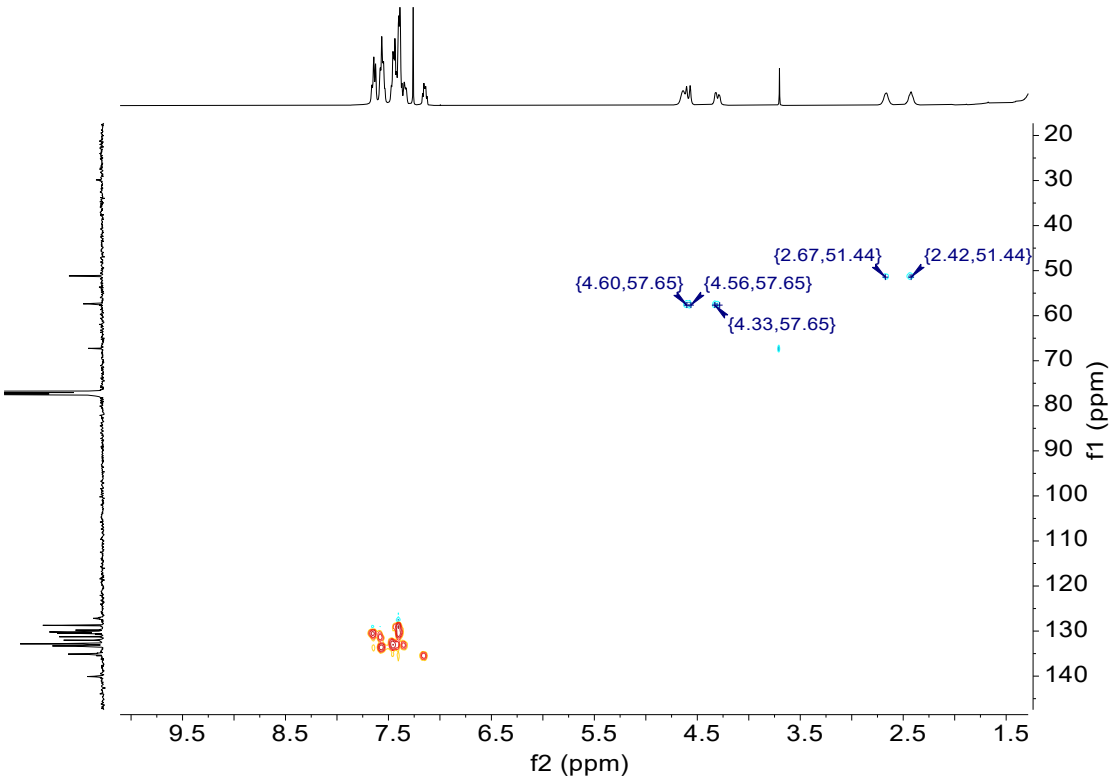

Fig. S7 ^{1}H-^{13}C HSQC NMR spectrum of **1** measured in $CDCl_3$.

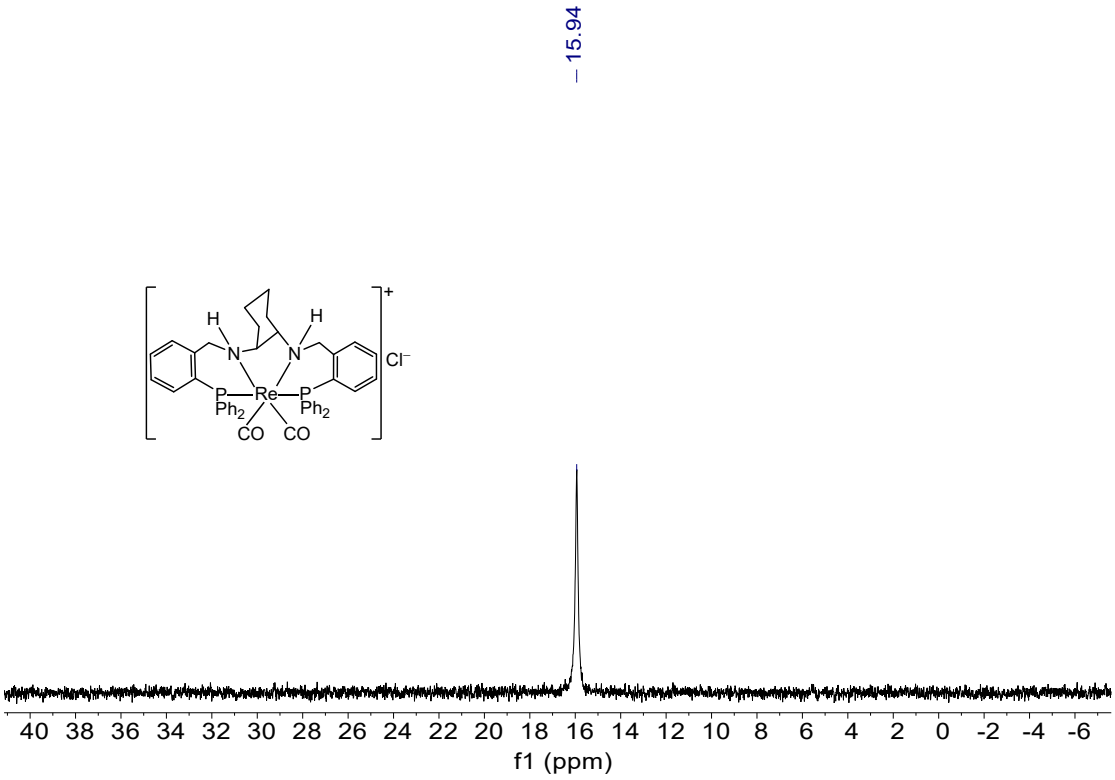

Fig. S8 $^{31}P\{^{1}H\}$ NMR spectrum of **2** measured in $CDCl_3$.

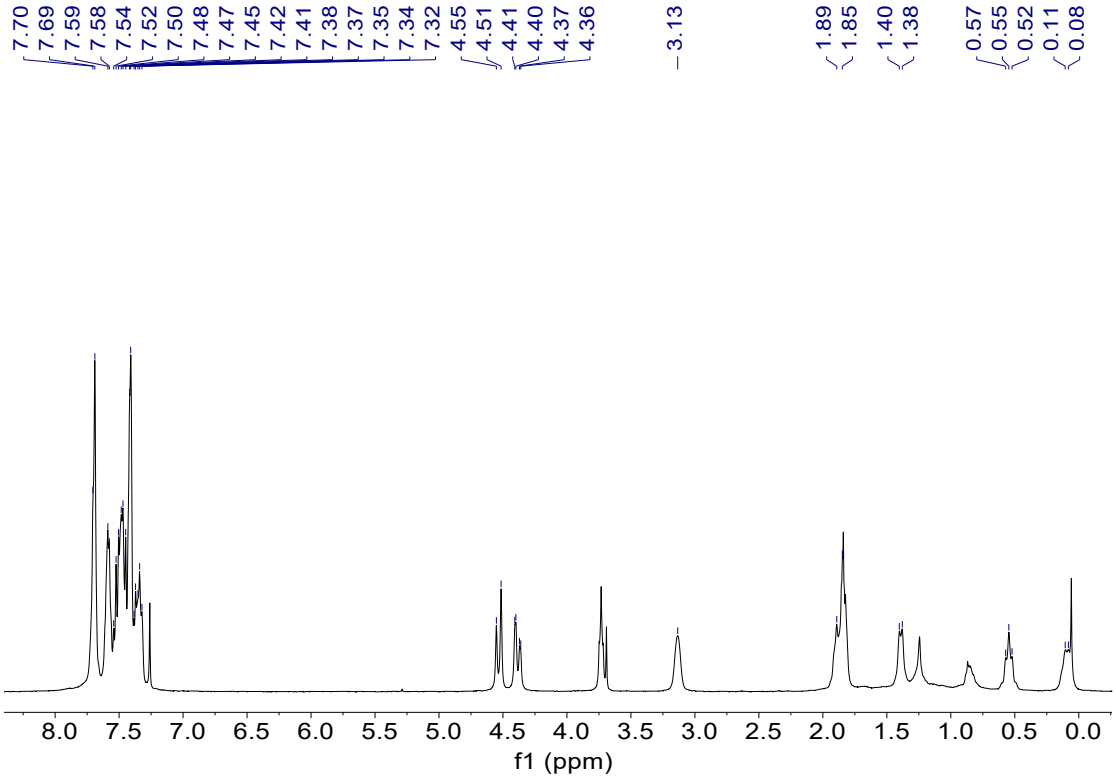

Fig. S9 ^{1}H NMR spectrum of **2** measured in $CDCl_3$.

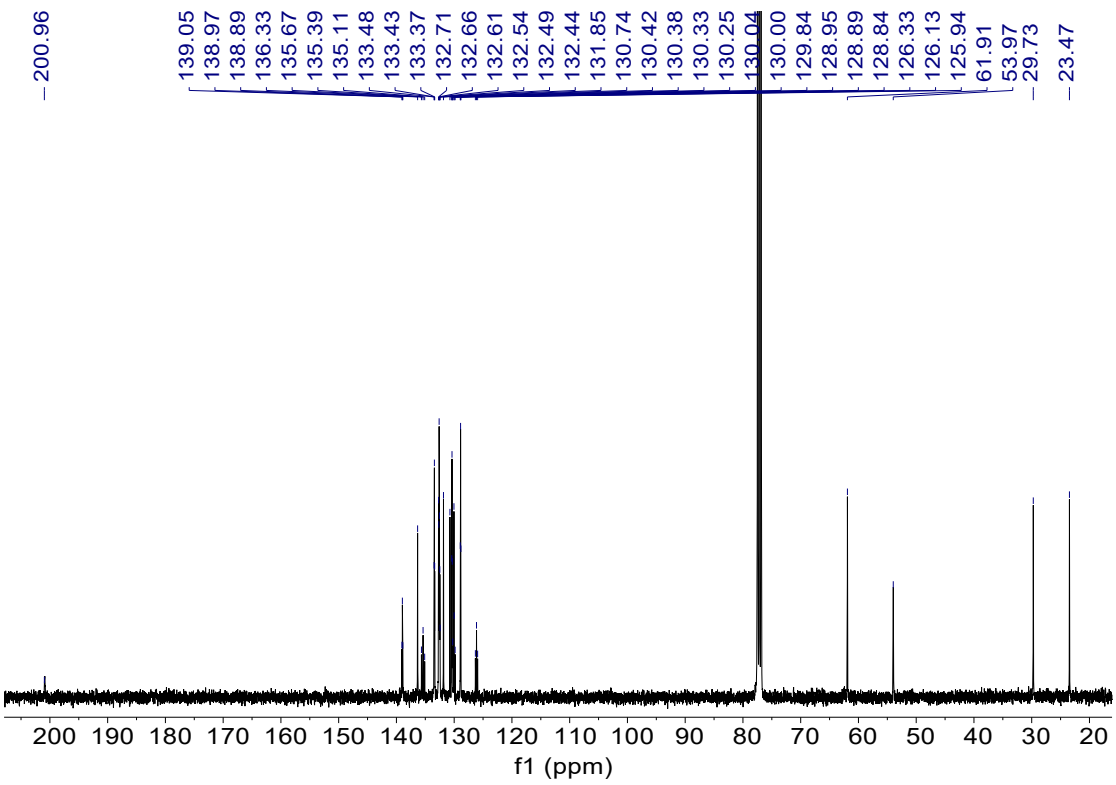

Fig. S10 $^{13}C\{^{1}H\}$ NMR spectrum of **2** measured in $CDCl_3$.

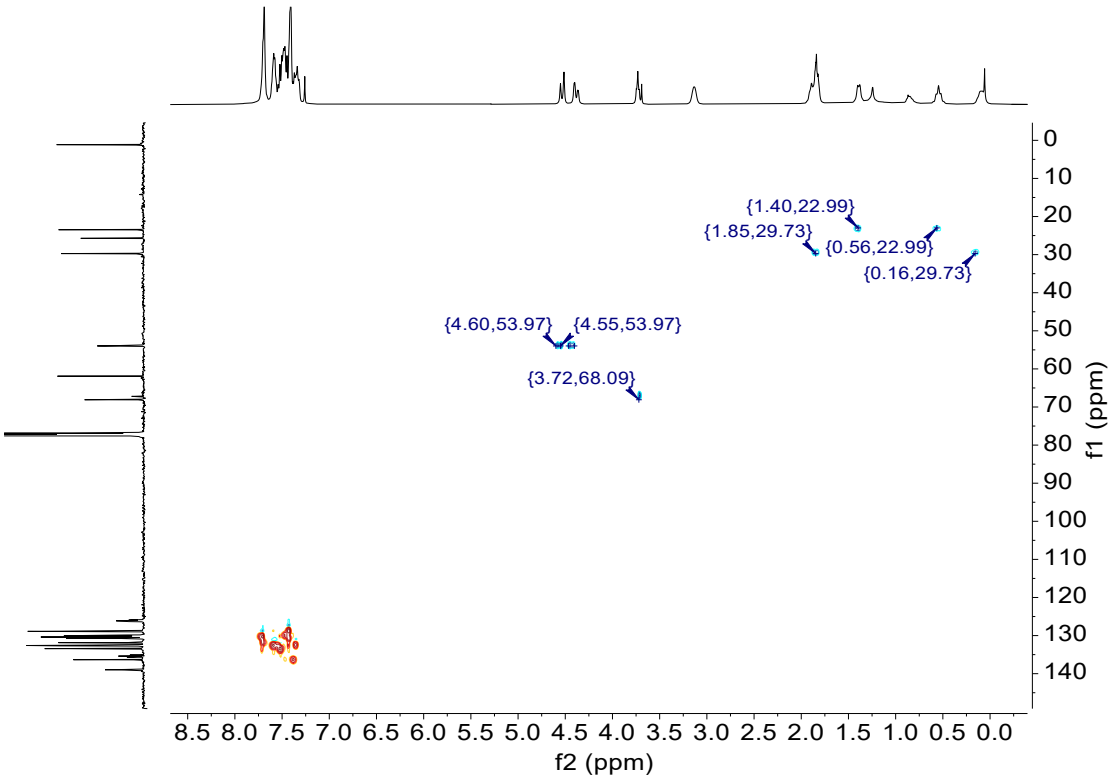

Fig. S11 ^{1}H-^{13}C HSQC NMR spectrum of **2** measured in $CDCl_3$.

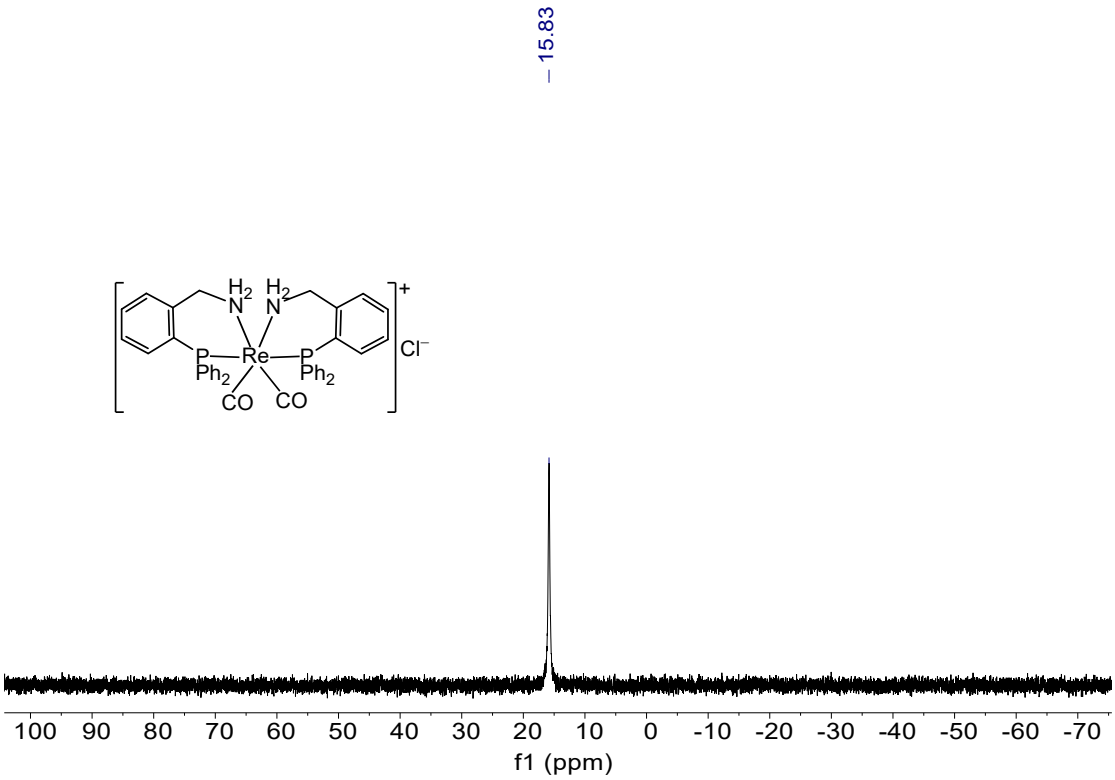

Fig. S12 $^{31}P\{^{1}H\}$NMR spectrum of **3** measured in $CDCl_3$.

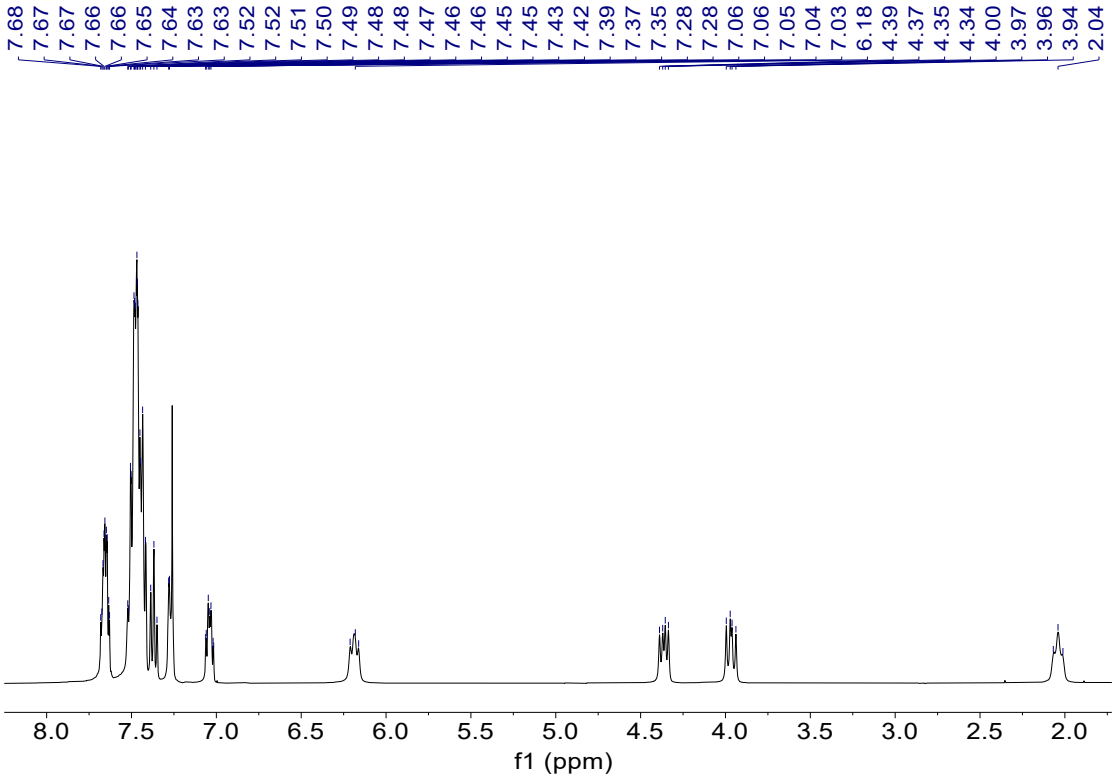

Fig. S13 ^{1}H NMR spectrum of **3** measured in $CDCl_3$.

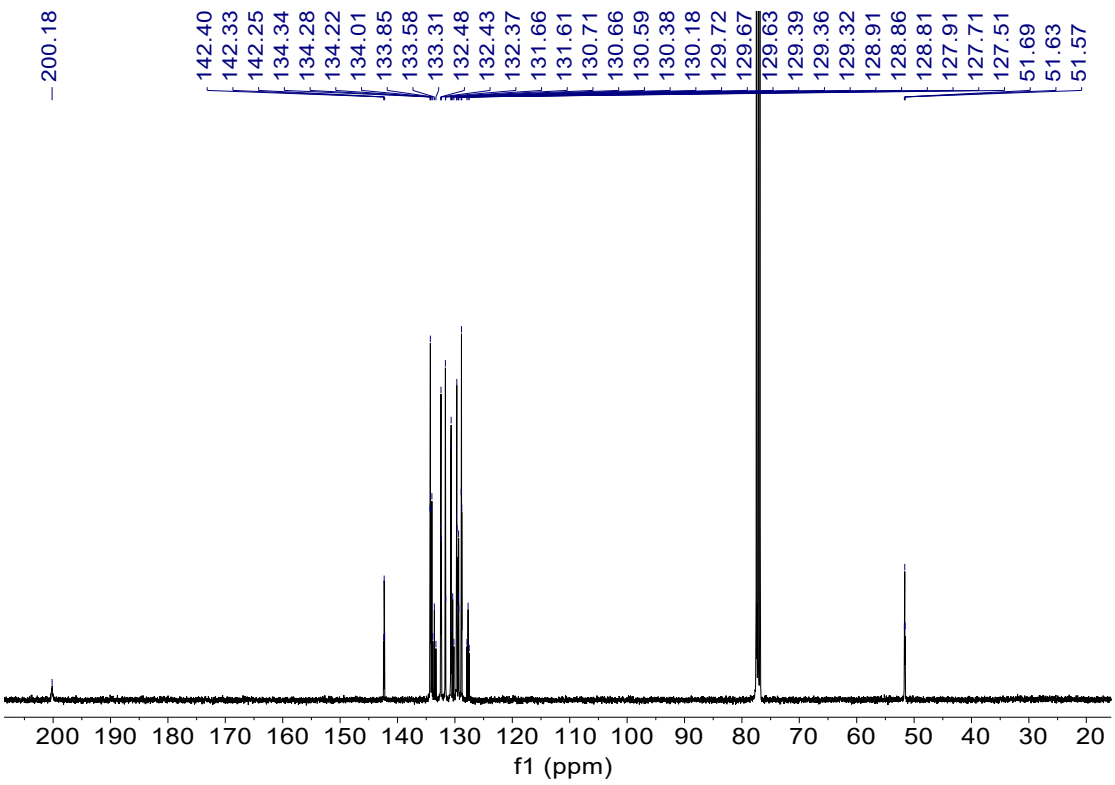

Fig. S14 $^{13}C\{^{1}H\}$ NMR spectrum of **3** measured in $CDCl_3$.

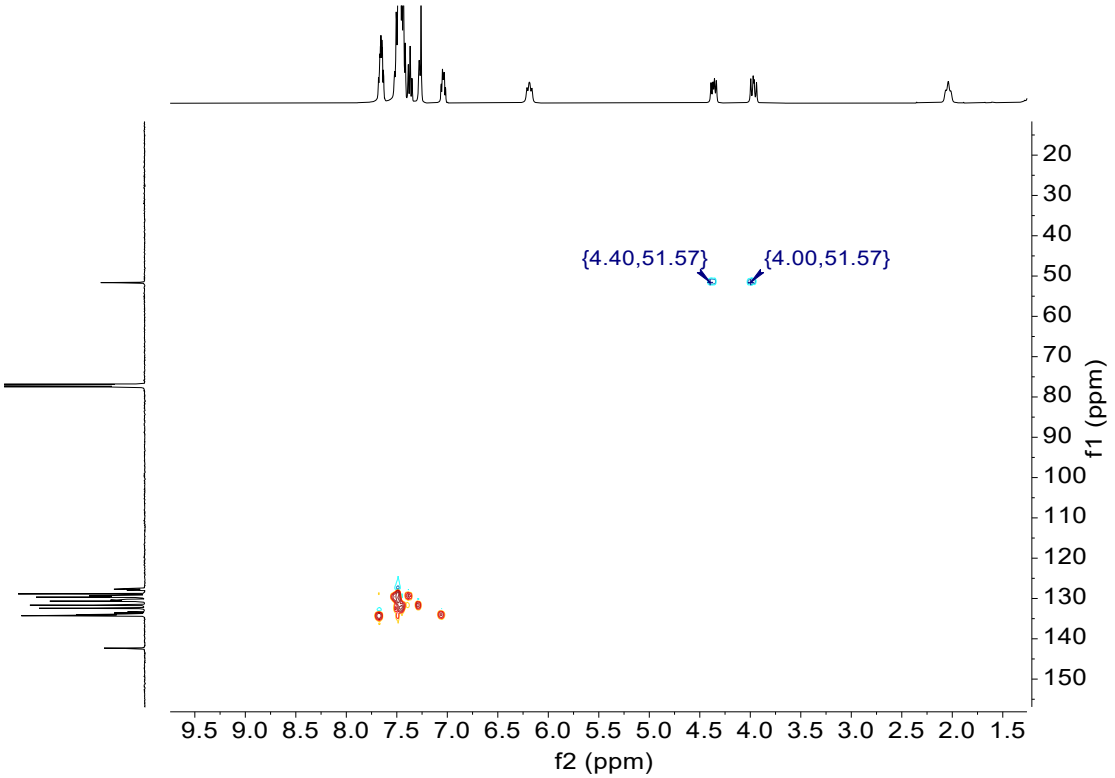

Fig. S15 ^{1}H-^{13}C HSQC NMR spectrum of **3** measured in $CDCl_3$.

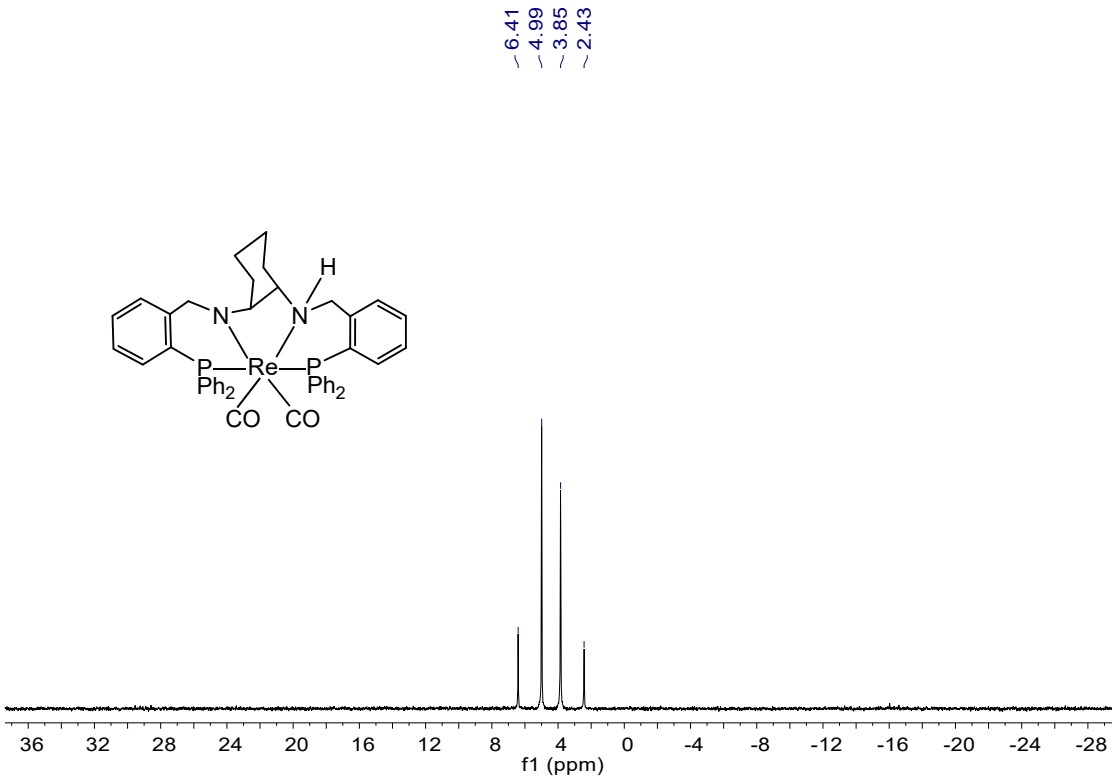

Fig. S16 $^{31}P\{^{1}H\}$ NMR spectrum of **4** measured in C_6D_6.

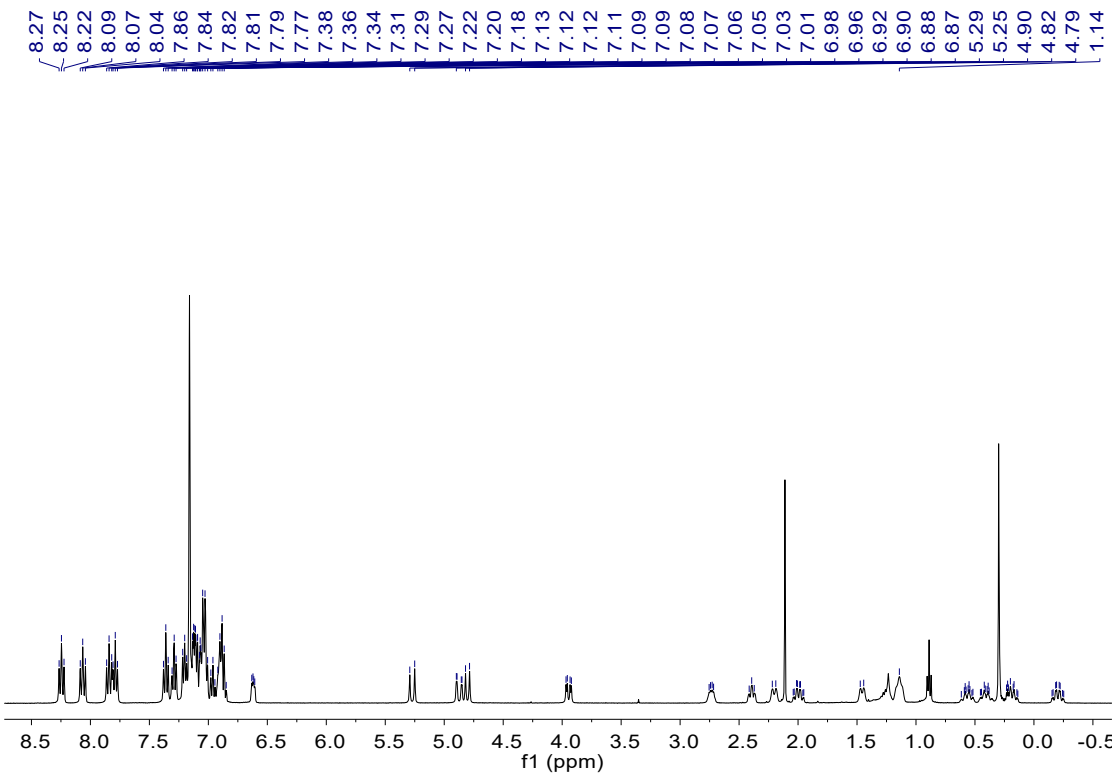

Fig. S17 ^{1}H NMR spectrum of **4** measured in C_6D_6.

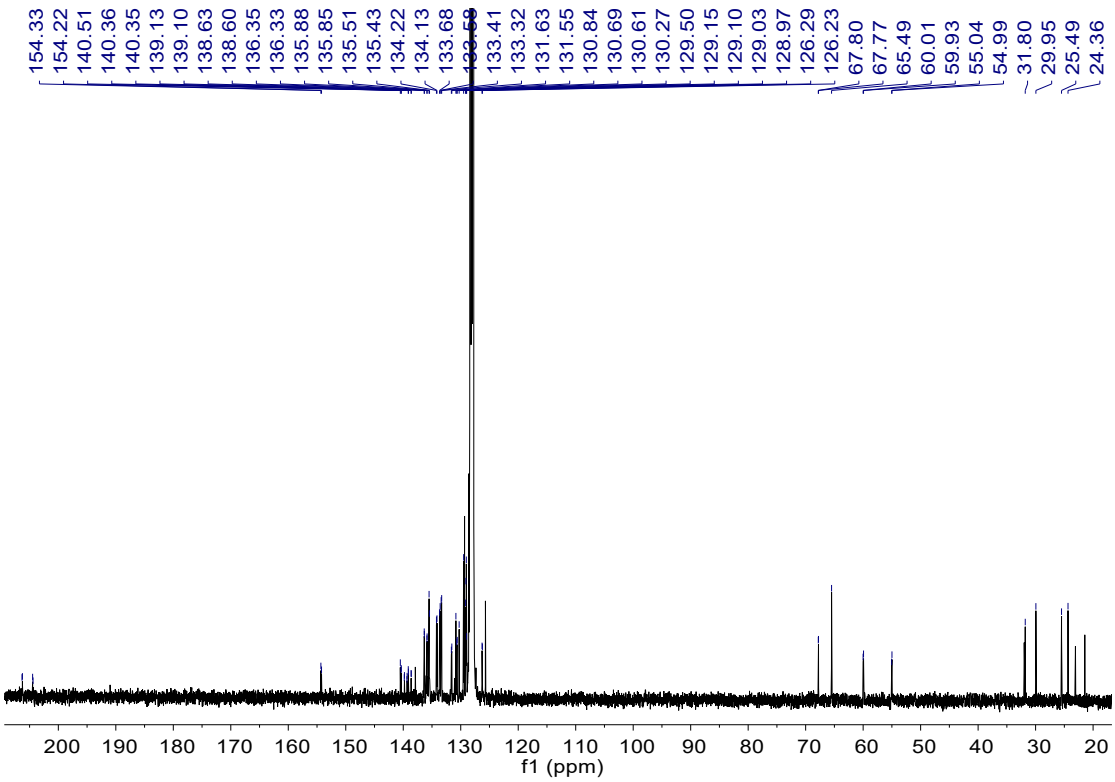

Fig. S18 $^{13}C\{^{1}H\}$ NMR spectrum of **4** measured in C_6D_6.

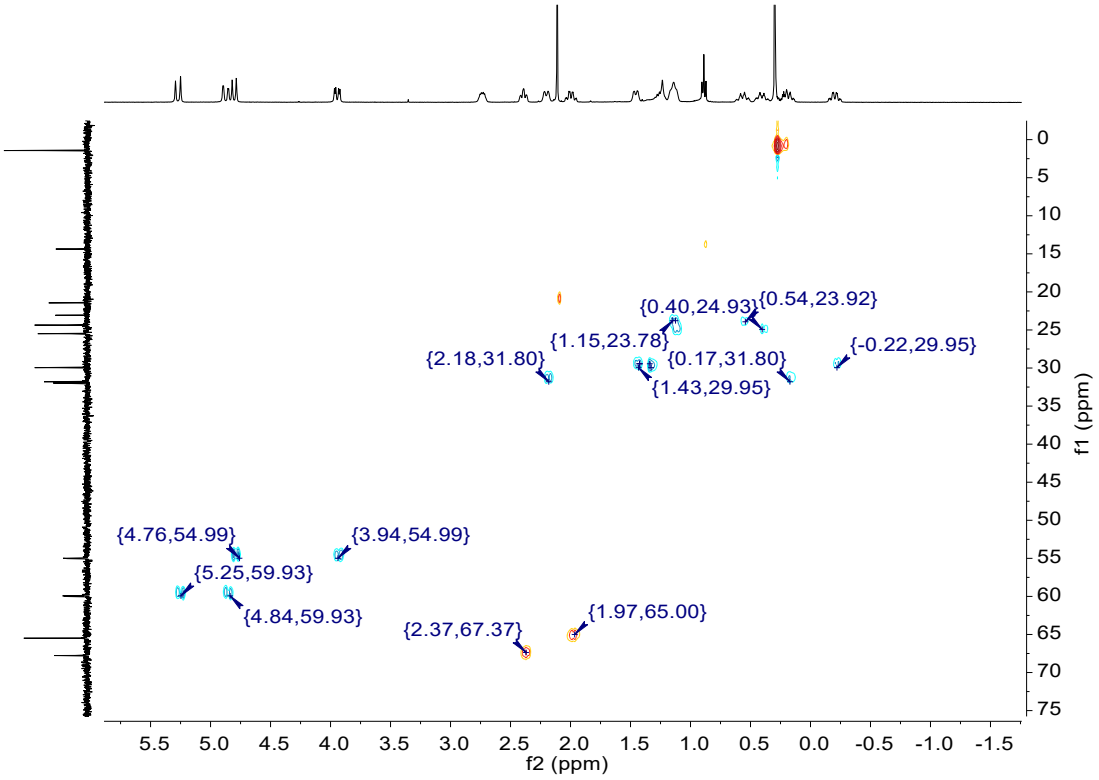

Fig. S19 ^{1}H-^{13}C HSQC NMR spectrum of **4** measured in C_6D_6.

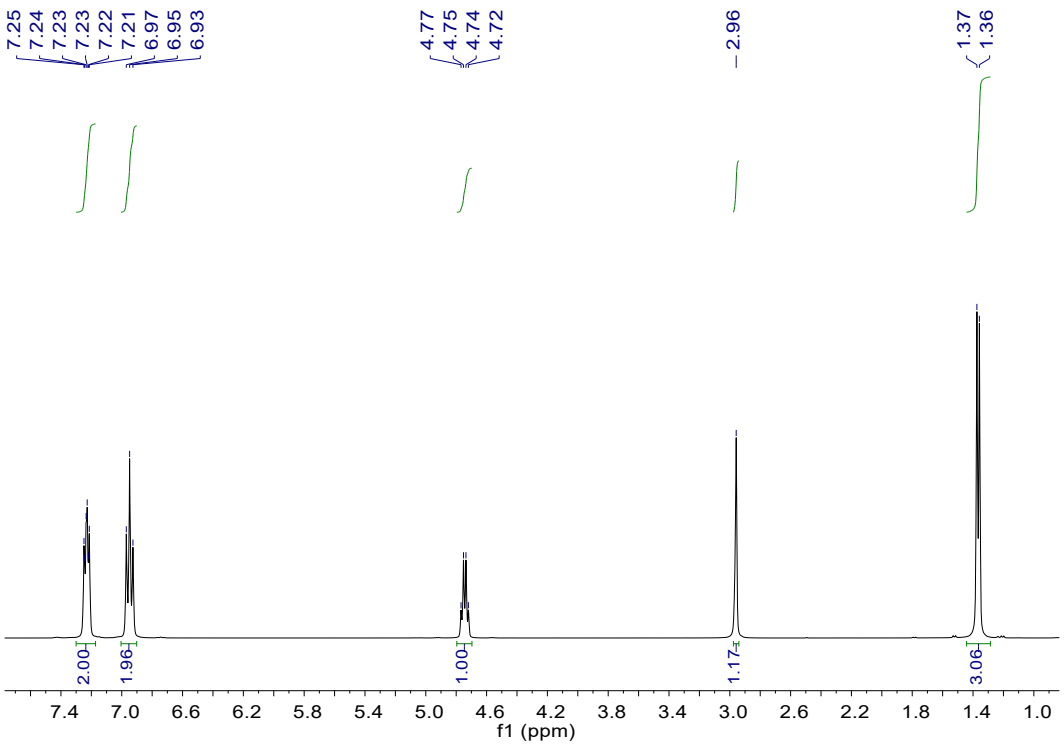

Fig. S20 ^{1}H NMR spectrum of **b1**.[6] ^{1}H NMR (400 MHz, $CDCl_3$, 298 k, ppm): δ = 1.36 (d, J_{HH} = 2.8 Hz, 3 H), 2.96 (s, 1 H), 4.75 (q, J_{HH} = 6.4, 6.4 Hz, 1 H), 6.95 (t, J_{HH} = 8.8 Hz, 2 H), 7.21-7.25 (m, 2 H).

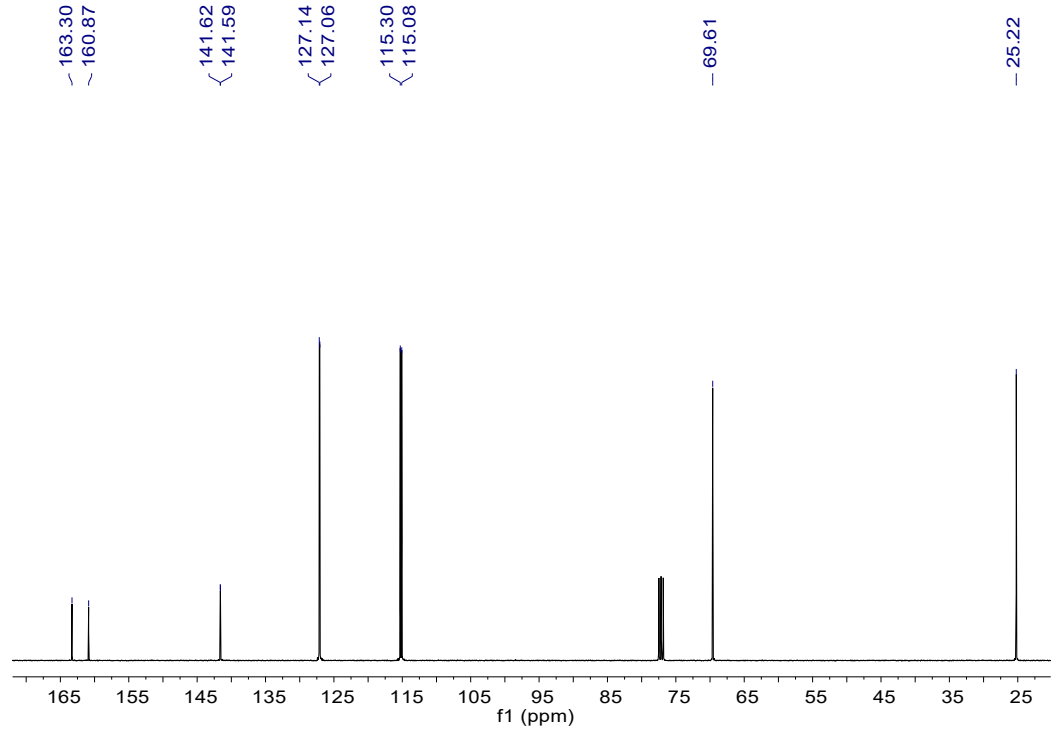

Fig. S21 ^{13}C{^{1}H} NMR spectrum of **b1**. ^{13}C{^{1}H} NMR (100 MHz, $CDCl_3$, 298 k, ppm): δ = 25.22, 69.61, 115.19 (d, J_{PC} = 21.2 Hz), 127.1 (d, J_{PC} = 8.0 Hz), 141.61 (d, J_{PC} = 3.0 Hz), 162.09 (d, J_{PC} = 243.4 Hz).

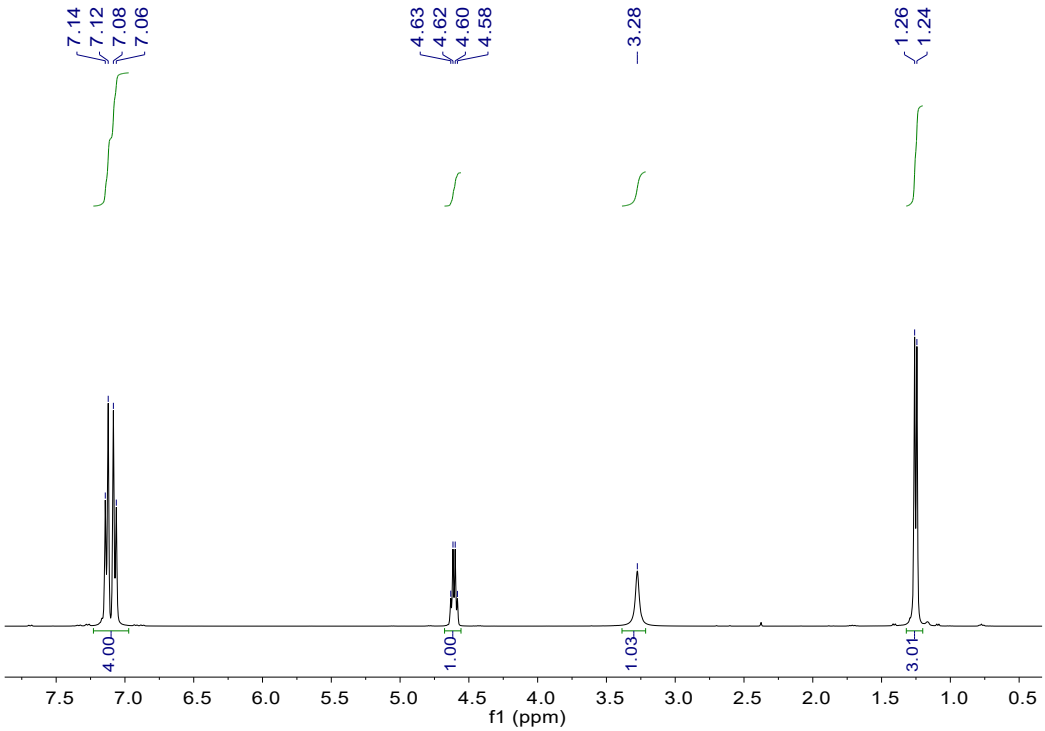

Fig. S22 ^{1}H NMR spectrum of **b2**.[6] ^{1}H NMR (400 MHz, $CDCl_3$, 298 k, ppm): δ = 1.25 (d, J_{HH} = 6.8 Hz, 3 H), 3.28 (br, 1 H), 4.61 (q, J_{HH} = 6.8, 6.4 Hz, 1 H), 7.06-7.14 (m, 4 H).

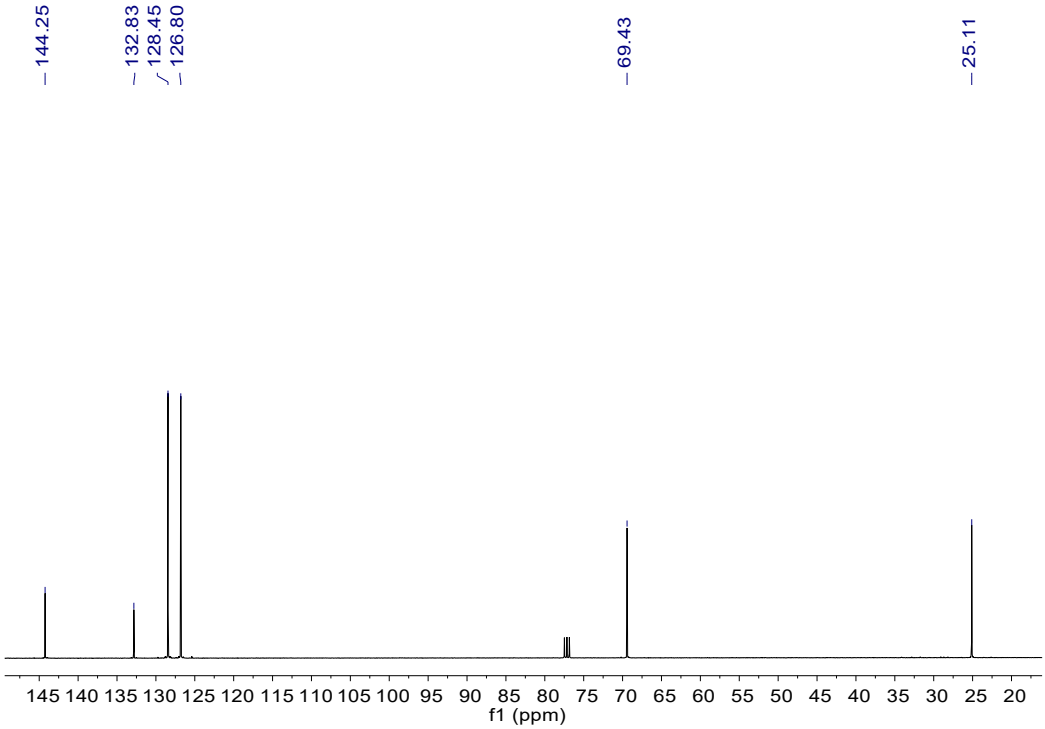

Fig. S23 ^{13}C{^{1}H} NMR spectrum of **b2**. ^{13}C{^{1}H} NMR (100 MHz, $CDCl_3$, 298 k, ppm): δ = 25.11, 69.43, 126.80, 128.45, 132.83, 144.25.

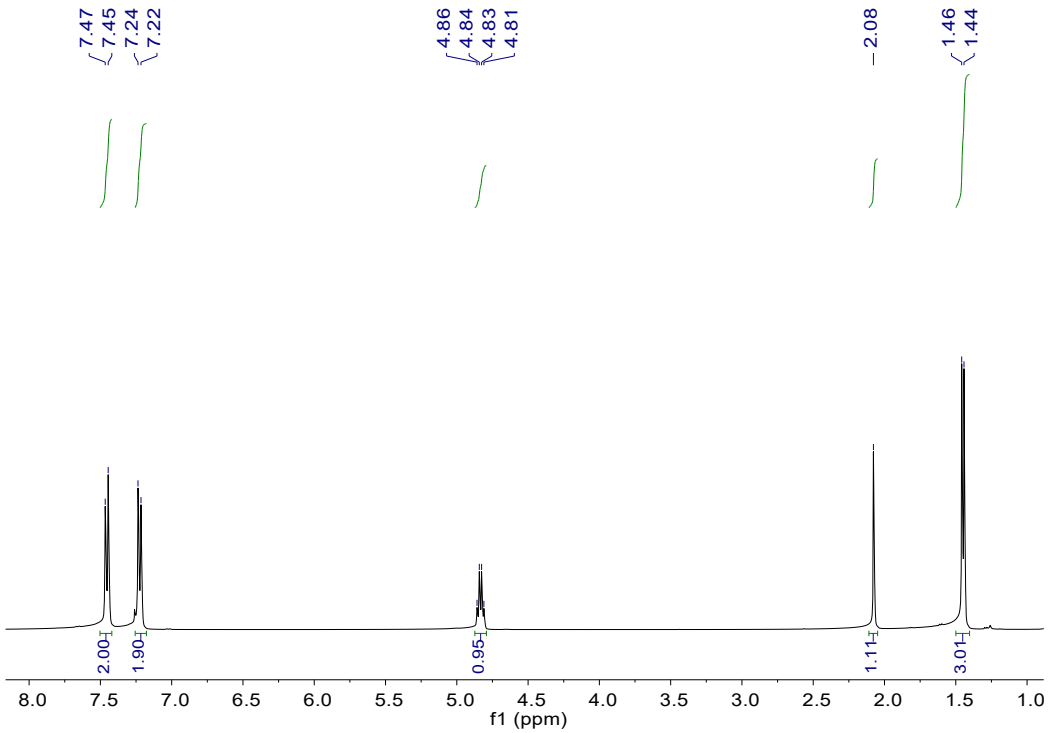

Fig. S24 ^{1}H NMR spectrum of **b3**.[7] ^{1}H NMR (400 MHz, $CDCl_3$, 298 k, ppm): δ = 1.45 (d, J_{HH} = 6.8 Hz, 3 H), 2.08 (s, 1 H), 4.84 (q, J_{HH} = 6.4, 6.4 Hz, 1 H), 7.23 (d, J_{HH} = 8.4 Hz, 2 H), 7.46 (d, J_{HH} = 8.4 Hz, 2 H).

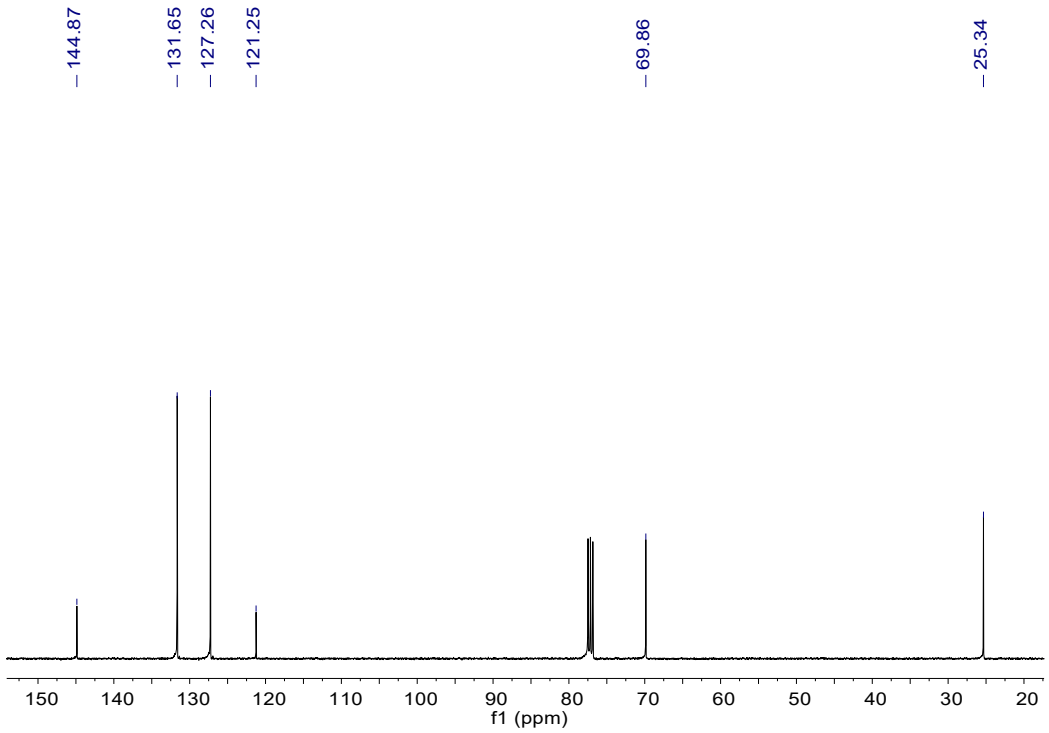

Fig. S25 ^{13}C{^{1}H} NMR spectrum of **b3**. ^{13}C{^{1}H} NMR (100 MHz, $CDCl_3$, 298 k, ppm): δ = 25.34, 69.86, 121.25, 127.26, 131.65, 144.87.

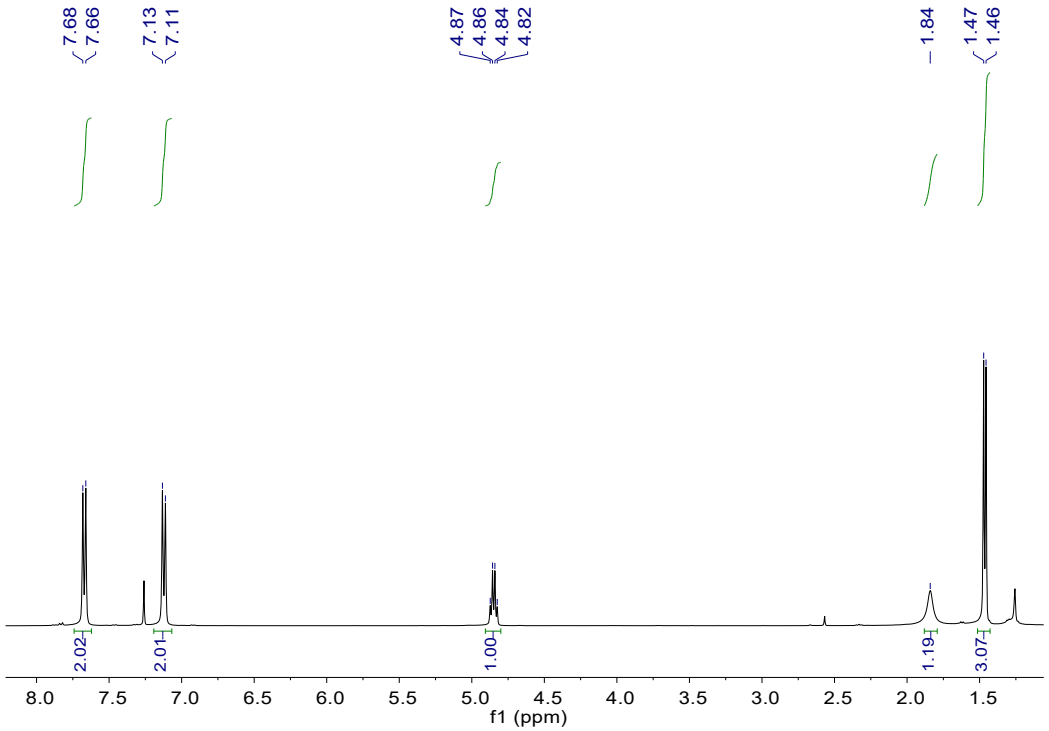

Fig. S26 ^{1}H NMR spectrum of **b4**.[6] ^{1}H NMR (400 MHz, $CDCl_3$, 298 k, ppm): δ = 1.46 (d, J_{HH} = 6.4 Hz, 3 H), 1.84 (br, 1 H), 4.85 (q, J_{HH} = 6.4, 6.4 Hz, 1 H), 7.12 (d, J_{HH} = 8.0 Hz, 2 H), 7.67 (d, J_{HH} = 8.4 Hz, 2 H).

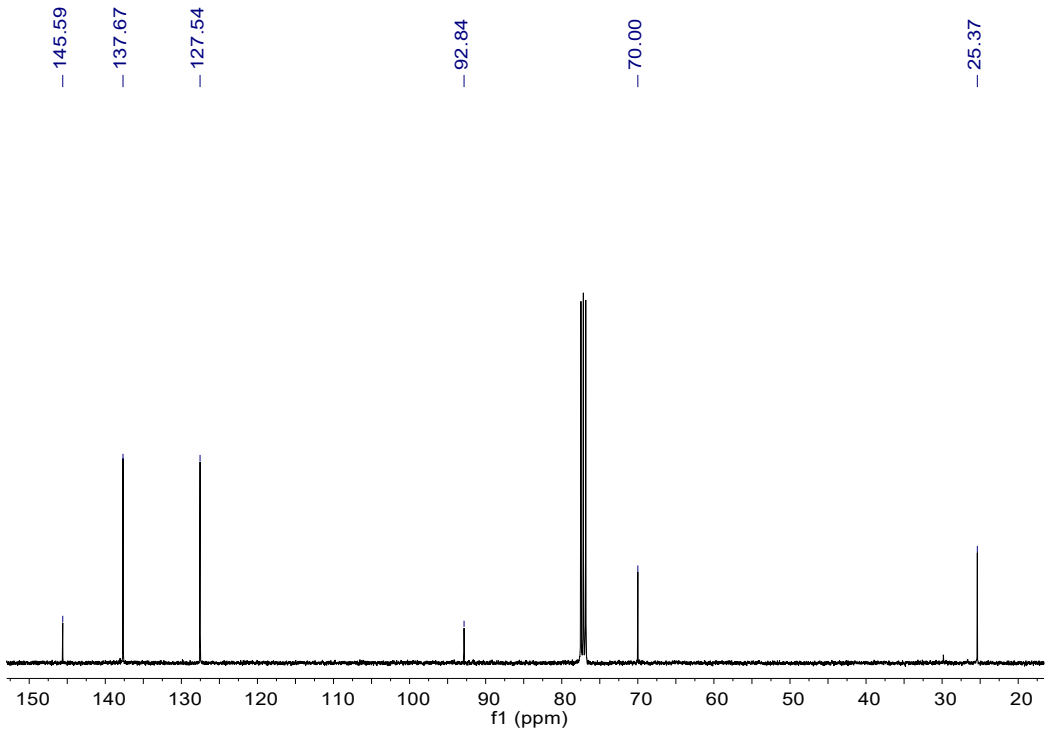

Fig. S27 ^{13}C{^{1}H} NMR spectrum of **b4**. ^{13}C{^{1}H} NMR (100 MHz, $CDCl_3$, 298 k, ppm): δ = 25.37, 70.00, 92.84, 127.54, 137.67, 145.59.

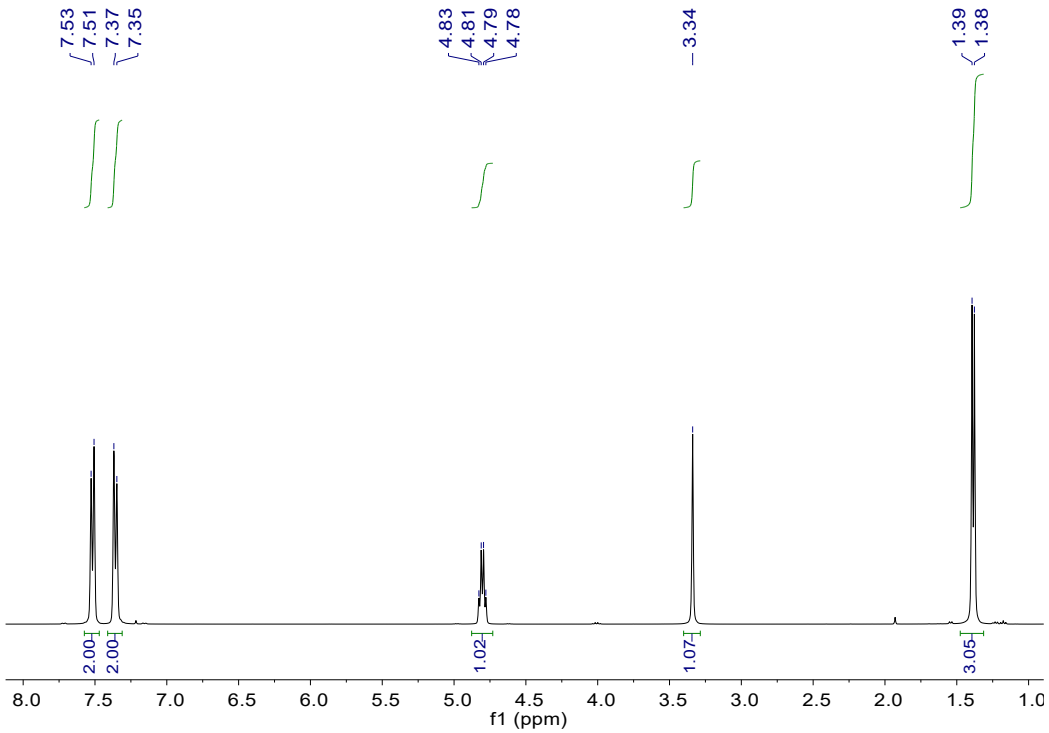

Fig. S28 ^{1}H NMR spectrum of **b5**.[6] ^{1}H NMR (400 MHz, $CDCl_3$, 298 k, ppm): δ = 1.38 (d, J_{HH} = 6.8 Hz, 3 H), 3.34 (s, 1 H), 4.80 (q, J_{HH} = 6.4, 6.4 Hz, 1 H), 7.36 (d, J_{HH} = 8.0 Hz, 2 H), 7.52 (d, J_{HH} = 8.0 Hz, 2 H).

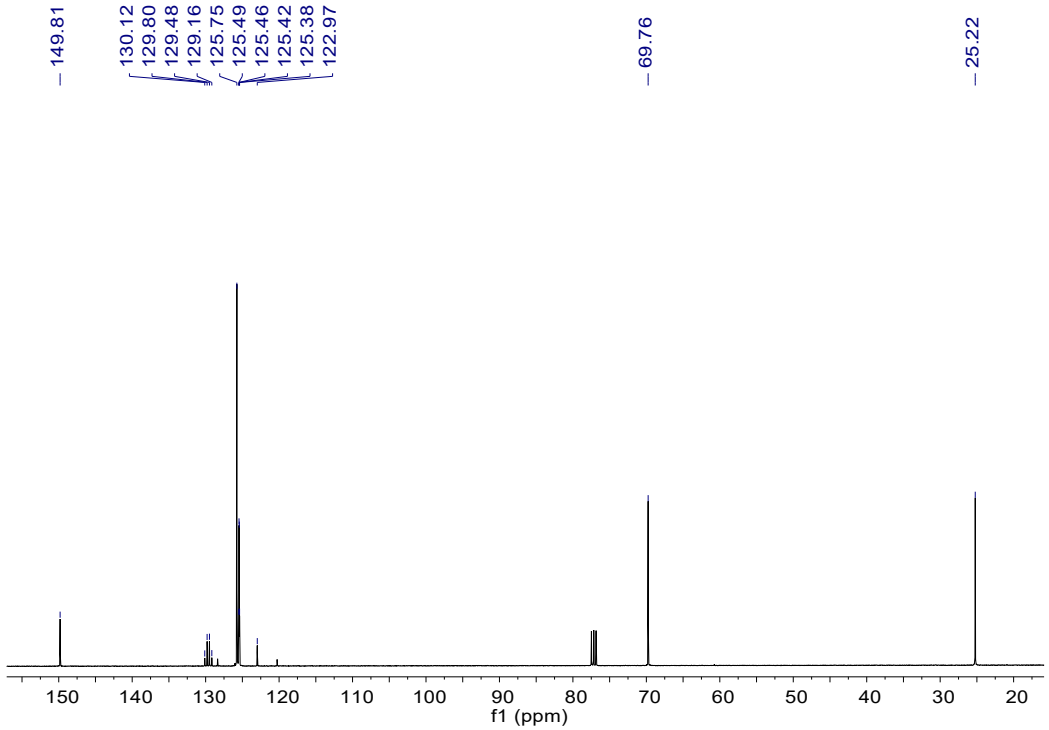

Fig. S29 ^{13}C{^{1}H} NMR spectrum of **b5**. ^{13}C{^{1}H} NMR (100 MHz, $CDCl_3$, 298 k, ppm): δ = 25.22, 69.76, 122.97, 125.44 (q, J_{PC} = 3.8, 3.7 Hz), 125.75, 129.14 (q, J_{PC} = 32.2, 32.1 Hz), 149.81.

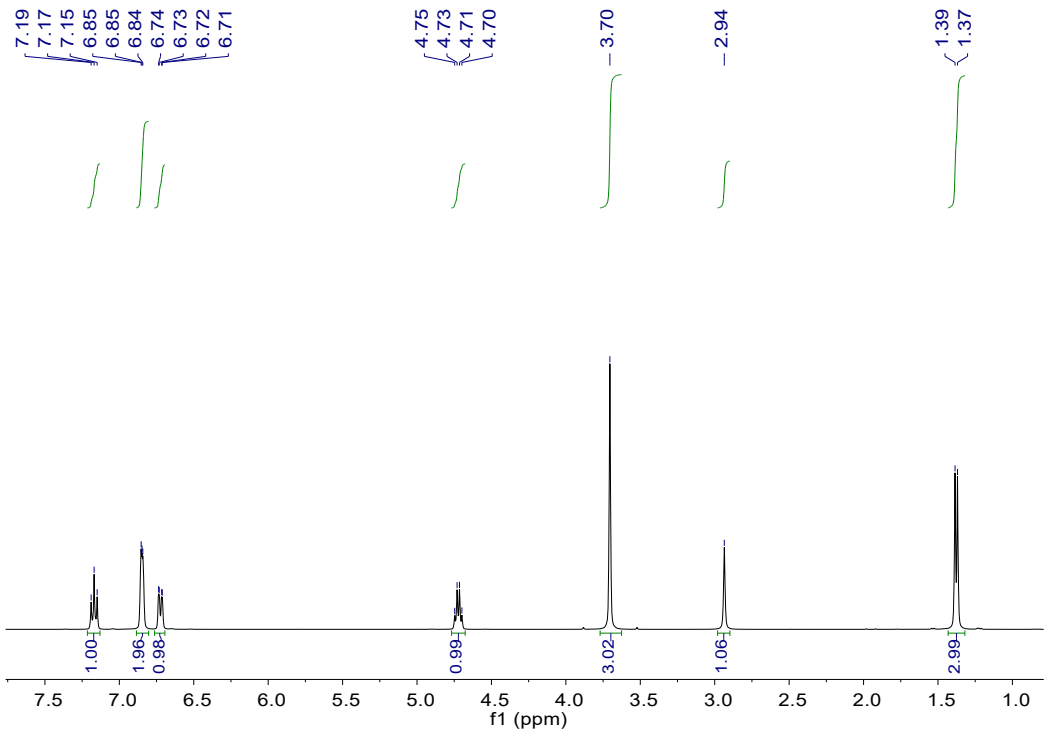

Fig. S30 ^{1}H NMR spectrum of **b6**.[6] ^{1}H NMR (400 MHz, $CDCl_3$, 298 k, ppm): δ = 1.38 (d, J_{HH} = 6.4 Hz, 3 H), 2.94 (s, 1 H), 3.70 (s, 3 H), 4.72 (q, J_{HH} = 6.4, 6.4 Hz, 1 H), 6.72 (dd, J_{HH} = 1.6, 6.8 Hz, 1 H), 6.85 (t, J_{HH} = 2.4 Hz, 2 H), 7.17 (t, J_{HH} = 8.0 Hz, 1 H).

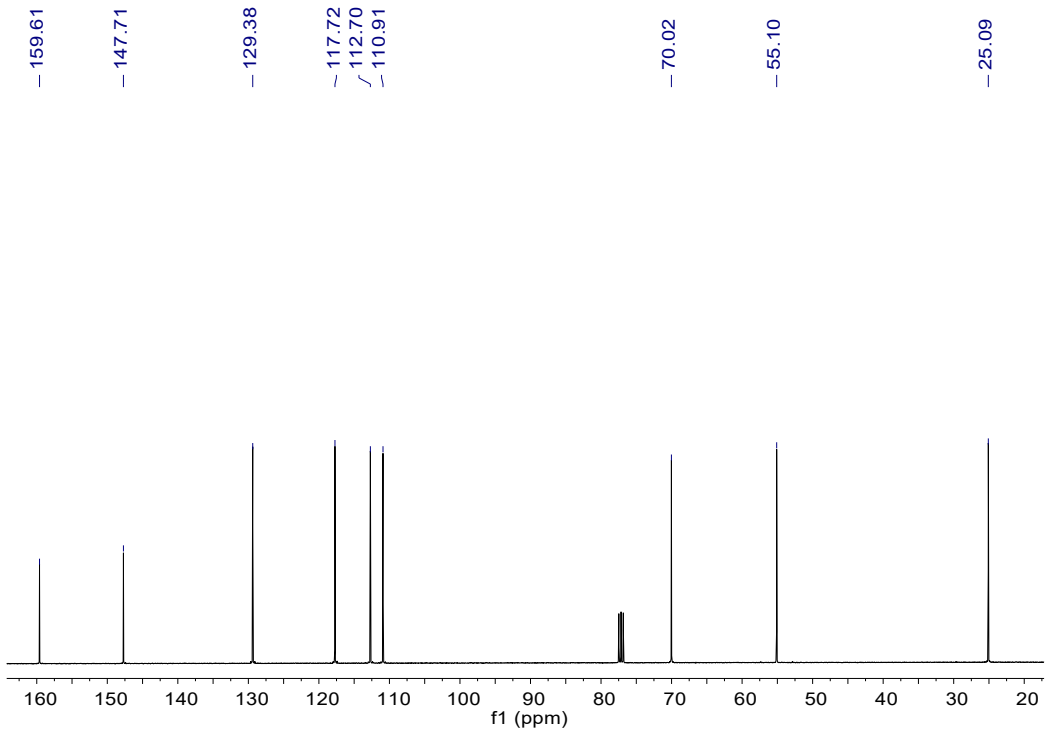

Fig. S31 ^{13}C{^{1}H} NMR spectrum of **b6**. ^{13}C{^{1}H} NMR (100 MHz, $CDCl_3$, 298 k, ppm): δ = 25.09, 55.10, 70.02, 110.91, 112.70, 117.72, 129.38, 147.71, 159.61.

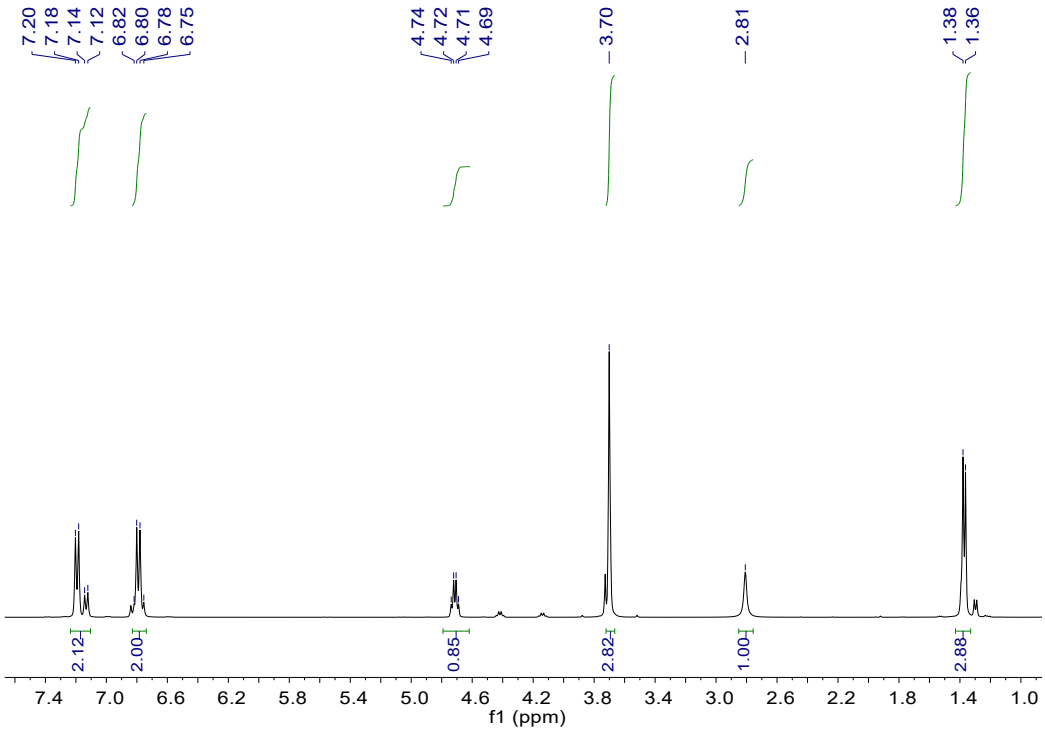

Fig. S32 ^{1}H NMR spectrum of **b7**.[6] ^{1}H NMR (400 MHz, $CDCl_3$, 298 k, ppm): δ = 1.37 (d, J_{HH} = 6.4 Hz, 3 H), 2.81 (s, 1 H), 3.70 (s, 3 H), 4.71 (q, J_{HH} = 6.4, 6.4 Hz, 1 H), 6.79 (q, J_{HH} = 6.8, 8.4 Hz, 2 H), 7.12-7.20 (m, 2 H).

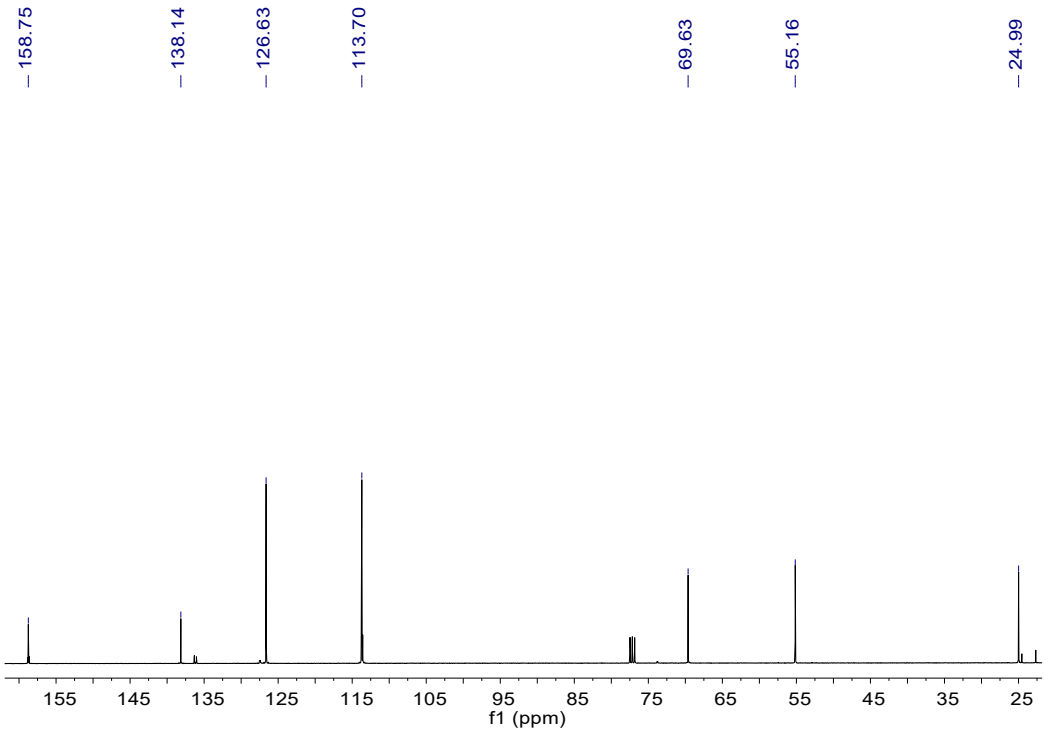

Fig. S33 ^{13}C{^{1}H} NMR spectrum of **b7**. ^{13}C{^{1}H} NMR (100 MHz, $CDCl_3$, 298 k, ppm): δ = 24.99, 55.16, 69.63, 113.70, 126.63, 138.14, 158.75.

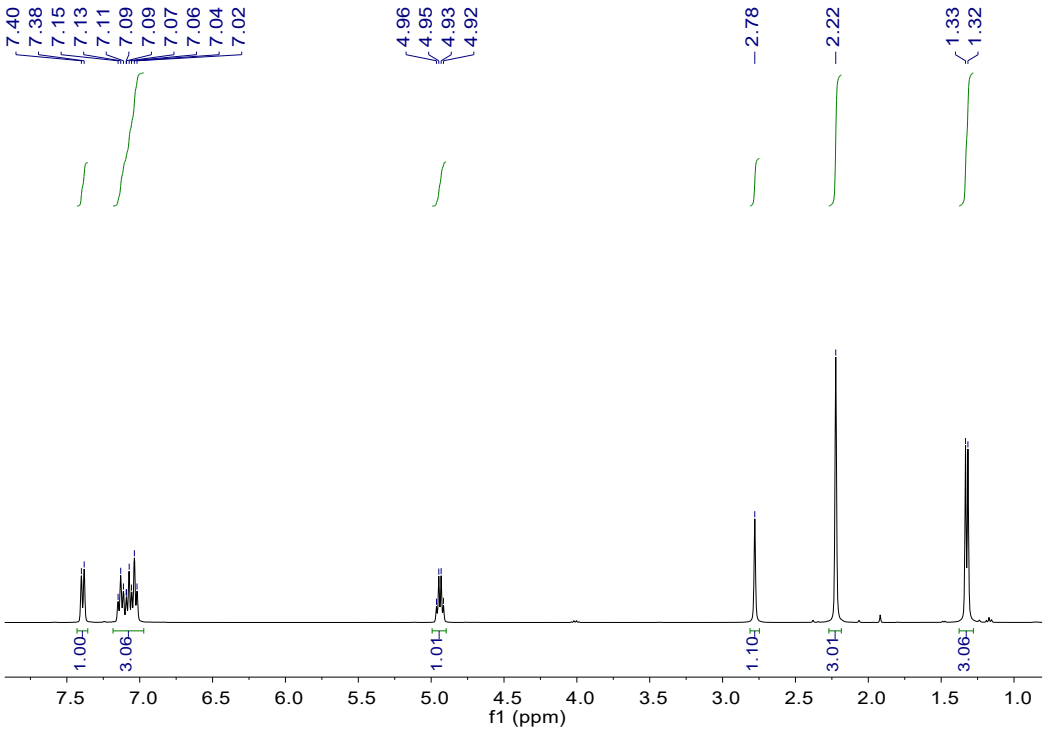

Fig. S34 ^{1}H NMR spectrum of **b8**.[6] ^{1}H NMR (400 MHz, $CDCl_3$, 298 k, ppm): δ = 1.32 (d, J_{HH} = 6.8 Hz, 3 H), 2.22 (s, 3 H), 2.78 (s, 1 H), 4.94 (q, J_{HH} = 6.4, 6.8 Hz, 1 H), 7.02-7.15 (m, 3 H), 7.39 (d, J_{HH} = 7.6 Hz, 1 H).

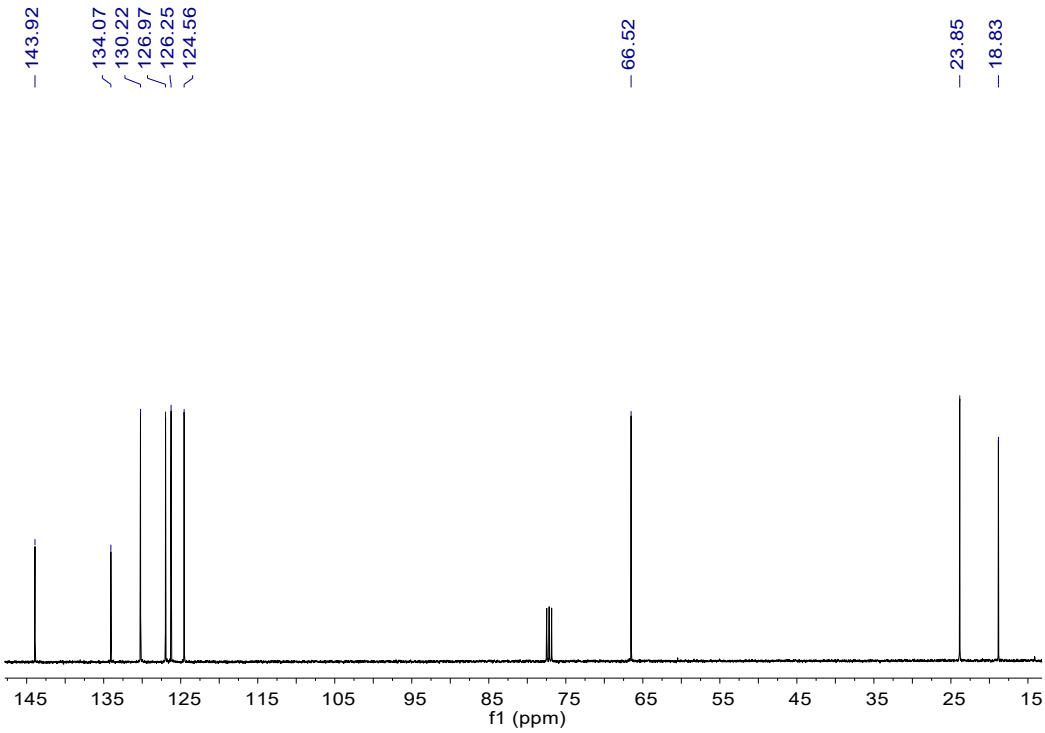

Fig. S35 ^{13}C{^{1}H} NMR spectrum of **b8**. ^{13}C{^{1}H} NMR (100 MHz, $CDCl_3$, 298 k, ppm): δ = 18.83, 23.85, 66.52, 124.56, 126.25, 126.97, 130.22, 134.07, 143.92.

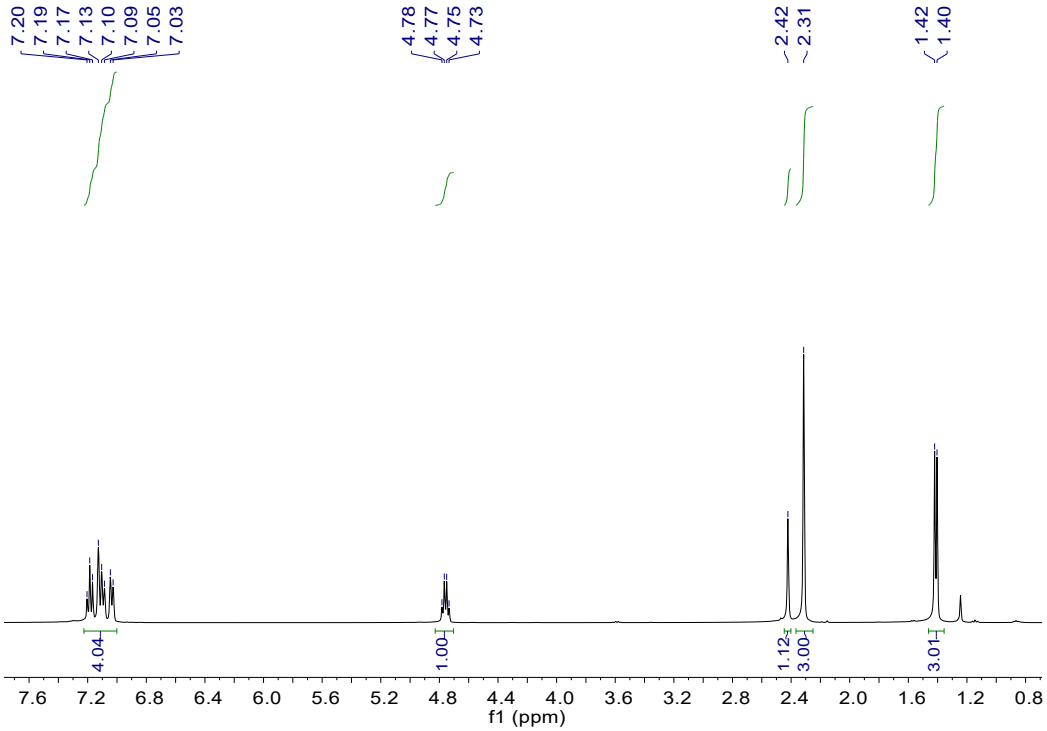

Fig. S36 ^{1}H NMR spectrum of **b9**.[8] ^{1}H NMR (400 MHz, $CDCl_3$, 298 k, ppm): δ = 1.41 (d, J_{HH} = 6.8 Hz, 3 H), 2.31 (s, 3 H), 2.42 (s, 1 H), 4.76 (q, J_{HH} = 6.8, 6.4 Hz, 1 H), 7.03-7.20 (m, 4 H).

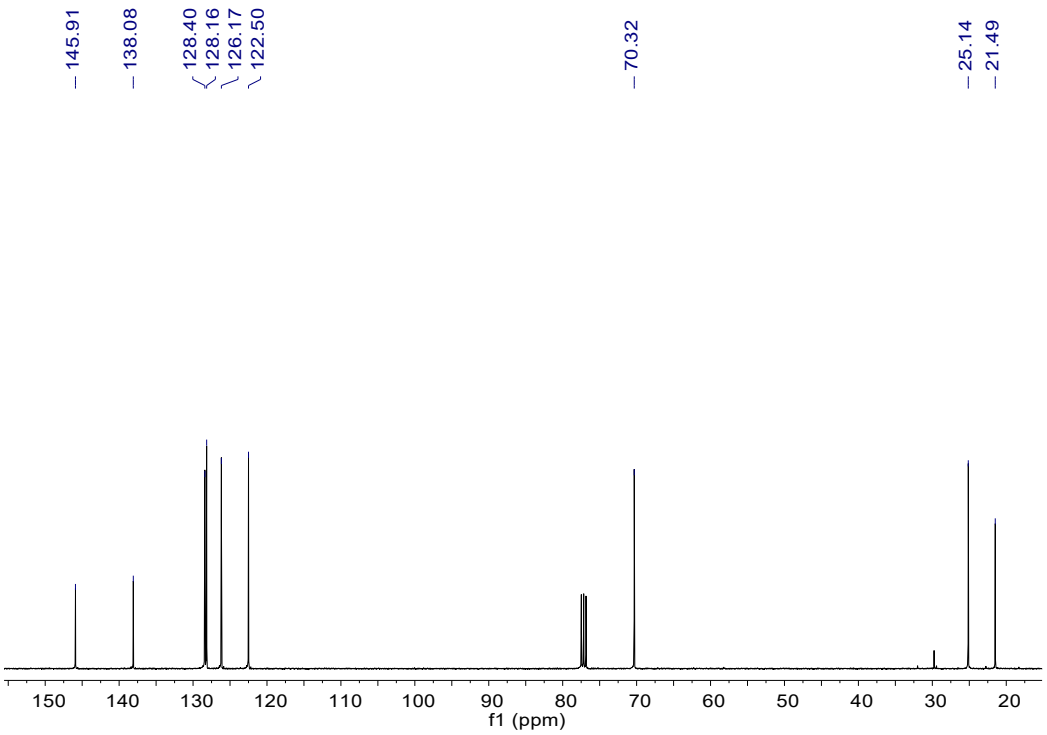

Fig. S37 ^{13}C{^{1}H} NMR spectrum of **b9**. ^{13}C{^{1}H} NMR (100 MHz, $CDCl_3$, 298 k, ppm): δ = 21.49, 25.14, 70.32, 122.50, 126.17, 128.16, 128.40, 138.08, 145.91.

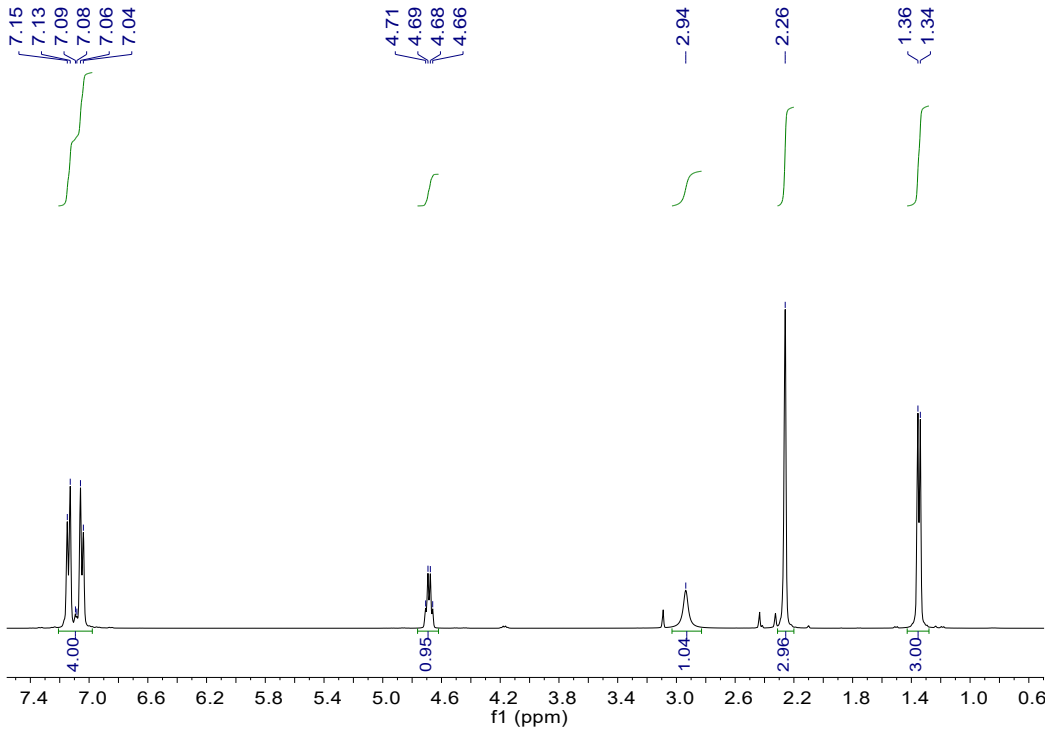

Fig. S38 ^{1}H NMR spectrum of **b10**.[6] ^{1}H NMR (400 MHz, $CDCl_3$, 298 k, ppm): δ = 1.35 (d, J_{HH} = 6.4 Hz, 3 H), 2.26 (s, 3 H), 2.94 (br, 1 H), 4.68 (q, J_{HH} = 6.4, 6.4 Hz, 1 H), 7.04-7.15 (m, 4 H).

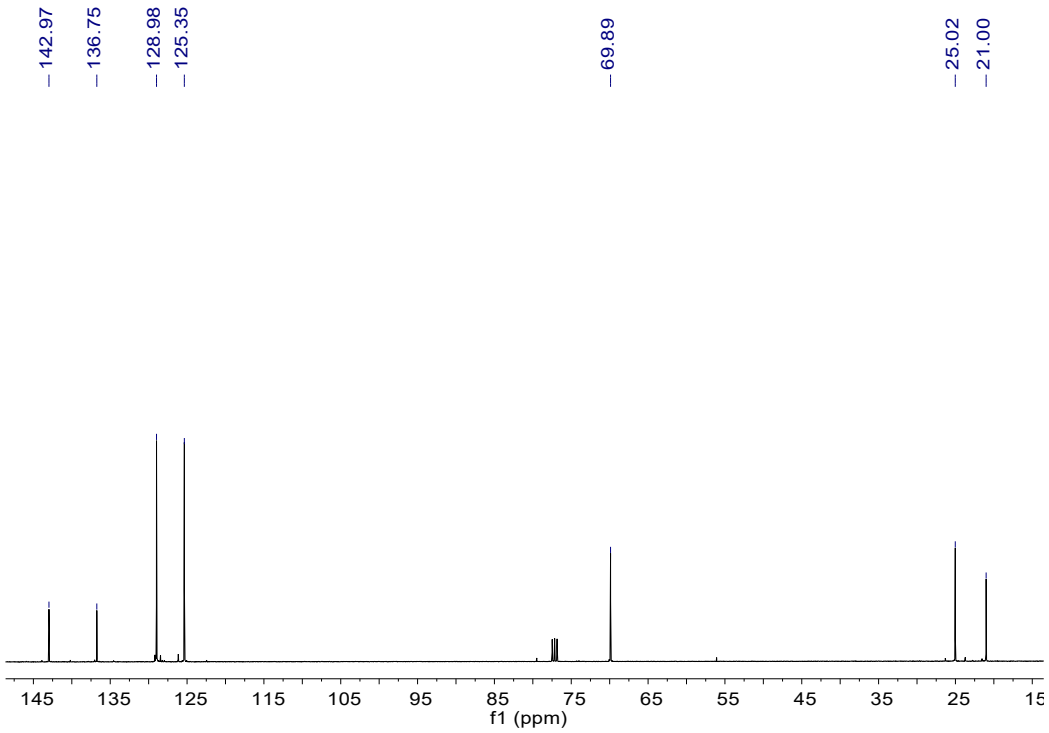

Fig. S39 ^{13}C{^{1}H} NMR spectrum of **b10**. ^{13}C{^{1}H} NMR (100 MHz, $CDCl_3$, 298 k, ppm): δ = 21.00, 25.02, 69.89, 125.35, 128.98, 136.75, 142.97.

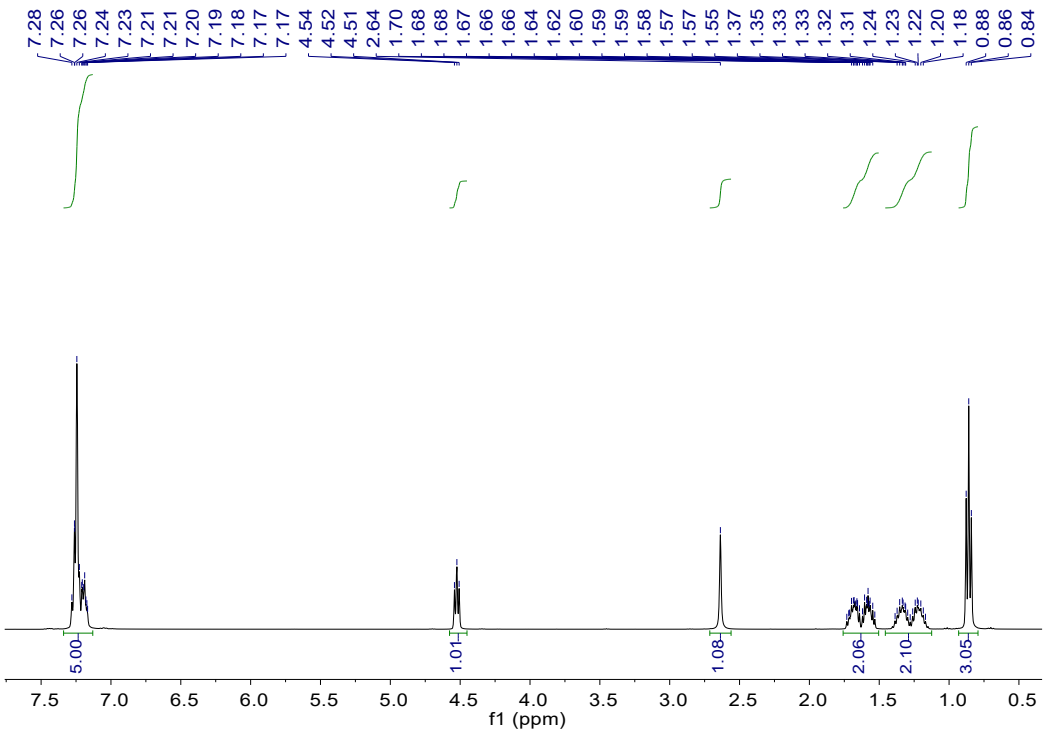

Fig. S40 ^{1}H NMR spectrum of **b13**.[7] ^{1}H NMR (400 MHz, $CDCl_3$, 298 k, ppm): δ = 0.86 (t, J_{HH} = 7.6 Hz, 3 H), 1.17-1.39 (m, 2 H), 1.53-1.73 (m, 2 H), 2.64 (s, 1 H), 4.52 (t, J_{HH} = 7.2 Hz, 1 H), 7.17-7.28 (m, 5 H).

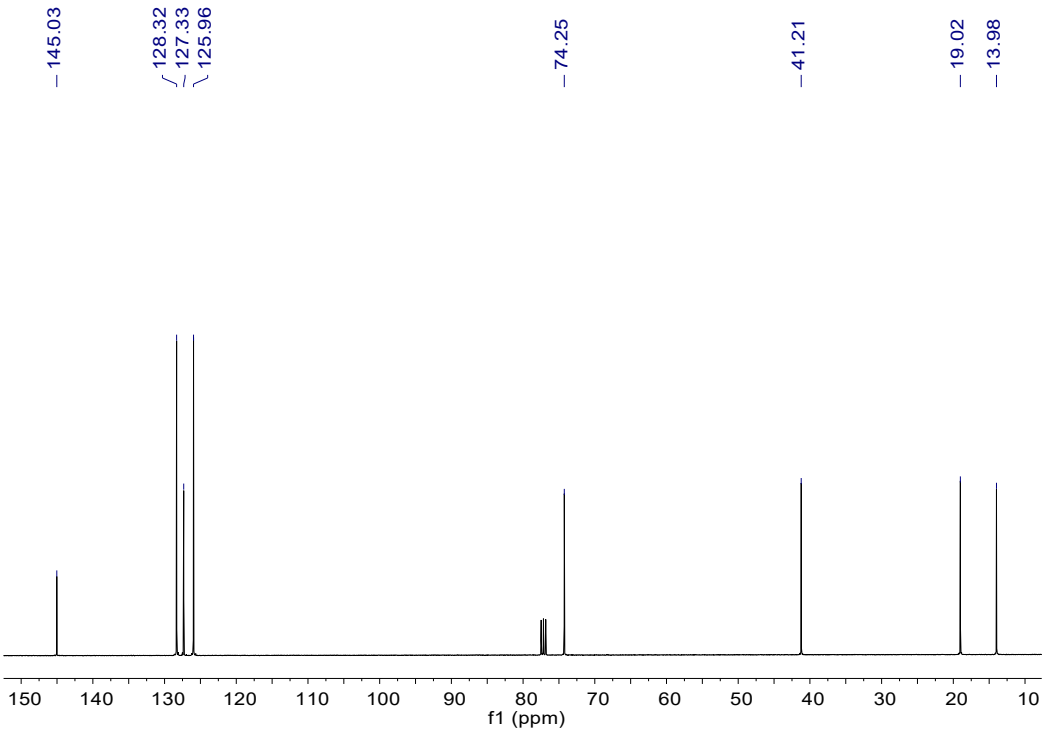

Fig. S41 ^{13}C{^{1}H} NMR spectrum of **b13**. ^{13}C{^{1}H} NMR (100 MHz, $CDCl_3$, 298 k, ppm): δ = 13.98, 19.02, 41.21, 74.25, 125.96, 127.33, 128.32, 145.03.

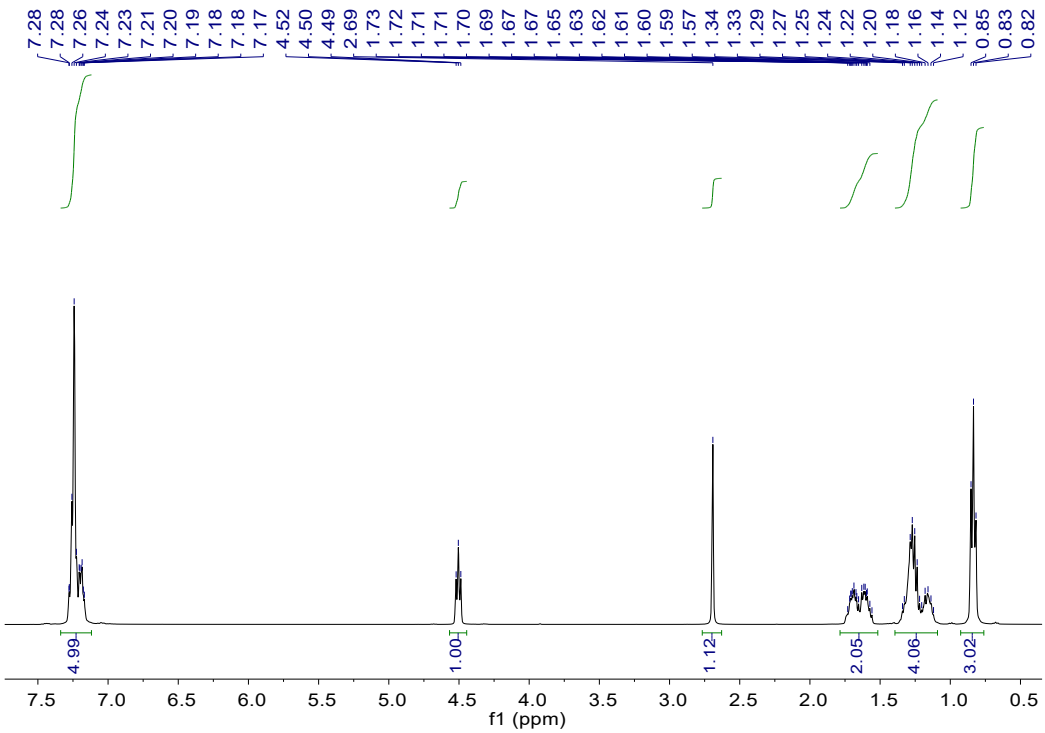

Fig. S42 ^{1}H NMR spectrum of **b14**.[9] ^{1}H NMR (400 MHz, $CDCl_3$, 298 k, ppm): δ = 0.83 (t, J_{HH} = 6.8 Hz, 3 H), 1.12-1.34 (m, 4 H), 1.56-1.73 (m, 2 H), 2.69 (s ,1 H), 4.50 (t, J_{HH} = 6.0 Hz, 1 H), 7.17-7.28 (m, 5 H).

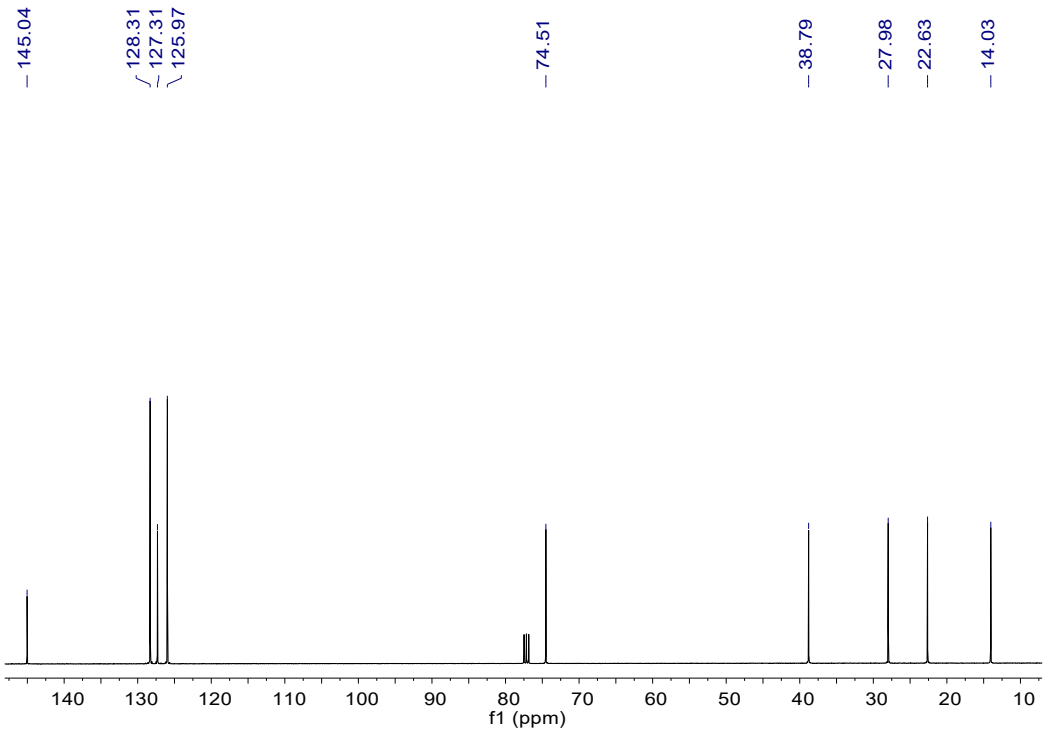

Fig. S43 ^{13}C{^{1}H} NMR spectrum of **b14**. ^{13}C{^{1}H} NMR (100 MHz, $CDCl_3$, 298 k, ppm): δ = 14.03, 22.63, 27.98, 38.79, 74.51, 125.97, 127.31, 128.31, 145.04.

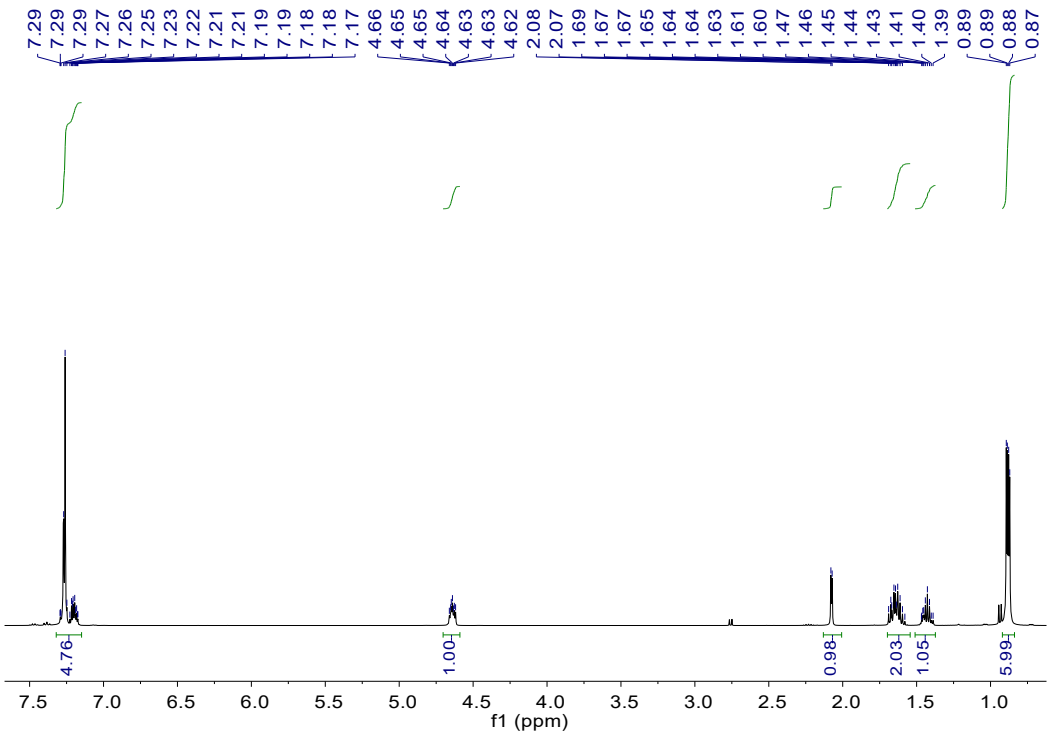

Fig. S44 ^{1}H NMR spectrum of **b15**.[6] ^{1}H NMR (400 MHz, $CDCl_3$, 298 k, ppm): δ = 0.88 (dd, J_{HH} = 2.8, 6.4 Hz, 6 H), 1.39-1.47 (m, 1 H), 1.58-1.69 (m, 1 H), 2.07 (d, J_{HH} = 3.2 Hz, 1 H), 4.62-4.66 (m, 1 H), 7.17-7.29 (m, 5 H).

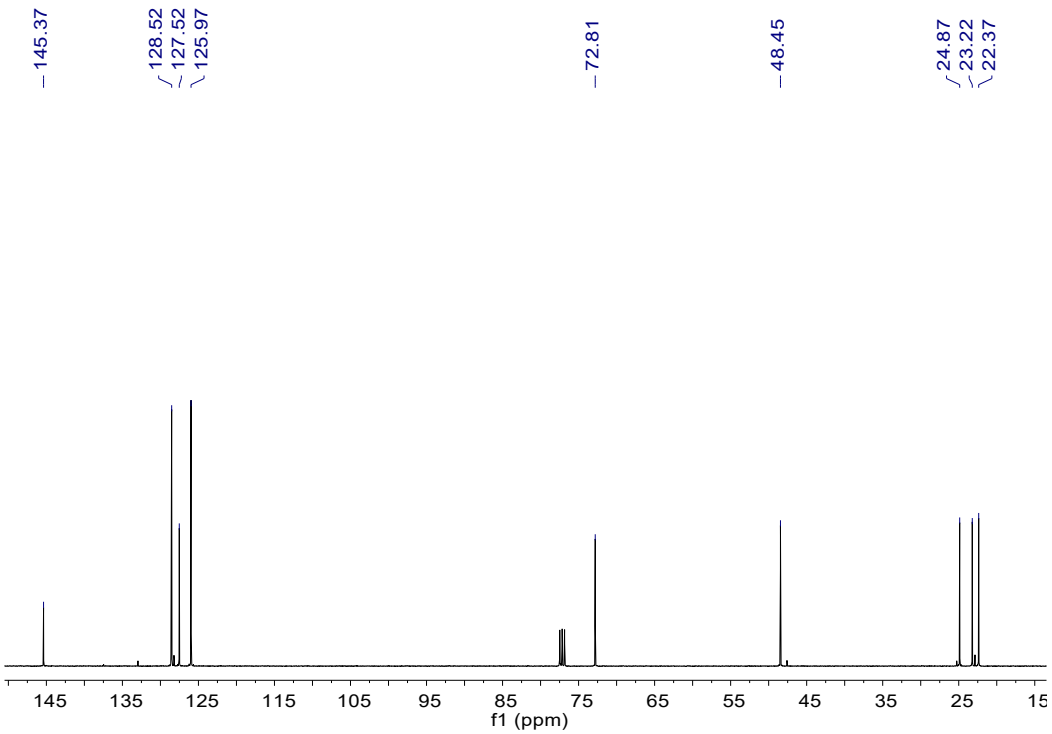

Fig. S45 ^{13}C{^{1}H} NMR spectrum of **b15**. ^{13}C{^{1}H} NMR (100 MHz, $CDCl_3$, 298 k, ppm): δ = 22.37, 23.22, 24.87, 48.45, 72.81, 125.97, 127.52, 128.52, 145.37.

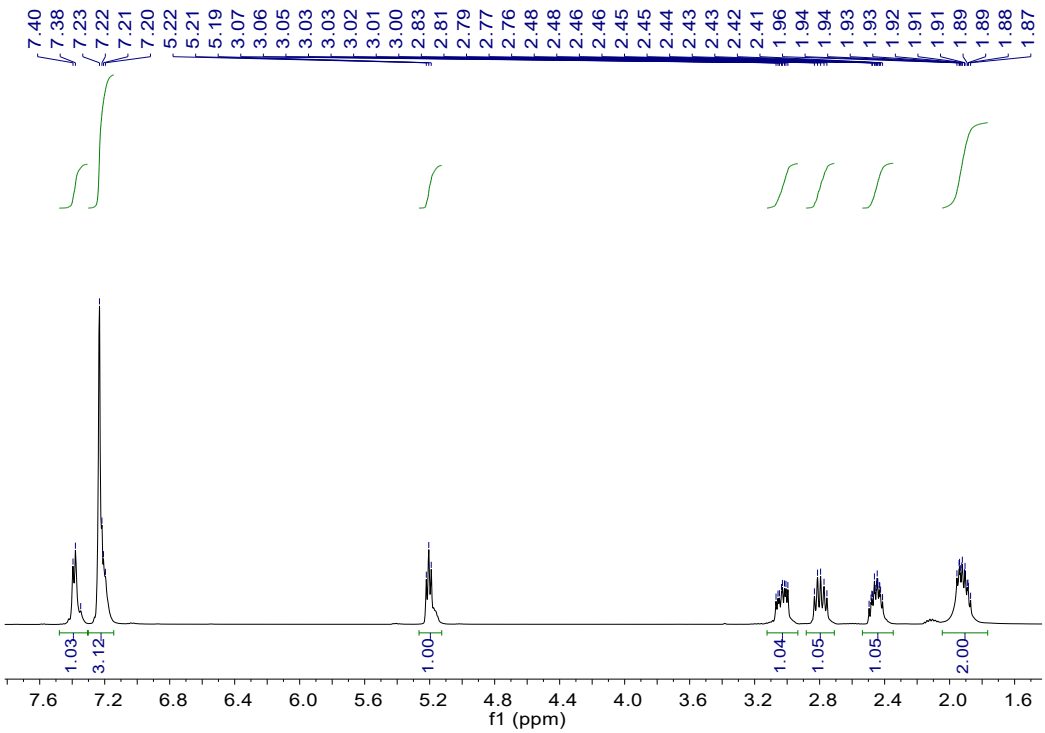

Fig. S46 ^{1}H NMR spectrum of **b16**.[6] ^{1}H NMR (400 MHz, $CDCl_3$, 298 k, ppm): δ = 1.87-1.96 (m, 2 H), 2.41-2.50 (m, 1 H), 2.76-2.83 (m, 1 H), 3.00-3.07 (m, 1 H), 5.21 (t, J_{HH} = 6.0 Hz, 1 H), 7.20-7.23 (m, 3 H), 7.35-7.40 (m, 1 H).

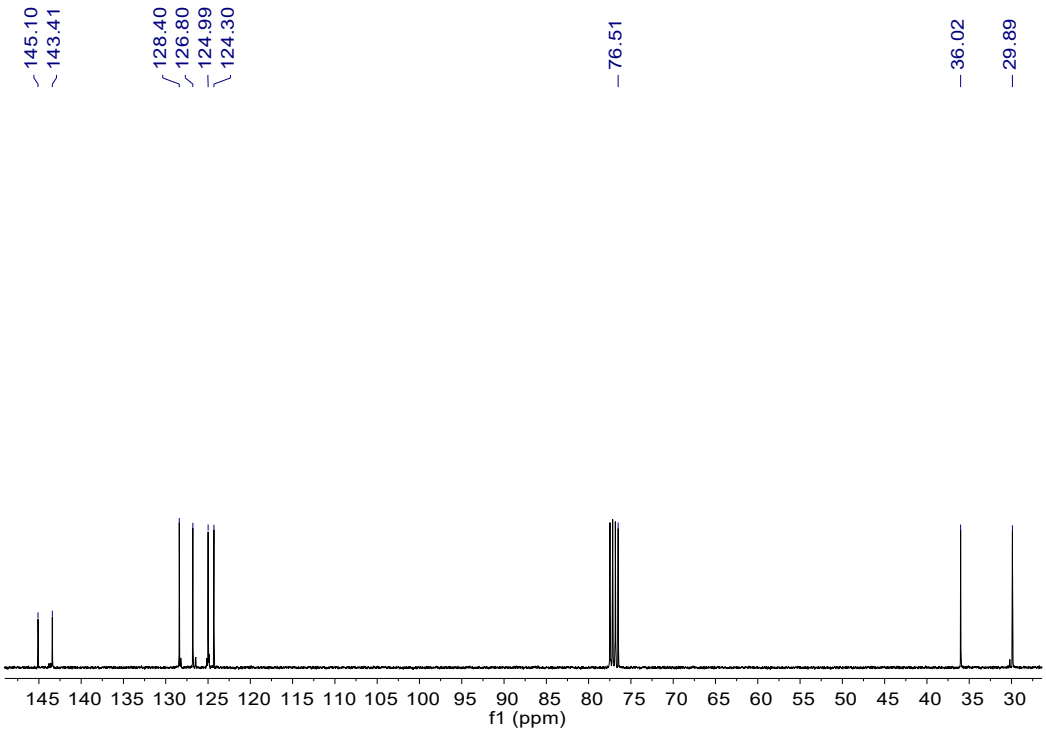

Fig. S47 ^{13}C{^{1}H} NMR spectrum of **b16**. ^{13}C{^{1}H} NMR (100 MHz, $CDCl_3$, 298 k, ppm): δ = 29.89, 36.02, 76.51, 124.30, 124.99, 126.80, 128.40, 143.41, 145.10.

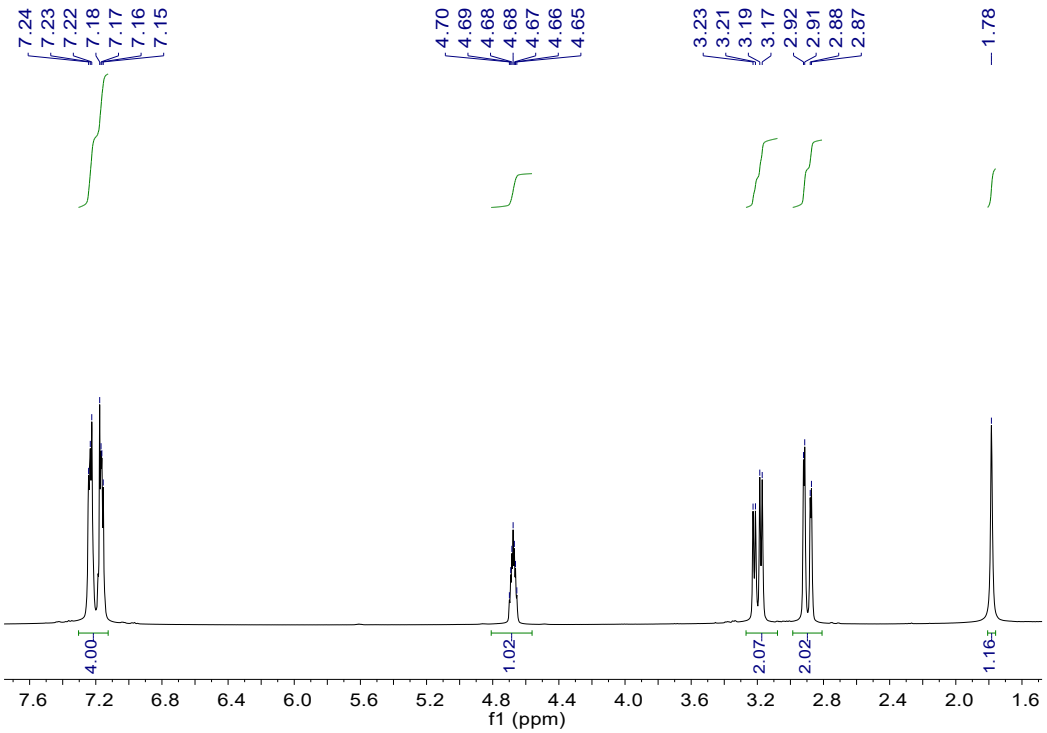

Fig. S48 ^{1}H NMR spectrum of **b17**.[6] ^{1}H NMR (400 MHz, $CDCl_3$, 298 k, ppm): δ = 1.78 (s, 1 H), 2.90 (dd, J_{HH} = 2.8, 13.6 Hz, 2 H), 3.20 (dd, J_{HH} = 6.0, 10.4 Hz, 2 H), 4.65-4.70 (m, 1 H), 7.15-7.24 (m, 4 H).

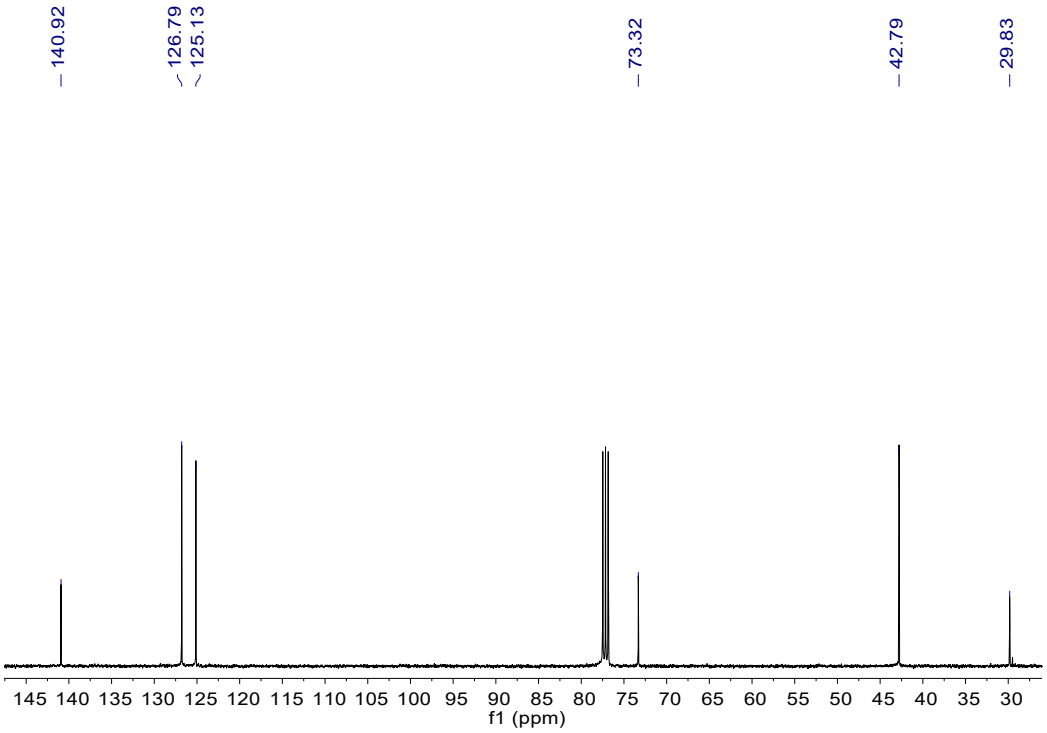

Fig. S49 ^{13}C{^{1}H} NMR spectrum of **b17**. ^{13}C{^{1}H} NMR (100 MHz, $CDCl_3$, 298 k, ppm): δ = 29.83, 42.79, 73.32, 125.13, 126.79, 140.92.

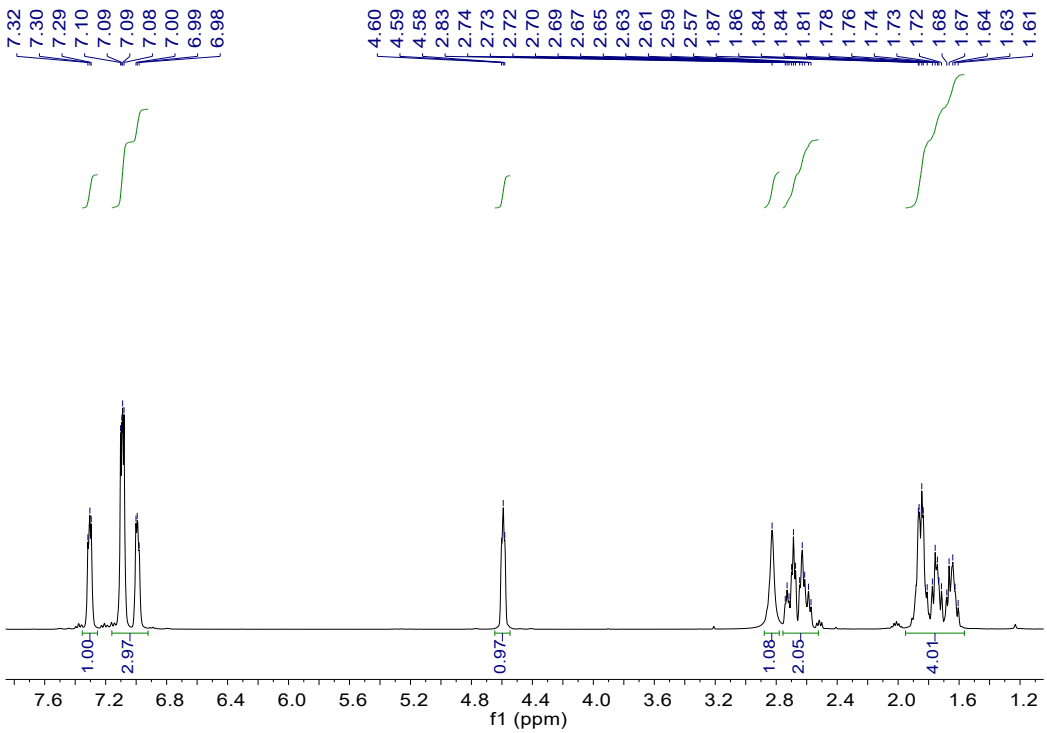

Fig. S50 ^{1}H NMR spectrum of **b18**.[6] ^{1}H NMR (400 MHz, $CDCl_3$, 298 k, ppm): δ = 1.61-1.87 (m, 4 H), 2.57-2.74 (m, 2 H), 2.83 (br, 1 H), 4.59 (t, J_{HH} = 4.4 Hz, 1 H), 6.98-7.10 (m, 3 H), 7.30 (t, J_{HH} = 4.4 Hz, 1 H).

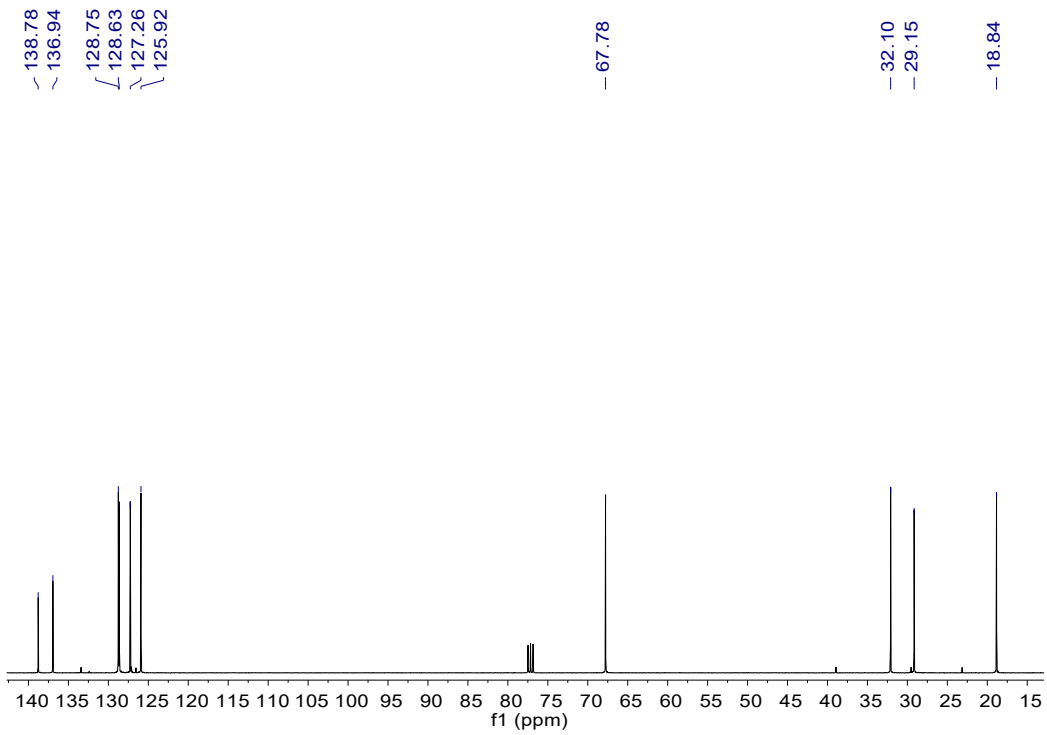

Fig. S51 ^{13}C{^{1}H} NMR spectrum of **b18**. ^{13}C{^{1}H} NMR (100 MHz, $CDCl_3$, 298 k, ppm): δ = 18.84, 29.15, 32.10, 67.78, 125.92, 127.26, 128.63, 128.75, 136.94, 138.78.

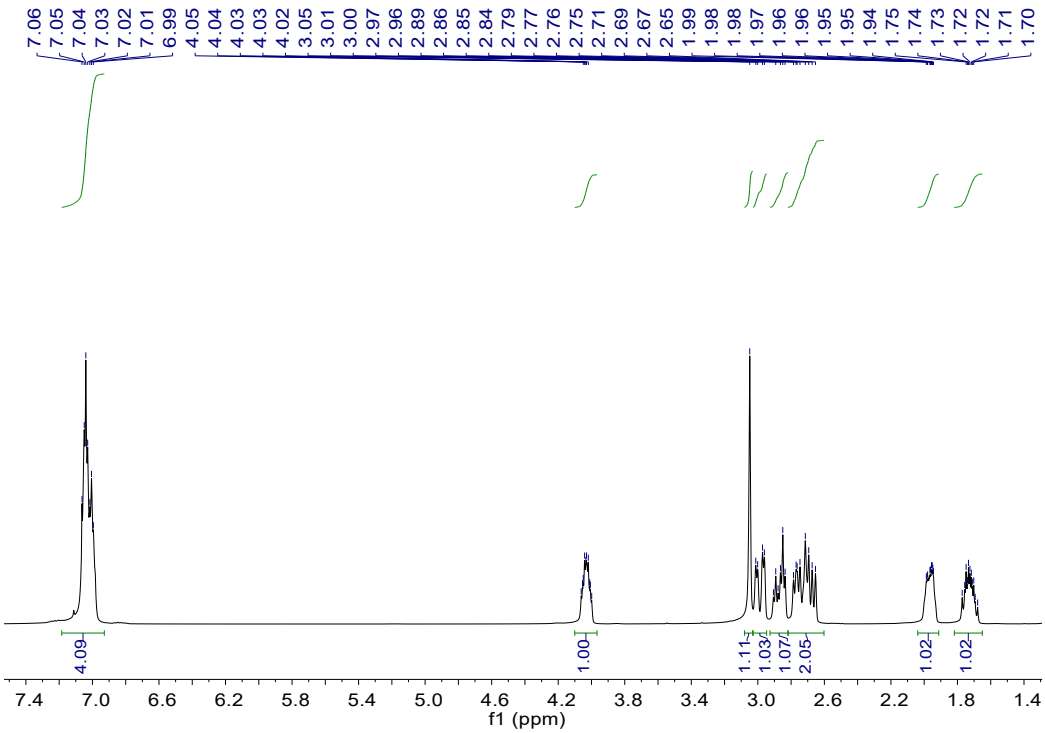

Fig. S52 ^{1}H NMR spectrum of **b19**.[6] ^{1}H NMR (400 MHz, $CDCl_3$, 298 k, ppm): δ = 1.68-1.77 (m, 1 H), 1.94-1.99 (m, 1 H), 2.65-2.79 (m, 2 H), 2.84-2.91 (m, 1 H), 2.98 (dd, J_{HH} = 4.4, 16.0 Hz, 1 H), 3.05 (s, 1 H), 4.00-4.06 (m, 1 H), 6.99-7.06 (m, 4 H).

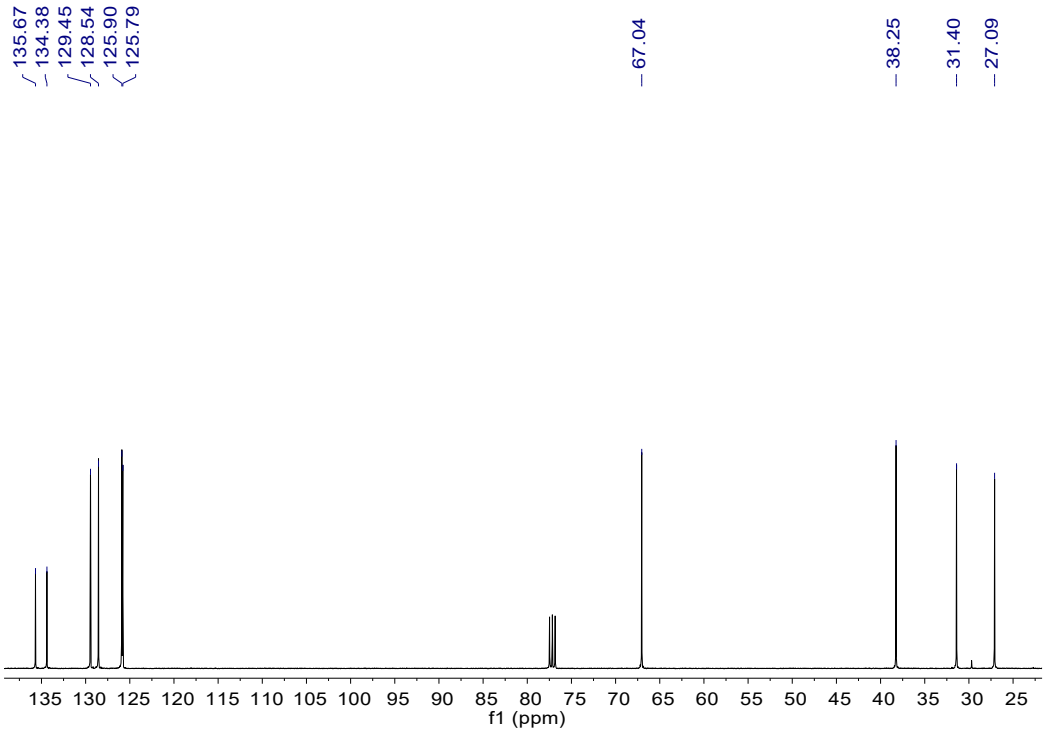

Fig. S53 ^{13}C{^{1}H} NMR spectrum of **b19**. ^{13}C{^{1}H} NMR (100 MHz, $CDCl_3$, 298 k, ppm): δ = 27.09, 31.40, 38.25, 67.04, 125.79, 125.90, 128.54, 129.45, 134.38, 135.67.

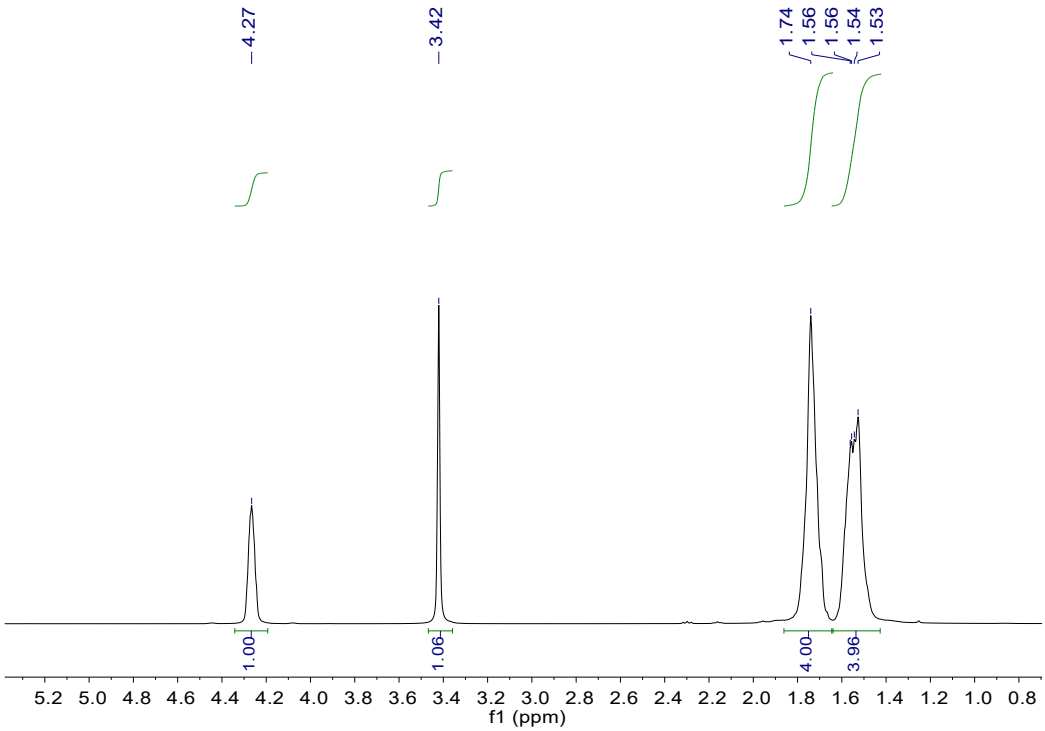

Fig. S54 ^{1}H NMR spectrum of **b20**.[7] ^{1}H NMR (400 MHz, $CDCl_3$, 298 k, ppm): δ = 1.53-1.56 (m, 4 H), 1.74 (br, 4 H), 3.42 (s, 1 H), 4.27 (s, 1 H).

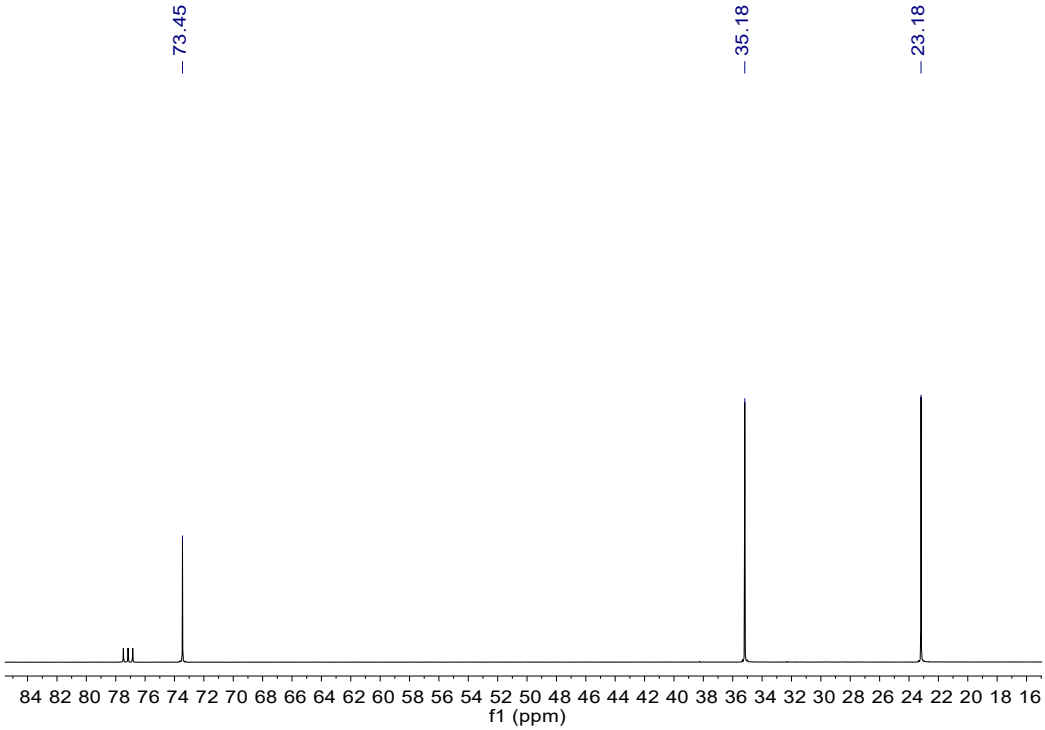

Fig. S55 ^{13}C{^{1}H} NMR spectrum of **b20**. ^{13}C{^{1}H} NMR (100 MHz, $CDCl_3$, 298 k, ppm): δ = 23.18, 35.18, 73.45.

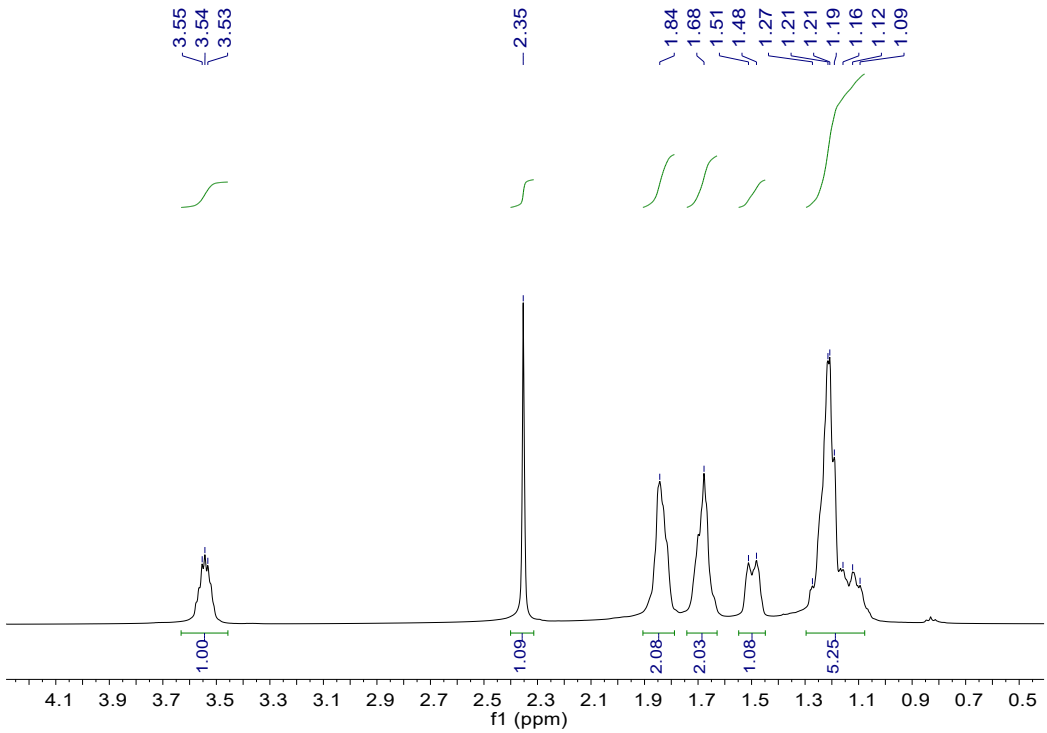

Fig. S56 ^{1}H NMR spectrum of **b21**.[7] ^{1}H NMR (400 MHz, $CDCl_3$, 298 k, ppm): δ = 1.09-1.27 (m, 5 H), 1.49 (d, J_{HH} = 12.0 Hz, 1 H), 1.68 (br, 2 H), 1.84 (br, 2 H), 2.35 (s, 1 H), 3.54 (t, J_{HH} = 1.0 Hz, 1 H).

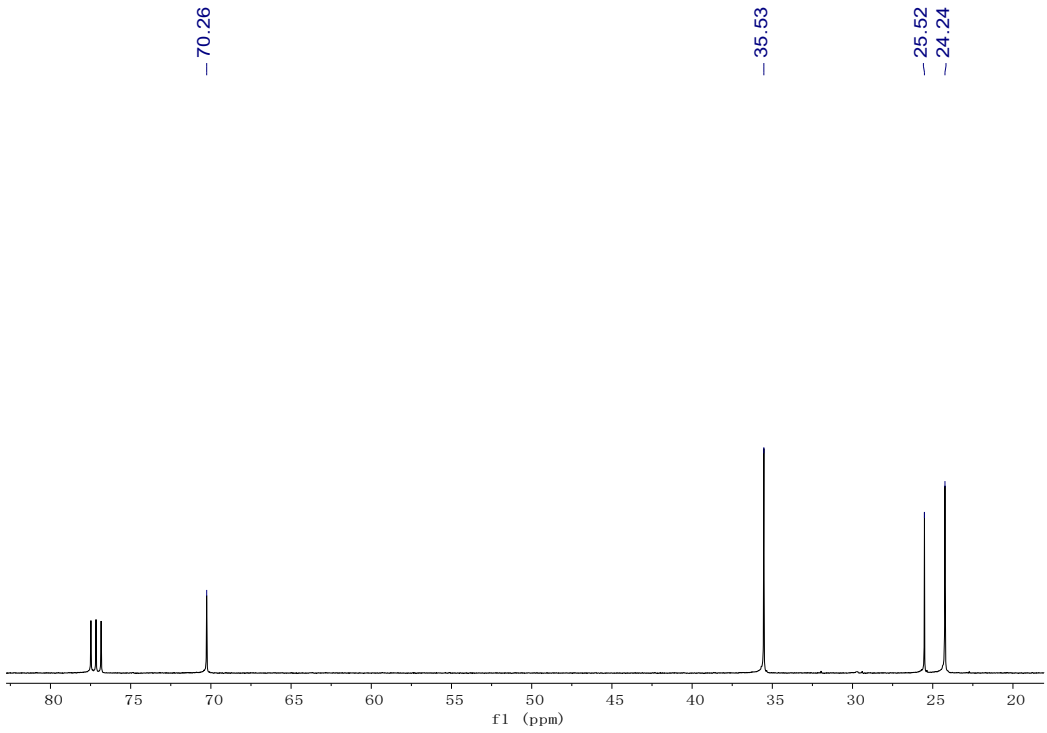

Fig. S57 ^{13}C{^{1}H} NMR spectrum of **b21**. ^{13}C{^{1}H} NMR (100 MHz, $CDCl_3$, 298 k, ppm): δ = 24.24, 25.52, 35.53, 70.26.

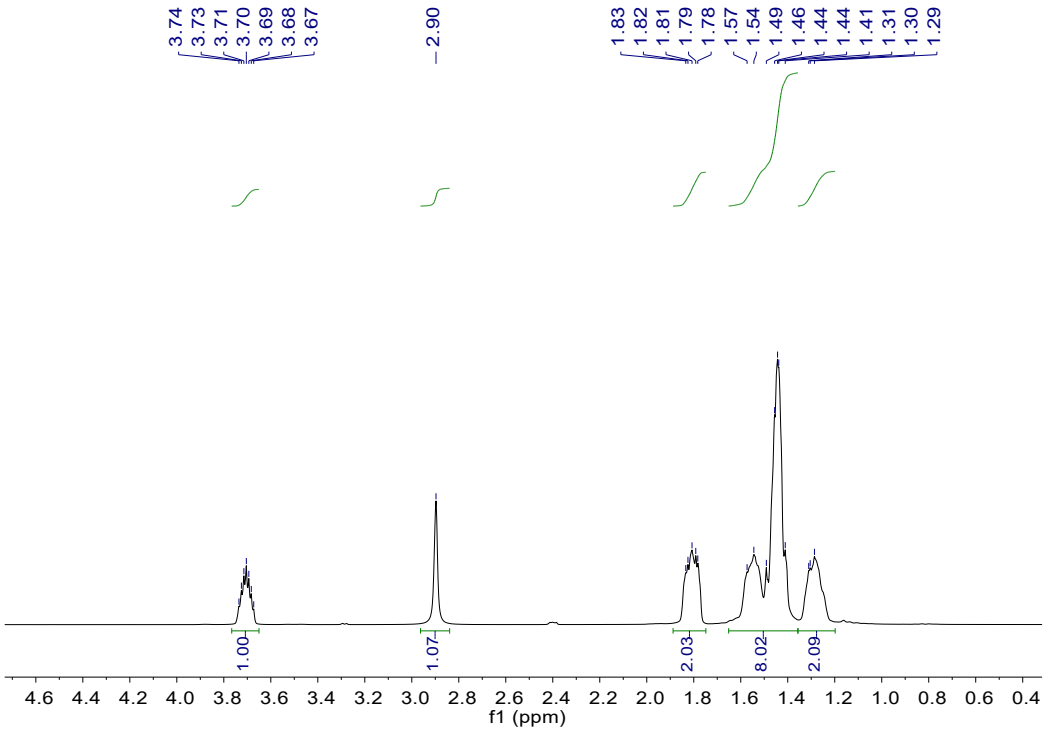

Fig. S58 ^{1}H NMR spectrum of **b22**.[6] ^{1}H NMR (400 MHz, $CDCl_3$, 298 k, ppm): δ = 1.29-1.31 (m, 2 H), 1.41-1.57 (m, 8 H), 1.78-1.83 (m, 2 H), 2.90 (s, 1 H), 3.67-3.74 (m, 1 H).

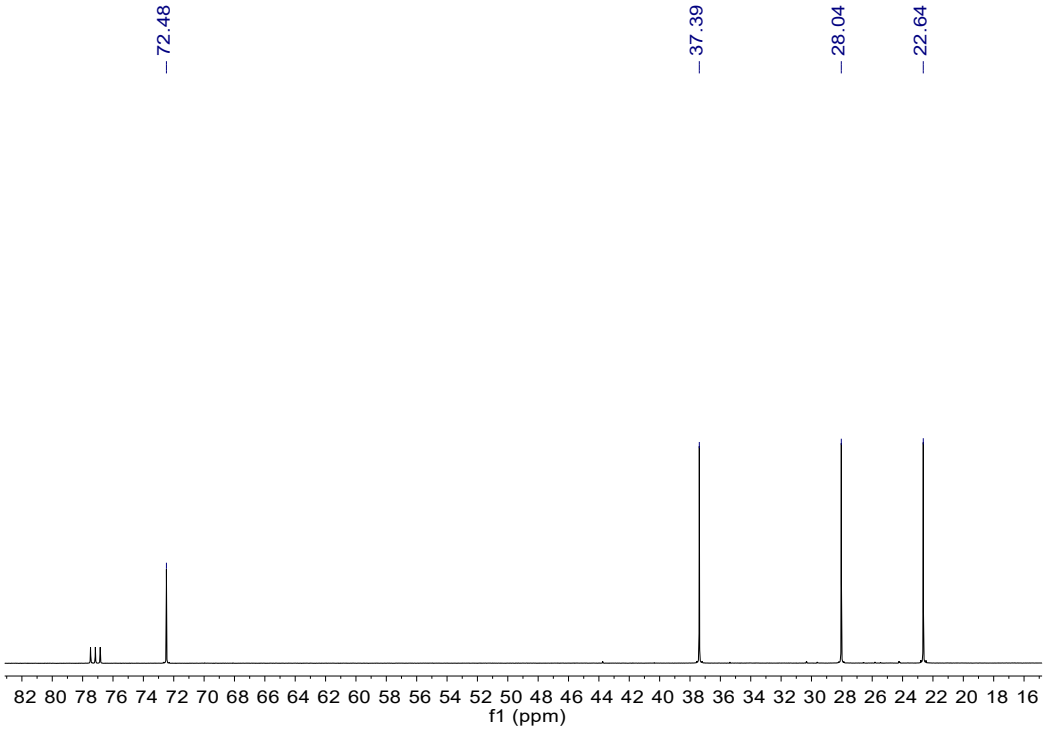

Fig. S59 $^{13}C\{^{1}H\}$ NMR spectrum of **b22**. $^{13}C\{^{1}H\}$ NMR (100 MHz, $CDCl_3$, 298 k, ppm): δ = 22.64, 28.04, 37.39, 72.48.

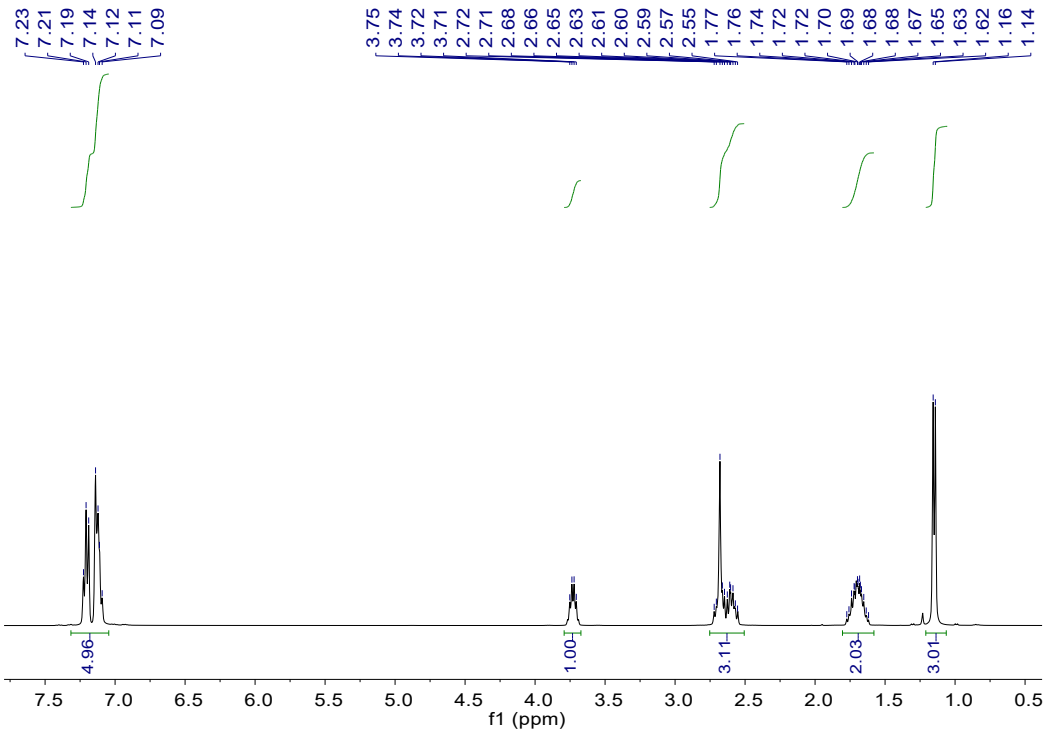

Fig. S60 ^{1}H NMR spectrum of **b23**.[6] ^{1}H NMR (400 MHz, $CDCl_3$, 298 k, ppm): δ = 1.15 (d, J_{HH} = 6.0 Hz, 3 H), 1.62-1.77 (m, 2 H), 2.55-2.72 (m, 3 H), 3.73 (q, J_{HH} = 6.0, 6.4 Hz, 1 H), 7.09-7.23 (m, 5 H).

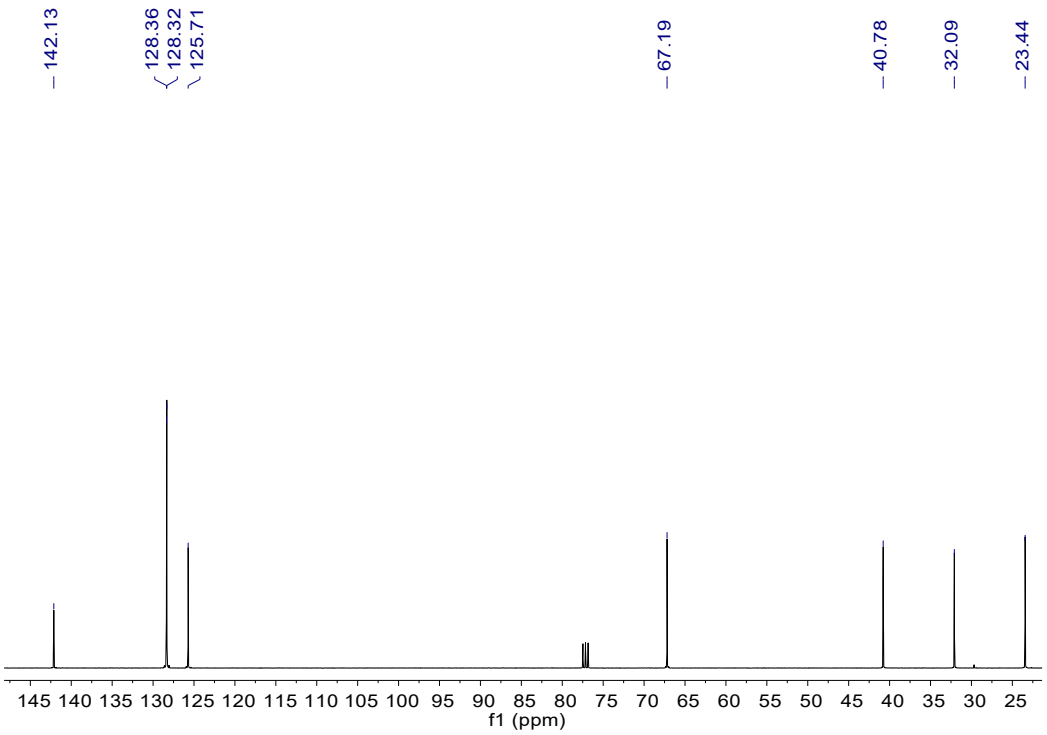

Fig. S61 ^{13}C{^{1}H} NMR spectrum of **b23**. ^{13}C{^{1}H} NMR (100 MHz, $CDCl_3$, 298 k, ppm): δ = 23.44, 32.09, 40.78, 67.19, 125.71, 128.32, 128.36, 142.13.

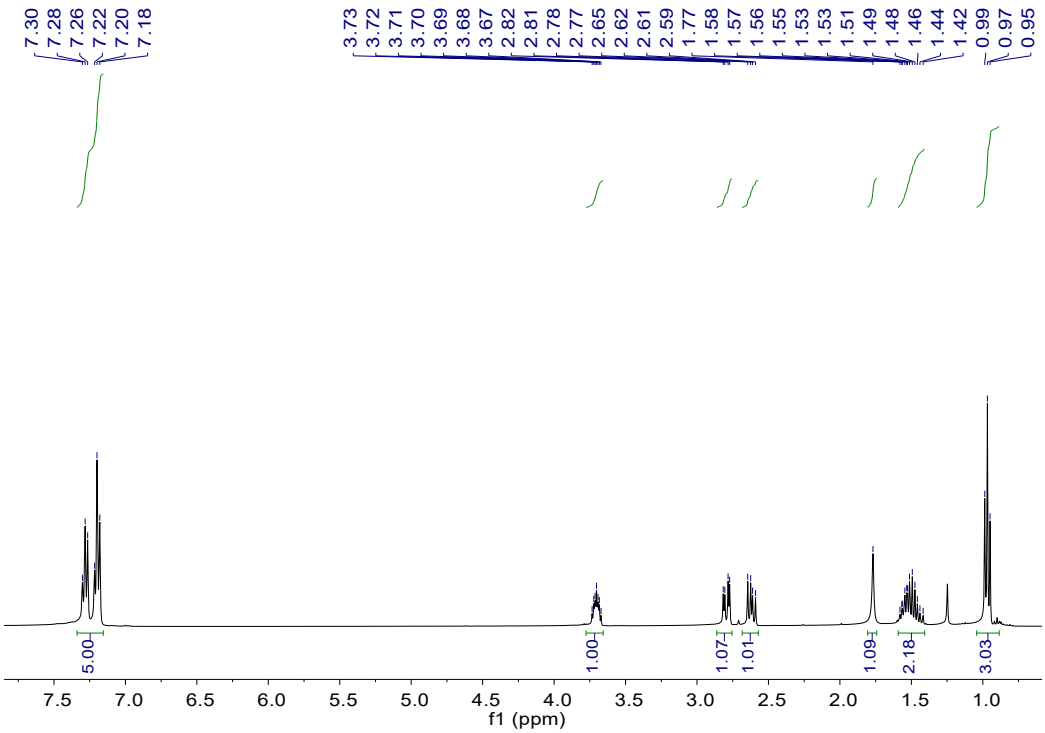

Fig. S62 ^{1}H NMR spectrum of **b24**.[10] ^{1}H NMR (400 MHz, $CDCl_3$, 298 k, ppm): δ = 0.97 (t, J_{HH} = 7.2 Hz, 3 H), 1.42-1.58 (m, 2 H), 1.77 (s, 1 H), 2.61 (dd, J_{HH} = 8.4, 5.2 Hz, 1 H), 2.79 (dd, J_{HH} = 4.4, 9.2 Hz, 1 H), 3.67-3.73 (m, 1 H), 7.18-7.30 (m, 5 H).

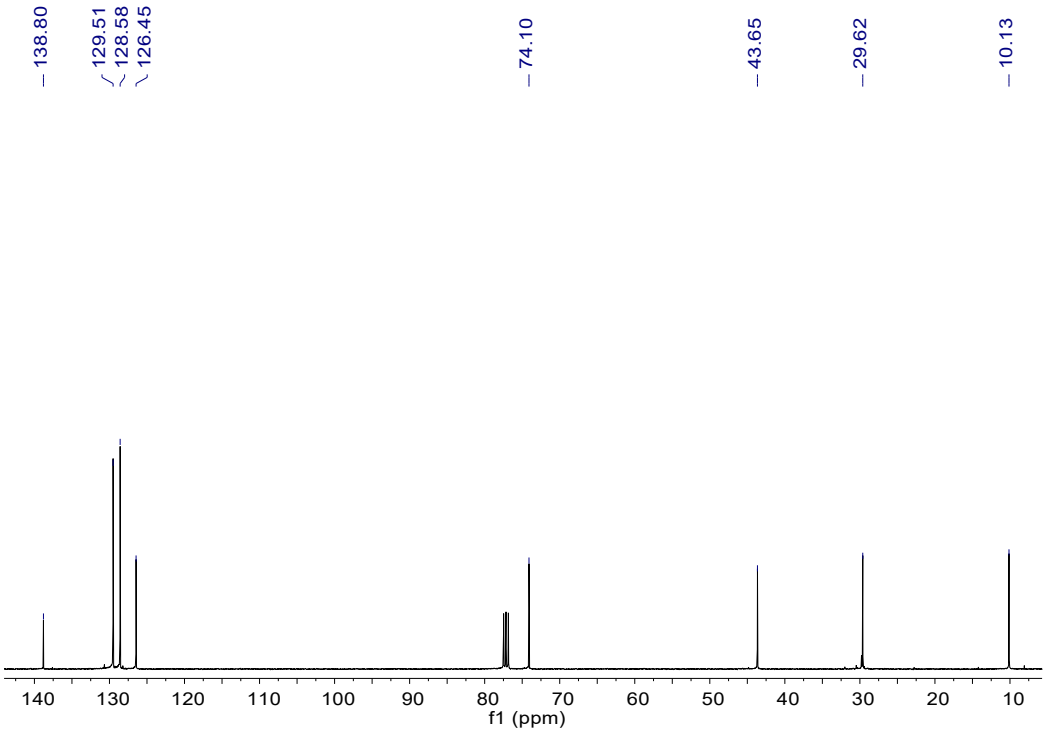

Fig. S63 ^{13}C{^{1}H} NMR spectrum of **b24**. ^{13}C{^{1}H} NMR (100 MHz, $CDCl_3$, 298 k, ppm): δ = 10.13, 29.62, 43.65, 74.10, 126.45, 128.58, 129.51, 138.80.

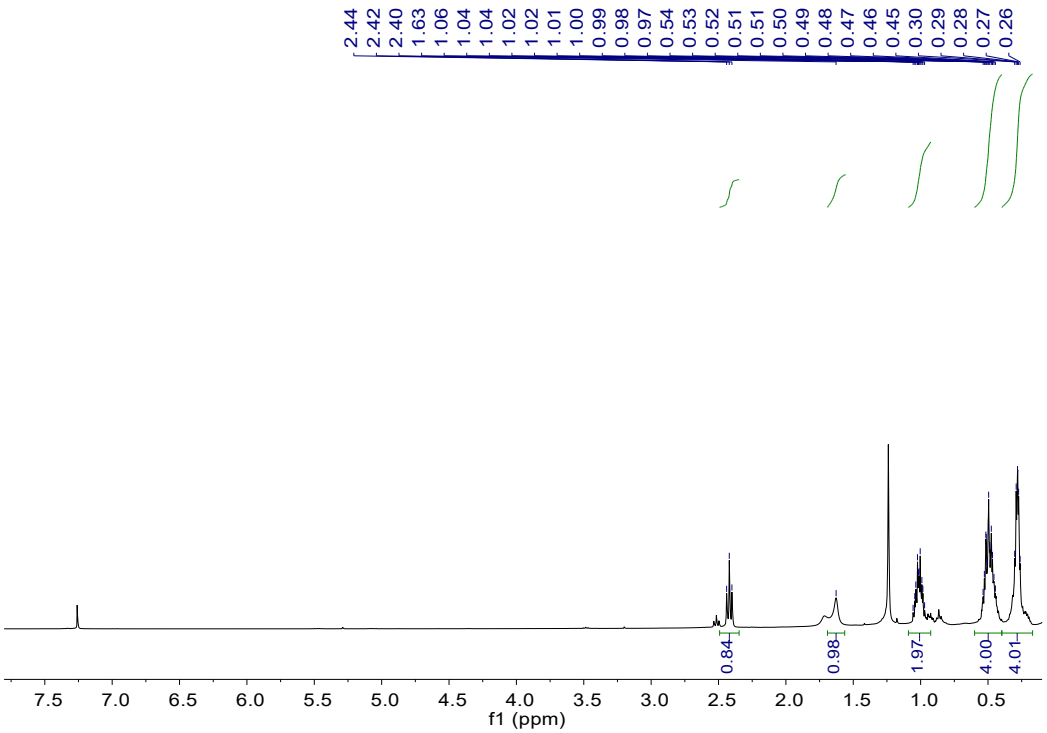

Fig. S64 ^{1}H NMR spectrum of **b25**.[11] ^{1}H NMR (400 MHz, $CDCl_3$, 298 k, ppm): δ = 0.26-0.30 (m, 4 H), 0.45-0.54 (m, 4 H), 0.97-1.06 (m, 2 H), 1.63 (br, 1 H), 2.42 (t, J_{HH} = 8.0 Hz, 1 H).

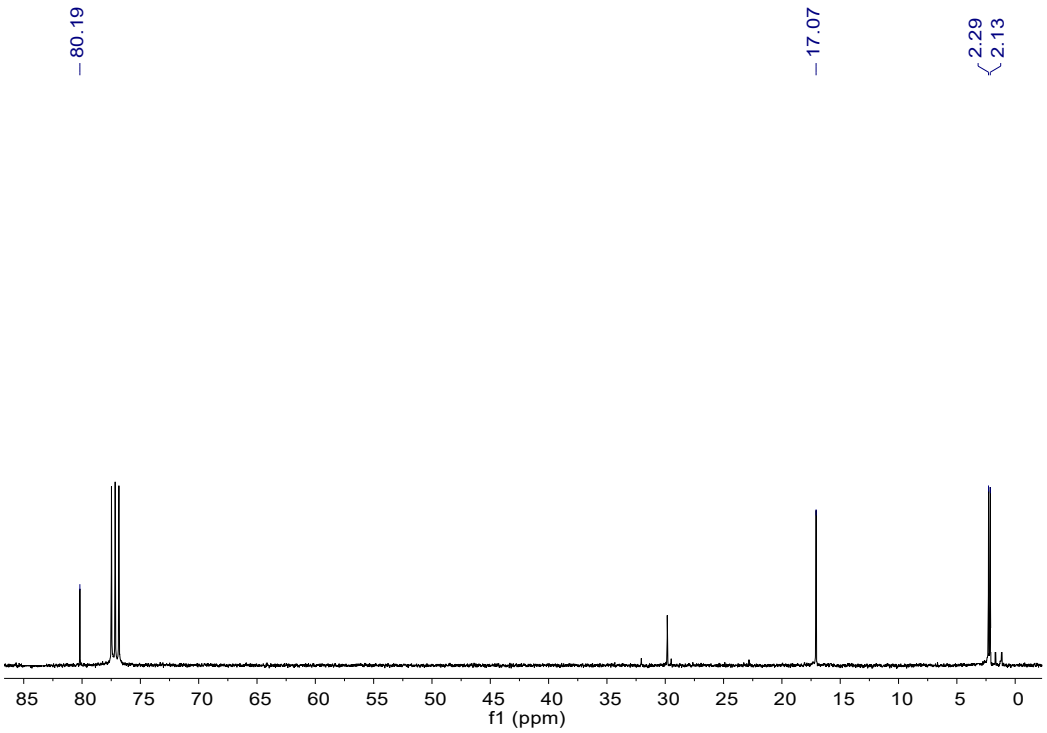

Fig. S65 ^{13}C{^{1}H} NMR spectrum of **b25**. ^{13}C{^{1}H} NMR (100 MHz, $CDCl_3$, 298 k, ppm): δ = 2.13, 2.29, 17.07, 80.19.

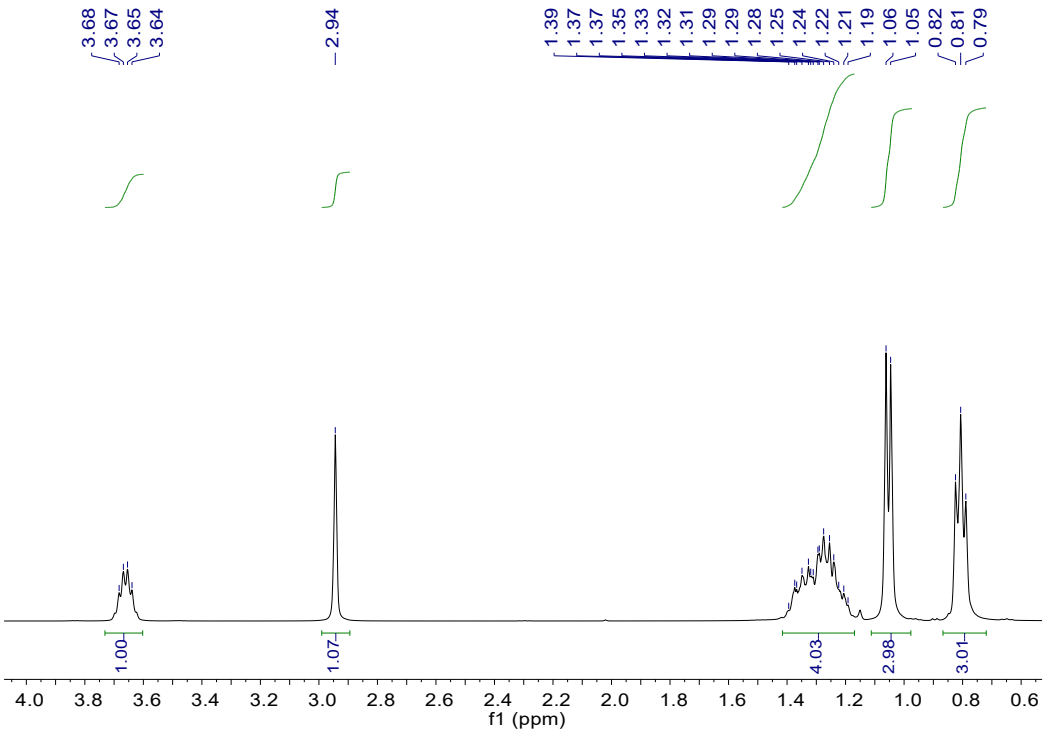

Fig. S66 ^{1}H NMR spectrum of **b26**.[12] ^{1}H NMR (400 MHz, $CDCl_3$, 298 k, ppm): δ = 0.81 (t, J_{HH} = 6.8 Hz, 1 H), 1.05 (d, J_{HH} = 6.4 Hz, 1 H), 1.19-1.39 (m, 4 H), 2.94 (s, 1 H), 3.66 (q, J_{HH} = 6.0, 5.6 Hz, 1 H).

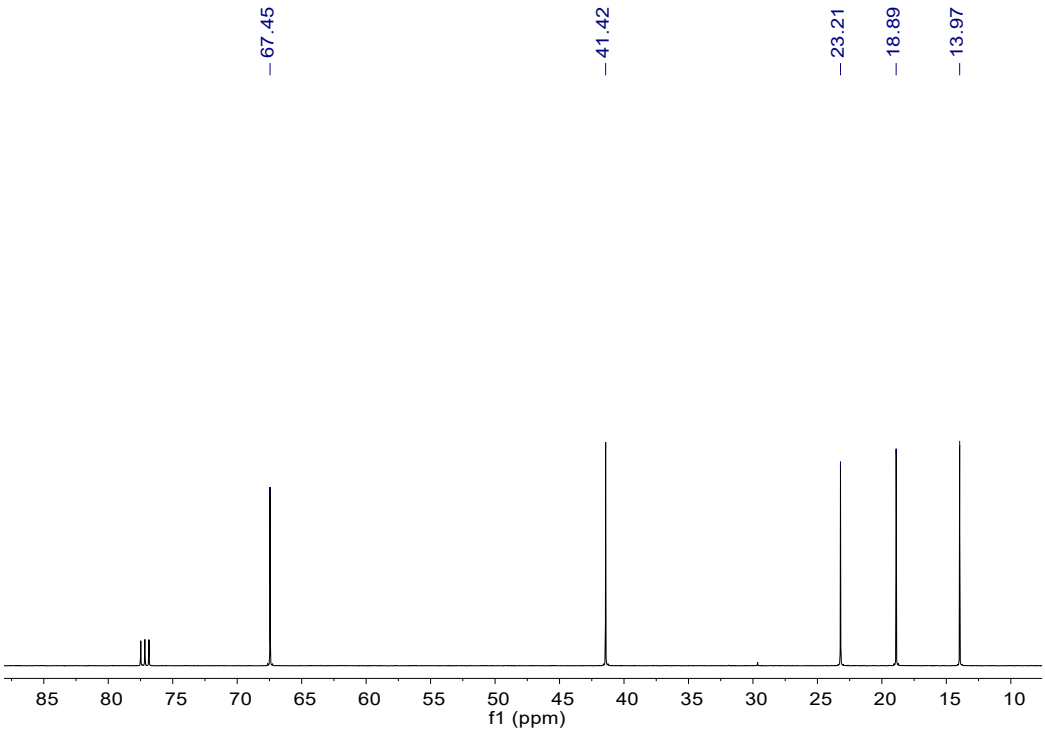

Fig. S67 ^{13}C{^{1}H} NMR spectrum of **b26**. ^{13}C{^{1}H} NMR (100 MHz, $CDCl_3$, 298 k, ppm): δ = 13.97, 18.89, 23.21, 41.42, 67.45.

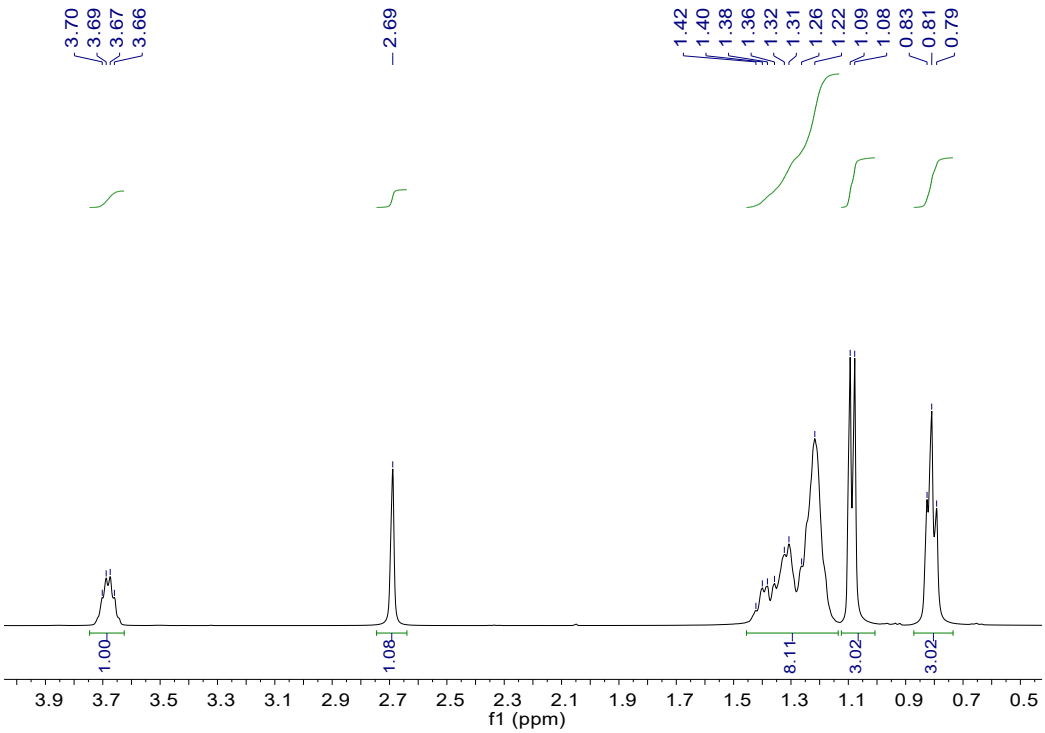

Fig. S68 ^{1}H NMR spectrum of **b27**.[9] ^{1}H NMR (400 MHz, $CDCl_3$, 298 k, ppm): δ = 0.81 (t, J_{HH} = 6.8 Hz, 3 H), 1.08 (d, J_{HH} = 6.0 Hz, 3 H), 1.22-1.42 (m, 8 H), 2.69 (s, 1 H), 3.68 (q, J_{HH} = 5.6, 5.6 Hz, 1 H).

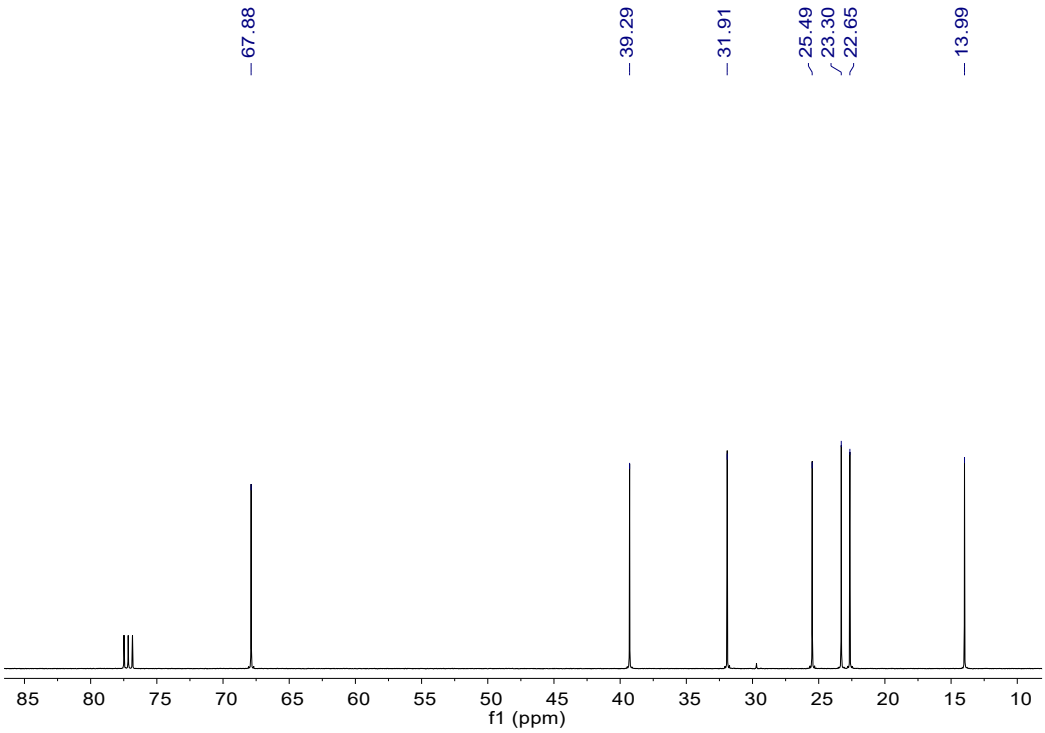

Fig. S69 ^{13}C{^{1}H} NMR spectrum of **b27**. ^{13}C{^{1}H} NMR (100 MHz, $CDCl_3$, 298 k, ppm): δ = 13.99, 22.65, 23.30, 25.49, 31.91, 39.29, 67.88.

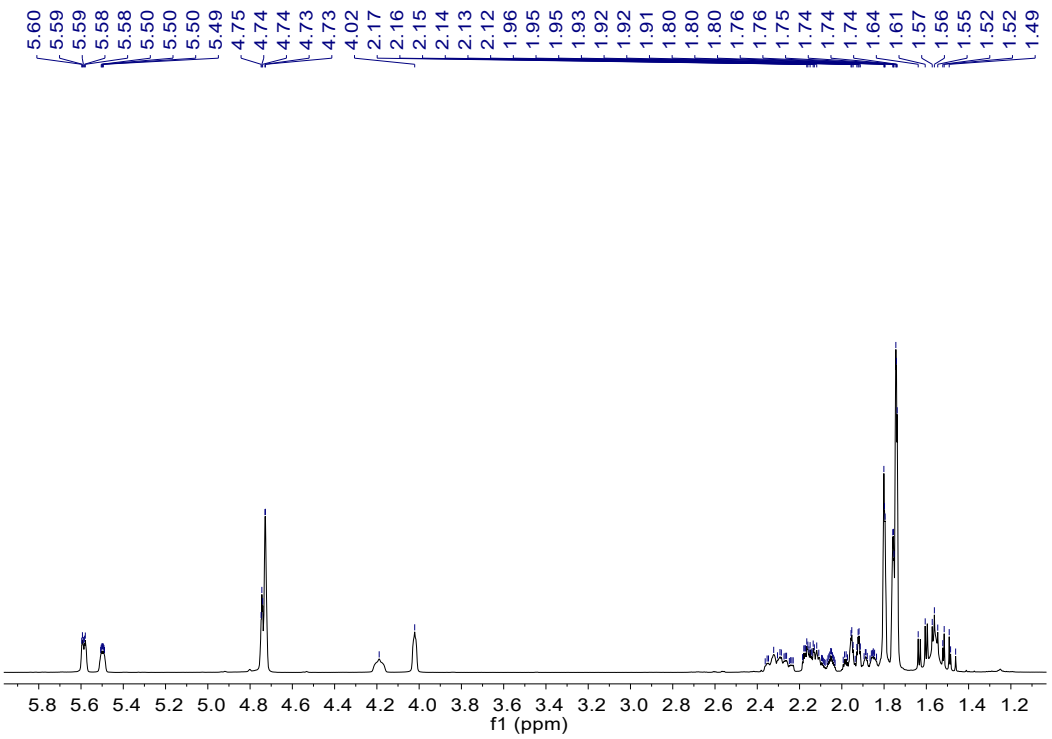

Fig. S70 ^{1}H NMR spectrum of **b28** (racemic mixture).[13] ^{1}H NMR (400 MHz, $CDCl_3$, 298 k, ppm): δ = 1.46-1.64 (m), 1.74-1.80 (m), 1.84-1.99(m), 2.03-2.19 (m), 2.23-2.36 (m), 4.02 (s), 4.19 (br), 4.73-4.75 (m), 5.49-5.51 (m), 5.58-5.60 (m).

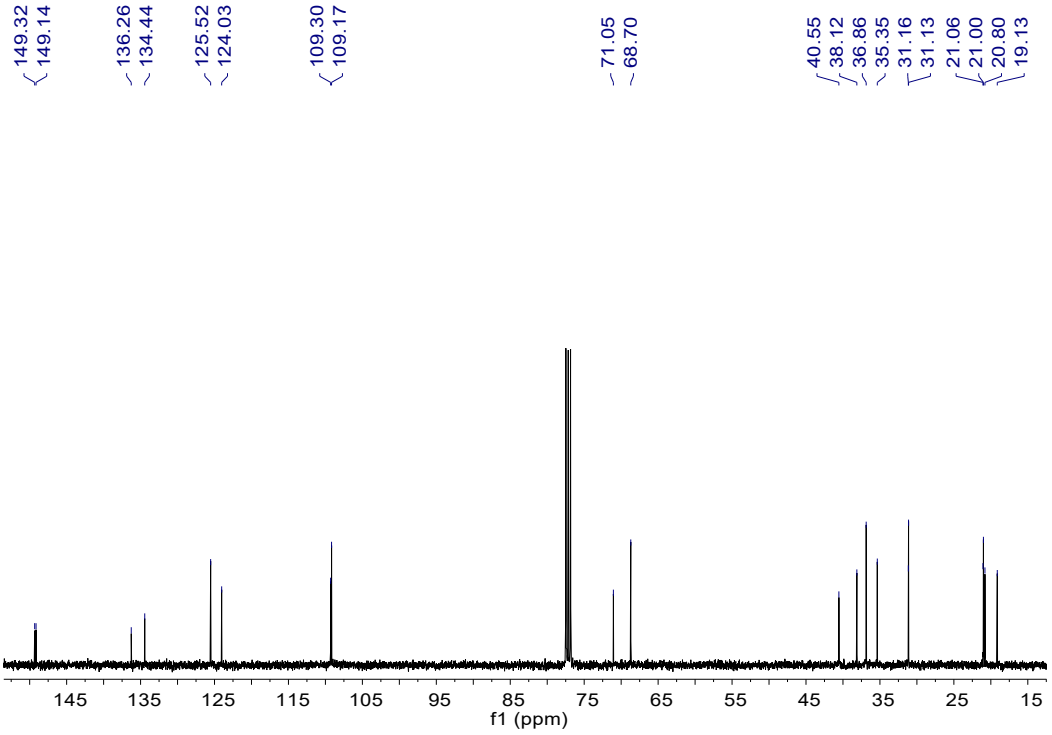

Fig. S71 ^{13}C{^{1}H} NMR spectrum of **b28**. ^{13}C{^{1}H} NMR (100 MHz, $CDCl_3$, 298 k, ppm): δ = 19.13, 20.80, 21.00, 21.06, 31.13, 31.16, 35.35, 36.86, 38.12, 40.55, 68.70, 71.05, 109.17, 109.30, 124.03, 125.52, 134.44, 136.26, 149.14, 149.32.

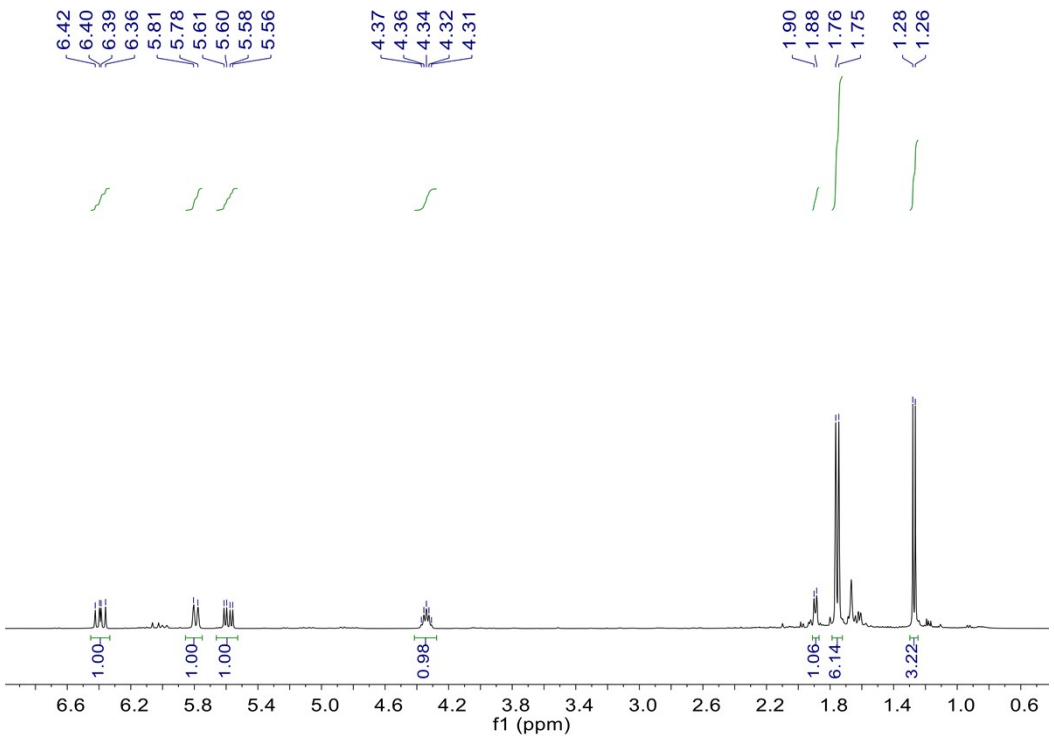

Fig. S72 ^{1}H NMR spectrum of **b29**.[14] ^{1}H NMR (400 MHz, $CDCl_3$, 298 k, ppm): δ = 1.27 (d, J_{HH} = 6.4 Hz, 3 H), 1.75 (d, J_{HH} = 7.6 Hz, 6 H), 1.89 (d, J_{HH} = 6.8 Hz, 1 H), 4.31-4.37 (m, 1 H), 5.59 (dd, J_{HH} = 6.8, 8.4 Hz, 1 H), 5.80 (d, J_{HH} = 11.2 Hz, 1 H), 5.59 (dd, J_{HH} = 11.2, 4.0 Hz, 1 H).

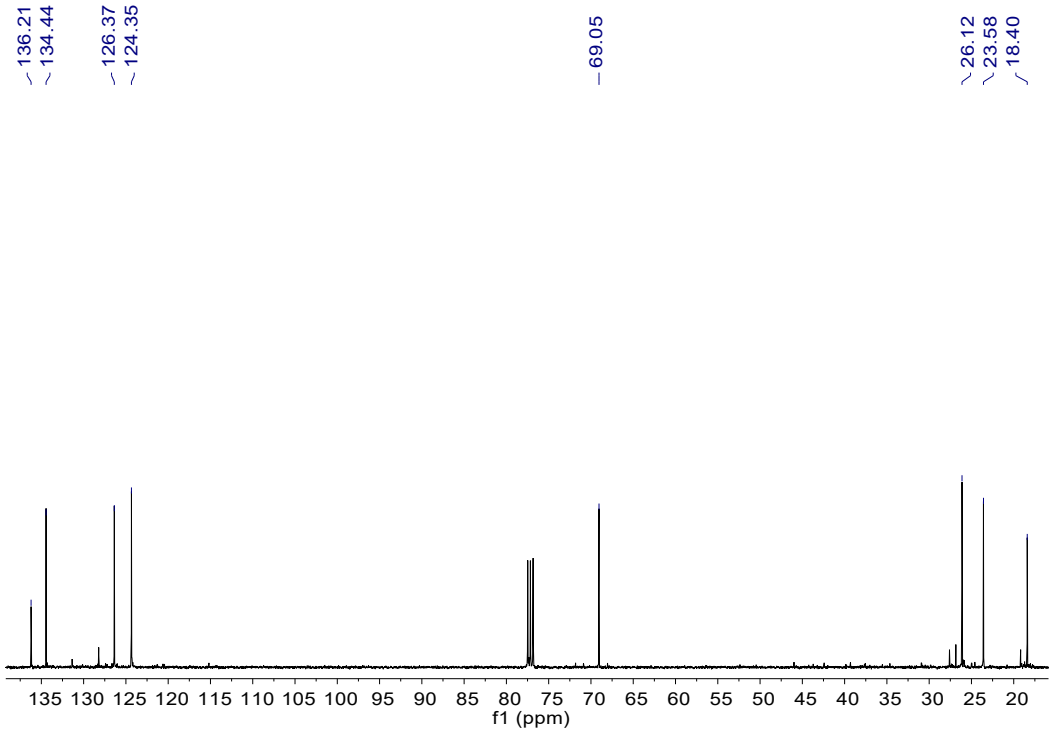

Fig. S73 ^{13}C{^{1}H} NMR spectrum of **b29**. ^{13}C{^{1}H} NMR (100 MHz, $CDCl_3$, 298 k, ppm): δ = 18.40, 23.58, 26.12, 69.05, 124.35, 126.37, 134.44, 136.21.

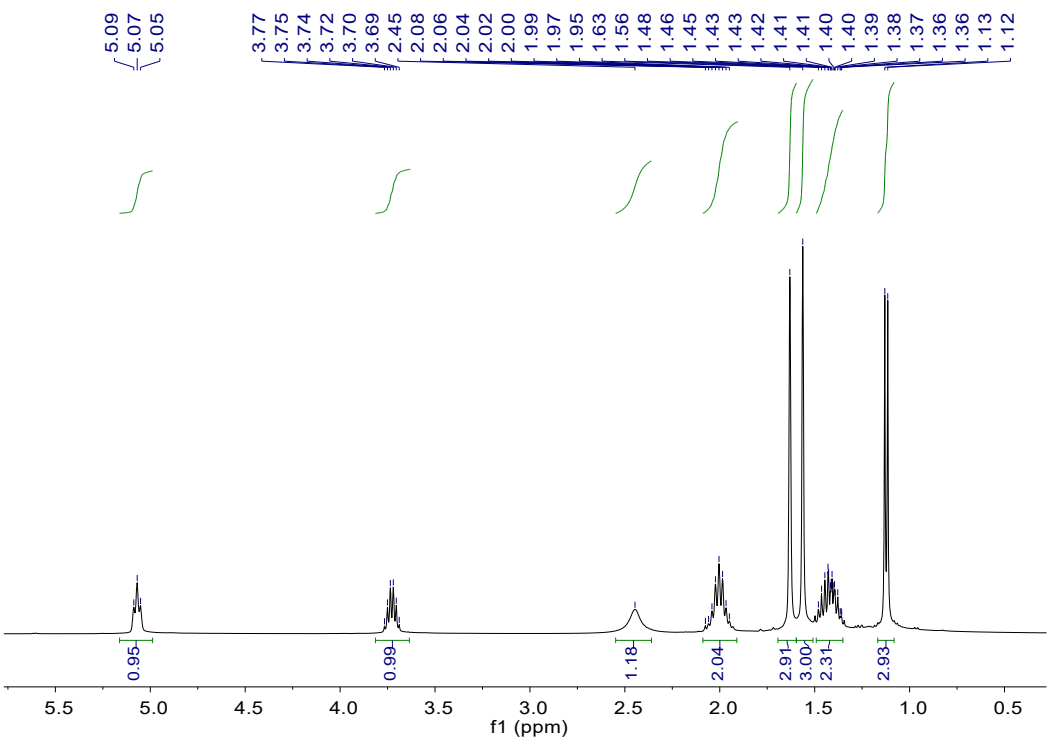

Fig. S74 ^{1}H NMR spectrum of **b30**.[15] ^{1}H NMR (400 MHz, $CDCl_3$, 298 k, ppm): δ = 1.12 (d, J_{HH} = 6.4 Hz, 3 H), 1.36-1.48 (m, 2 H), 1.56 (s, 3 H), 1.63 (s, 3 H), 1.95-2.08 (m, 2 H), 2.45 (br, 1 H), 3.69-3.77 (m, 1 H), 5.07 (t, J_{HH} = 7.2 Hz, 1 H).

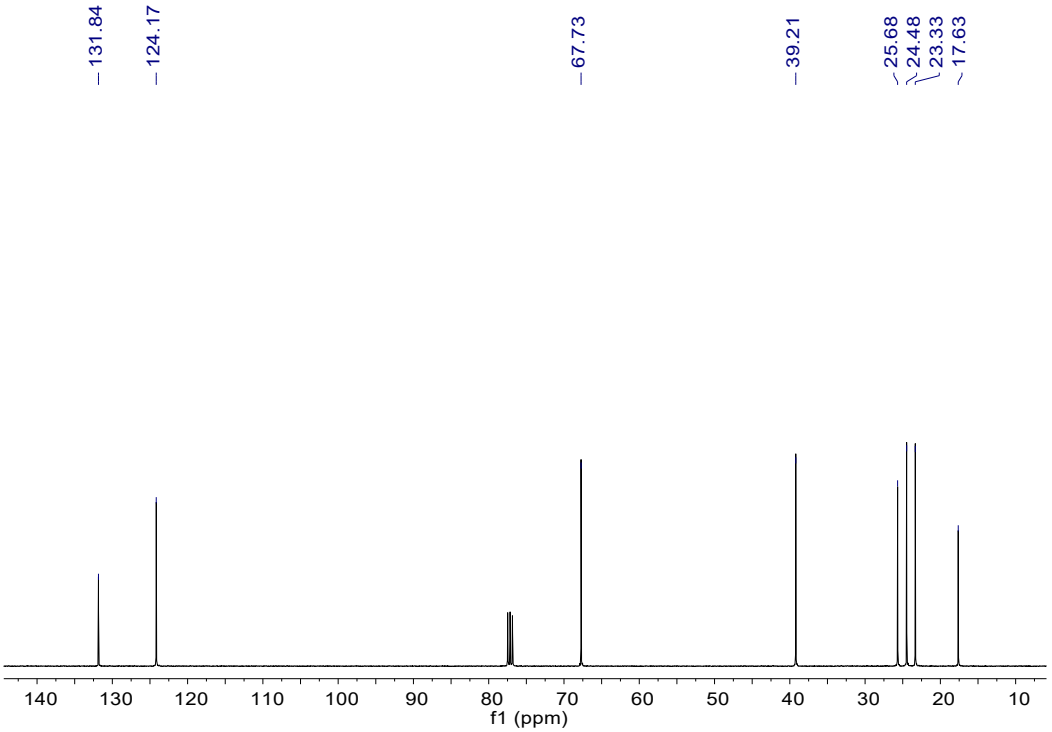

Fig. S75 ^{13}C{^{1}H} NMR spectrum of **b30**. ^{13}C{^{1}H} NMR (100 MHz, $CDCl_3$, 298 k, ppm): δ = 17.63, 23.33, 24.48, 25.68, 39.21, 67.73, 124.17, 131.84.

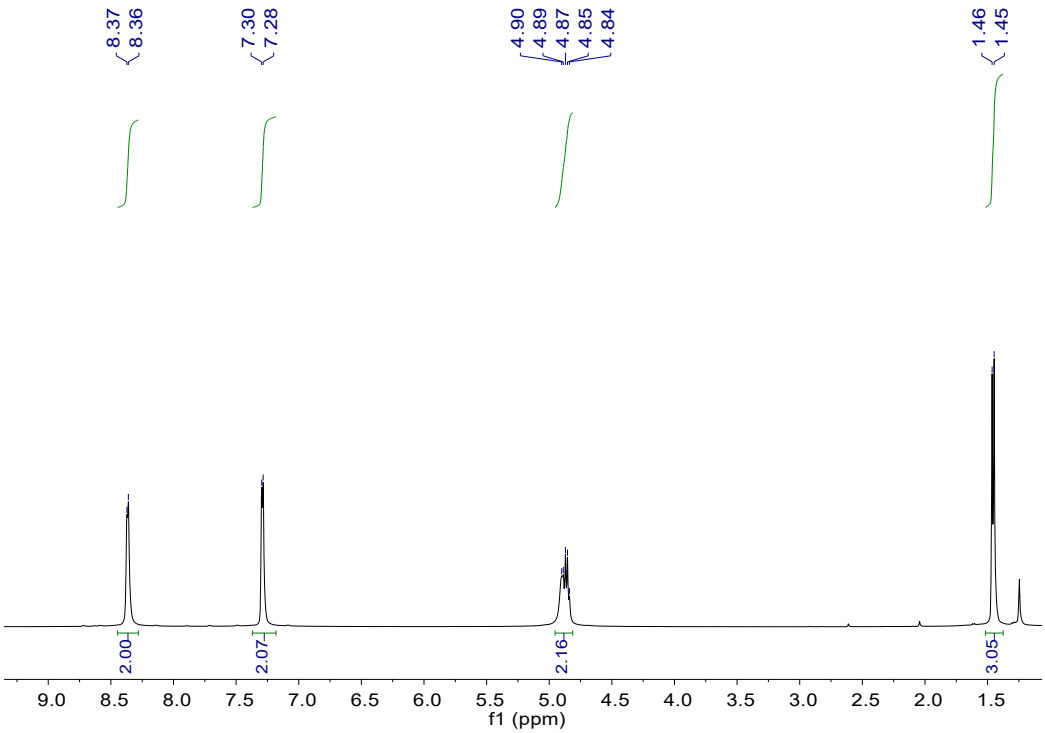

Fig. S76 ^{1}H NMR spectrum of **b31**.[16] ^{1}H NMR (400 MHz, $CDCl_3$, 298 k, ppm): δ = 1.45 (d, J_{HH} = 6.8 Hz, 3 H), 4.84-4.90 (m, 2 H), 7.29 (d, J_{HH} = 4.8 Hz, 2 H), 8.36 (d, J_{HH} = 4.4 Hz, 2 H).

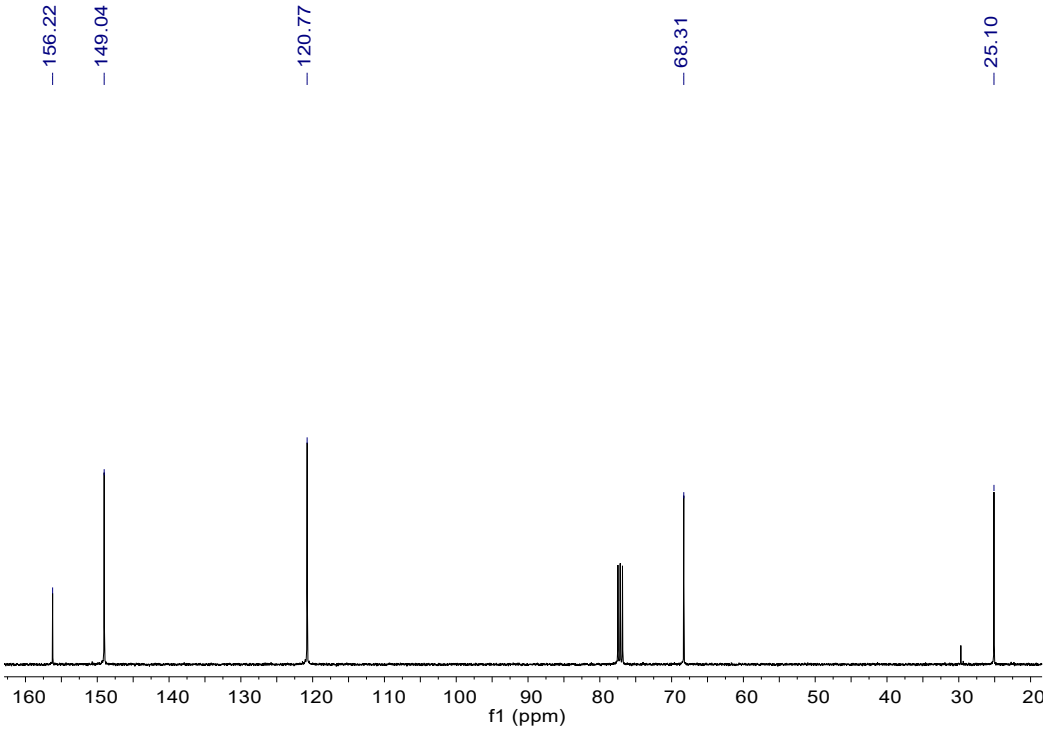

Fig. S77 ^{13}C{^{1}H} NMR spectrum of **b31**. ^{13}C{^{1}H} NMR (100 MHz, $CDCl_3$, 298 k, ppm): δ = 25.10, 68.31, 120.77, 149.04, 156.22.

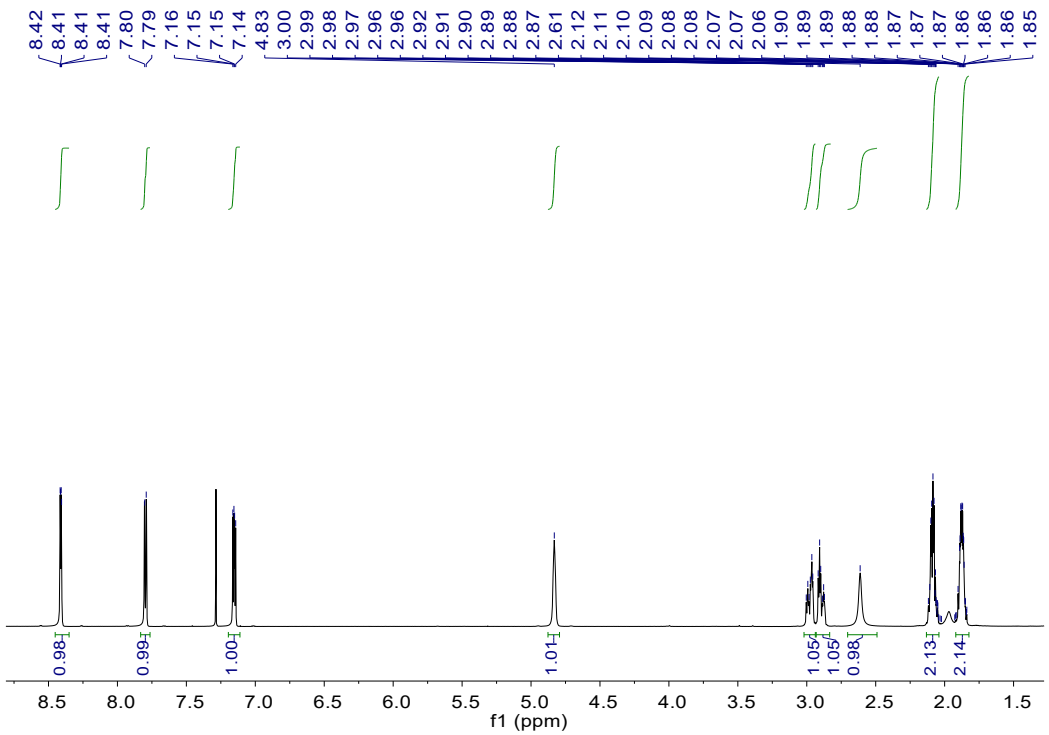

Fig. S78 ^{1}H NMR spectrum of **b32**.[8] ^{1}H NMR (400 MHz, $CDCl_3$, 298 k, ppm): δ = 1.84-1.93 (m, 2 H), 2.02-2.12 (m, 2 H), 2.61 (s, 1 H), 2.87-2.92 (m, 1 H), 2.96-3.00 (m, 1 H), 4.83 (s, 1 H), 7.15 (dd, J_{HH} = 3.2, 2.0 Hz, 1 H), 7.79 (d, J_{HH} = 5.2 Hz, 1 H), 8.41 (dd, J_{HH} = 1.2, 2.0 Hz, 1 H).

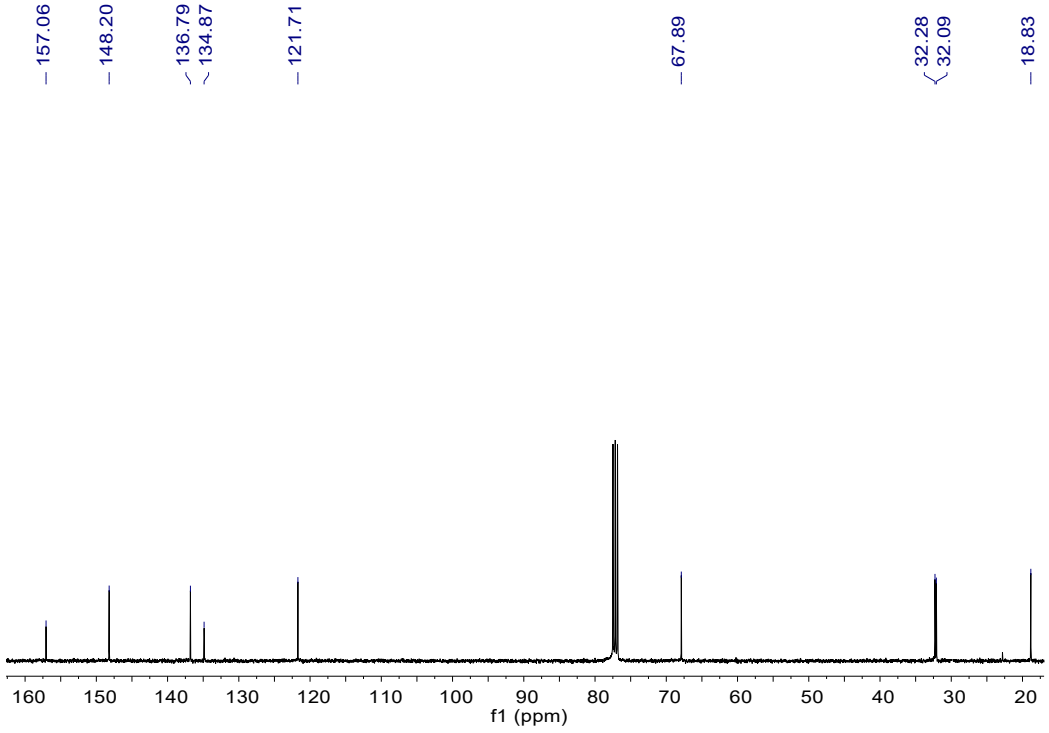

Fig. S79 ^{13}C{^{1}H} NMR spectrum of **b32**. ^{13}C{^{1}H} NMR (100 MHz, $CDCl_3$, 298 k, ppm): δ = 18.83, 32.09, 32.28, 67.89, 121.71, 134.87, 136.79, 148.20, 157.06.

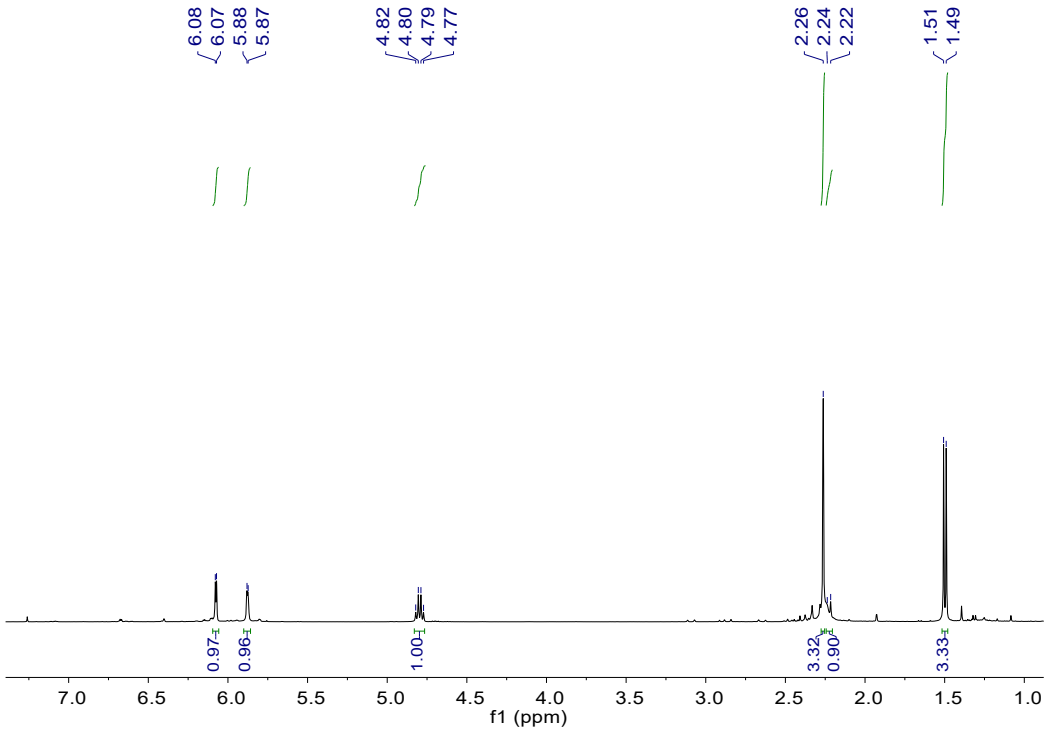

Fig. S80 ^{1}H NMR spectrum of **b33**.[6] ^{1}H NMR (400 MHz, $CDCl_3$, 298 k, ppm): δ = 1.50 (d, J_{HH} = 6.8 Hz, 3 H), 2.23 (d, J_{HH} = 8.8 Hz, 1 H), 2.26 (s, 3 H), 4.79 (d, J_{HH} = 6.4, 13.2 Hz, 1 H), 5.87 (d, J_{HH} = 2.8 Hz, 1 H), 6.07 (d, J_{HH} = 2.8 Hz, 1 H).

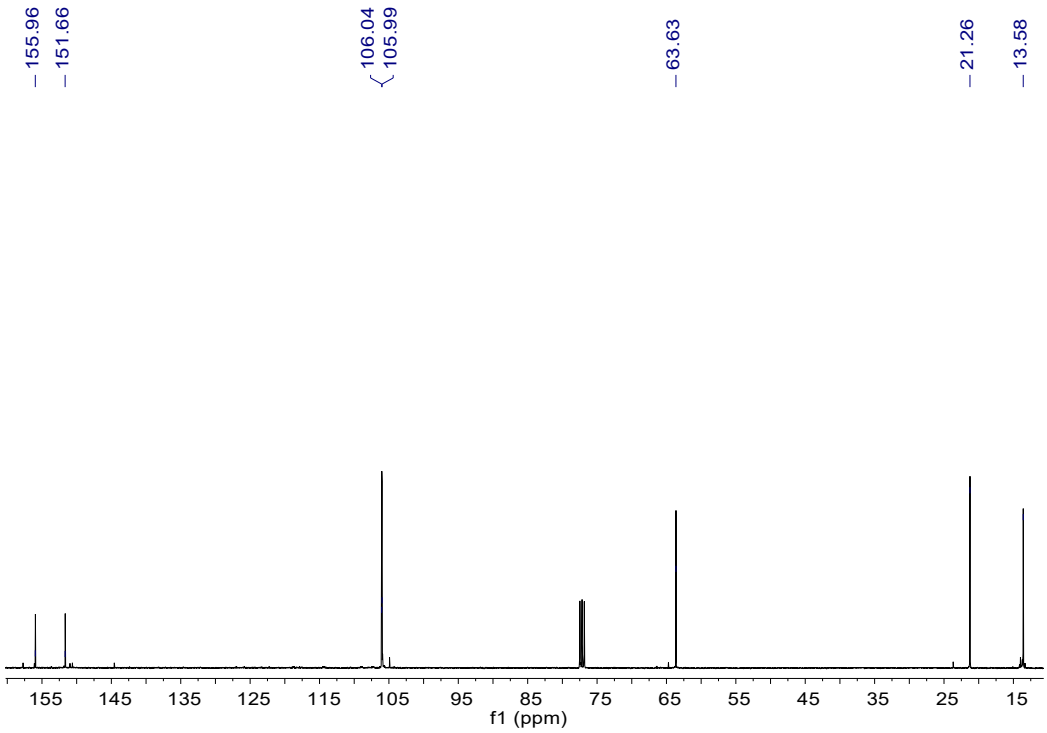

Fig. S81 ^{13}C{^{1}H} NMR spectrum of **b33**. ^{13}C{^{1}H} NMR (100 MHz, $CDCl_3$, 298 k, ppm): δ = 13.58, 21.26, 63.63, 105.99, 106.04, 151.66, 155.96.

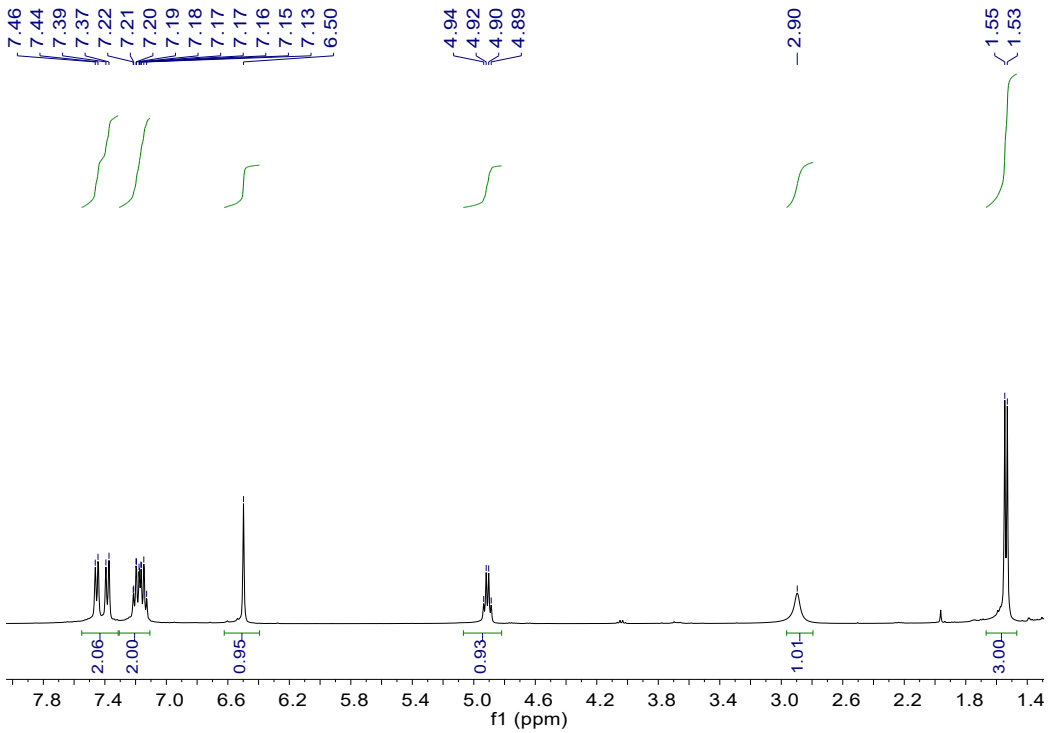

Fig. S82 ^{1}H NMR spectrum of **b34**.[6] ^{1}H NMR (400 MHz, $CDCl_3$, 298 k, ppm): δ = 1.54 (d, J_{HH} = 6.4 Hz, 3 H), 2.90 (br, 1 H), 4.91 (q, J_{HH} = 6.4, 6.8 Hz, 1 H), 6.50 (s, 1 H), 7.13-7.22 (m, 2 H), 7.42 (dd, J_{HH} = 6.8, 20.8 Hz, 2 H).

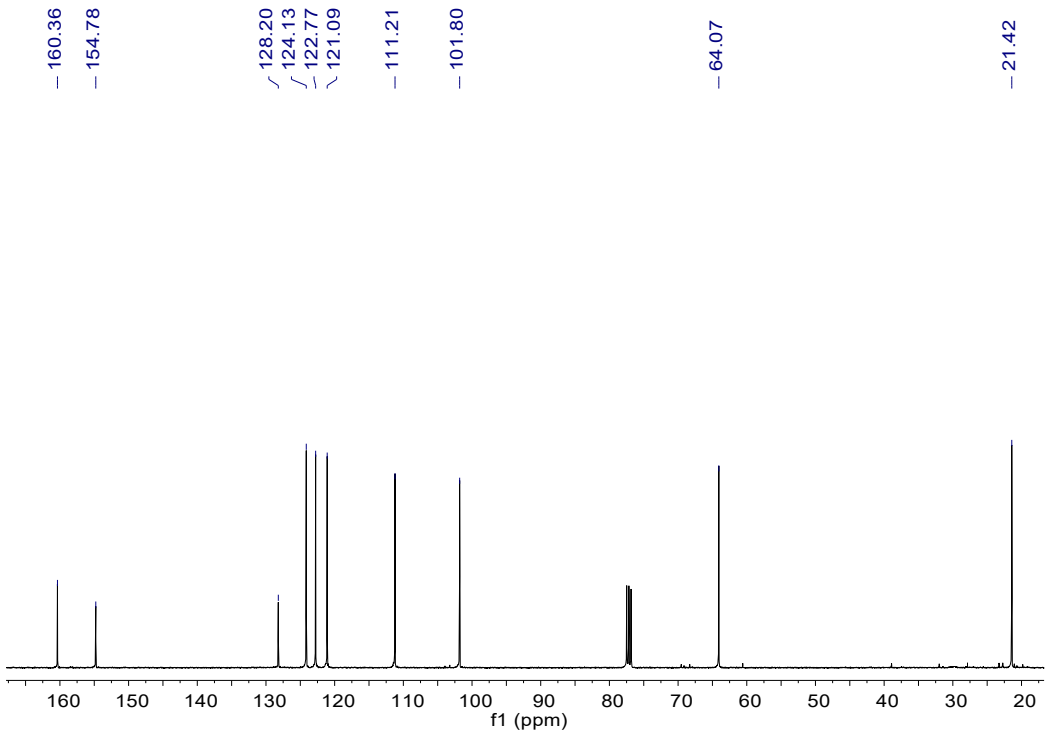

Fig. S83 ^{13}C{^{1}H} NMR spectrum of **b34**. ^{13}C{^{1}H} NMR (100 MHz, $CDCl_3$, 298 k, ppm): δ = 21.42, 64.07, 101.80, 111.21, 121.09, 122.77, 124.13, 128.20, 154.78, 160.36.

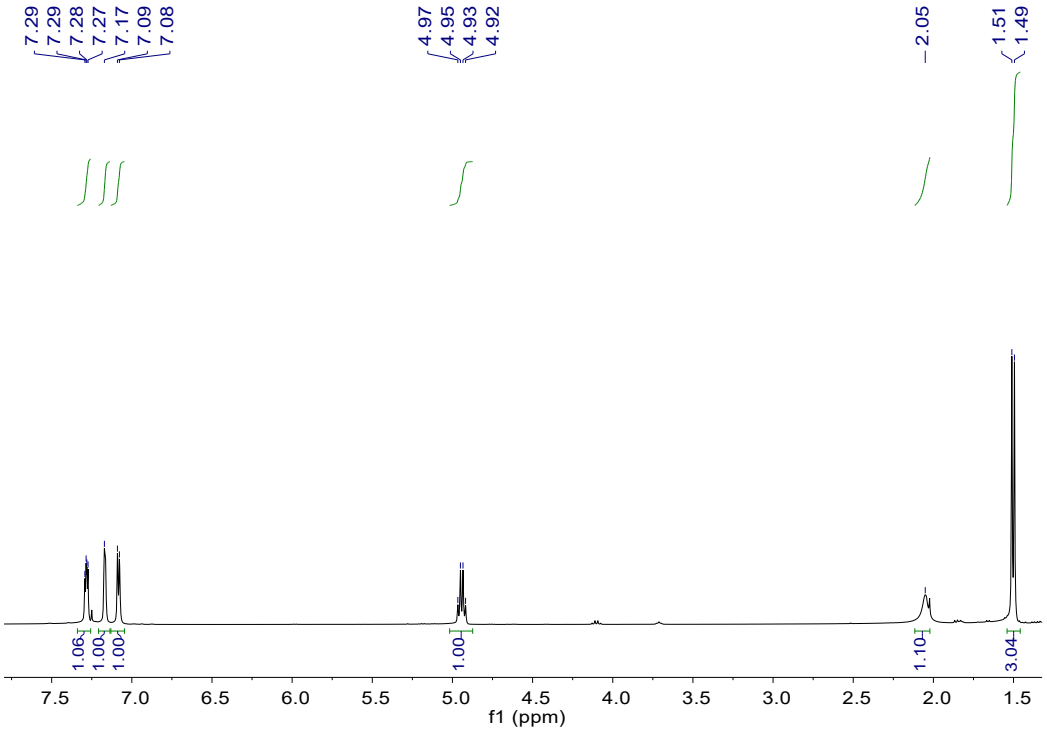

Fig. S84 ^{1}H NMR spectrum of **b35**.[8] ^{1}H NMR (400 MHz, $CDCl_3$, 298 k, ppm): δ = 1.50 (d, J_{HH} = 6.4 Hz, 3 H), 2.05 (br, 1 H), 4.94 (q, J_{HH} = 6.4, 6.4 Hz, 1 H), 7.08 (d, J_{HH} = 5.2 Hz, 1 H), 7.17 (br, 1 H), 7.28 (dd, J_{HH} = 3.2, 2.0 Hz, 1 H).

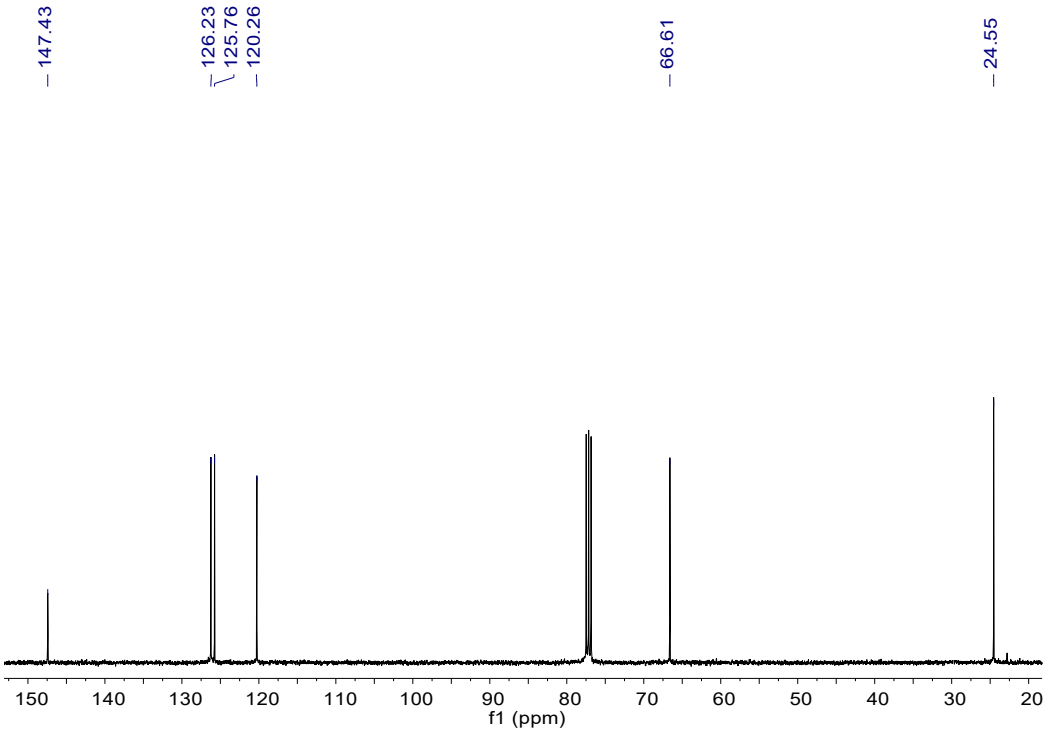

Fig. S85 ^{13}C{^{1}H} NMR spectrum of **b35**. ^{13}C{^{1}H} NMR (100 MHz, $CDCl_3$, 298 k, ppm): δ = 24.55, 66.61, 120.26, 125.76, 126.23, 147.43.

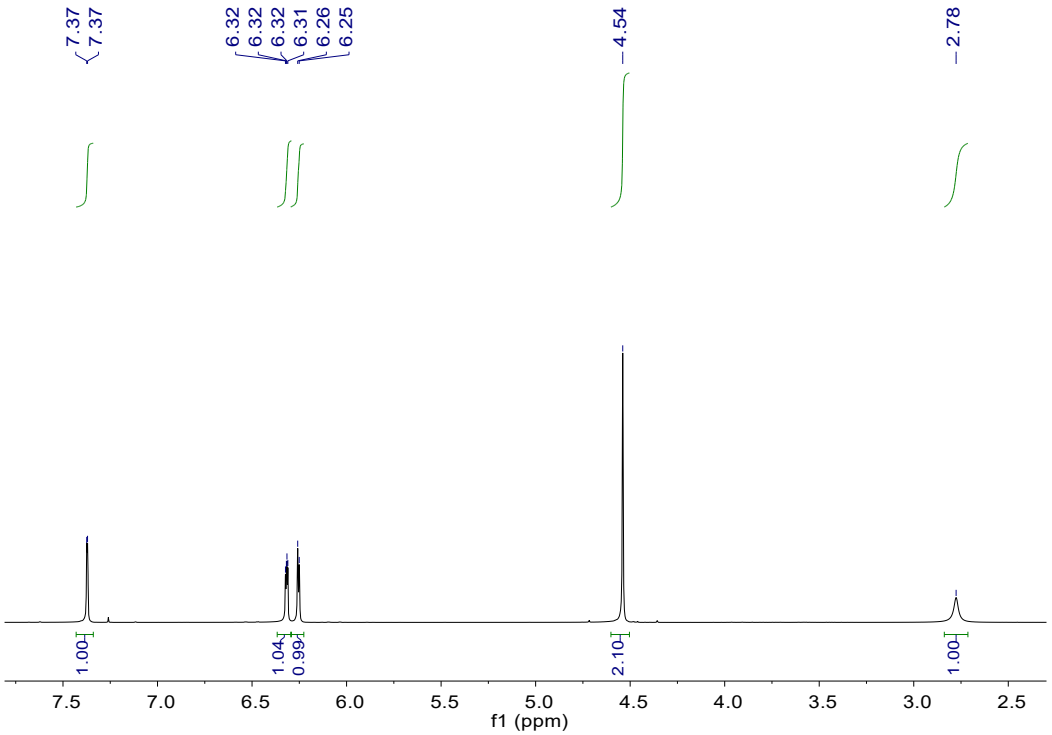

Fig. S86 ^{1}H NMR spectrum of **b36**.[17] ^{1}H NMR (400 MHz, $CDCl_3$, 298 k, ppm): δ = 2.78 (br, 1 H), 4.54 (s, 2 H), 6.25 (d, J_{HH} = 2.8 Hz, 1 H), 6.32 (dd, J_{HH} = 2.0, 3.2 Hz, 1 H), 7.37 (d, J_{HH} = 1.6 Hz, 1 H).

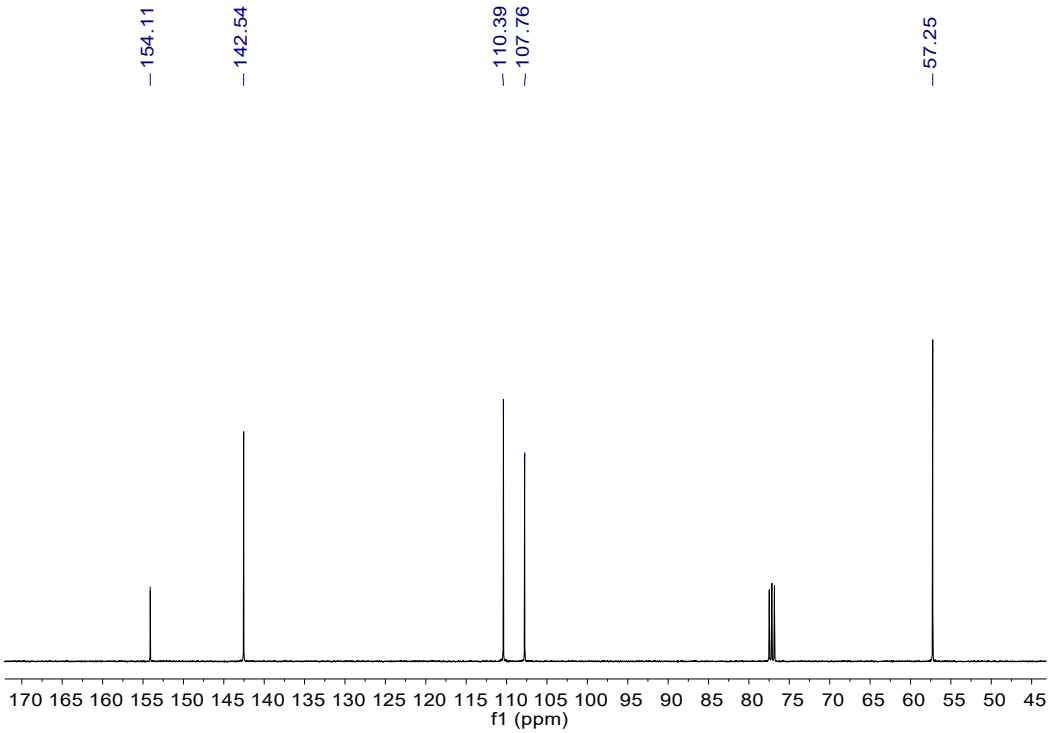

Fig. S87 ^{13}C{^{1}H} NMR spectrum of **b36**. ^{13}C{^{1}H} NMR (100 MHz, $CDCl_3$, 298 k, ppm): δ = 57.25, 107.76, 110.39, 142.54, 154.11.

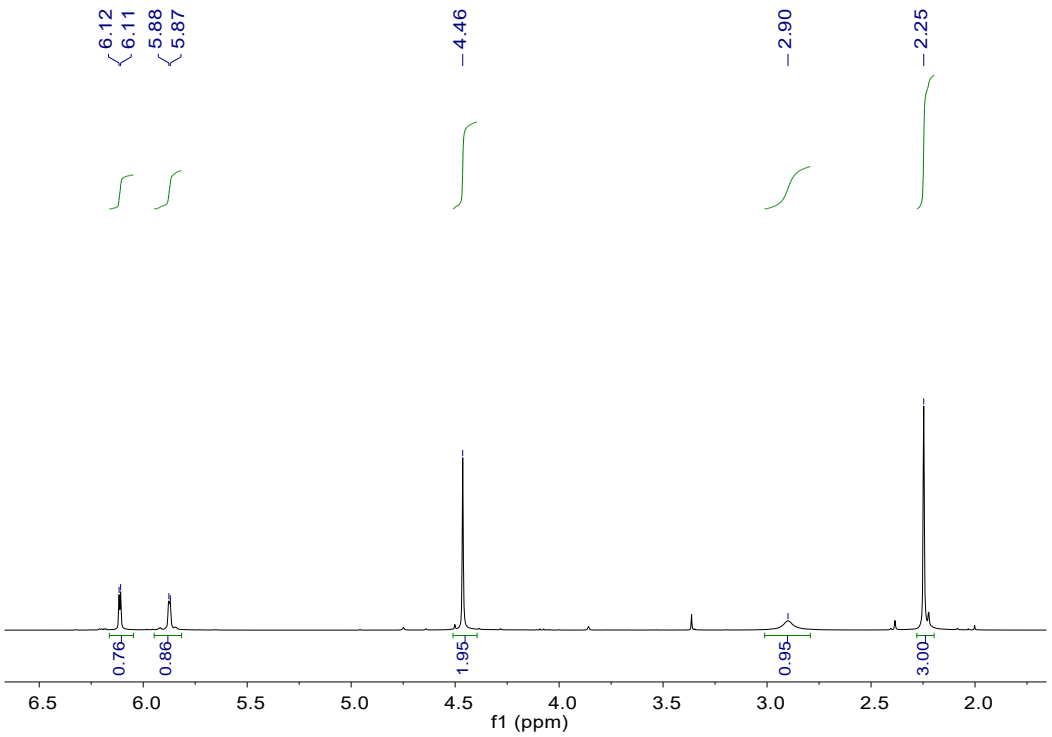

Fig. S88 ^{1}H NMR spectrum of **b37**.[17] ^{1}H NMR (400 MHz, $CDCl_3$, 298 k, ppm): δ = 2.25(s, 3 H), 2.90 (br, 1 H), 4.46 (s, 2 H), 5.87 (d, J_{HH} = 3.2 Hz, 1 H), 6.12 (d, J_{HH} = 2.8 Hz, 1 H).

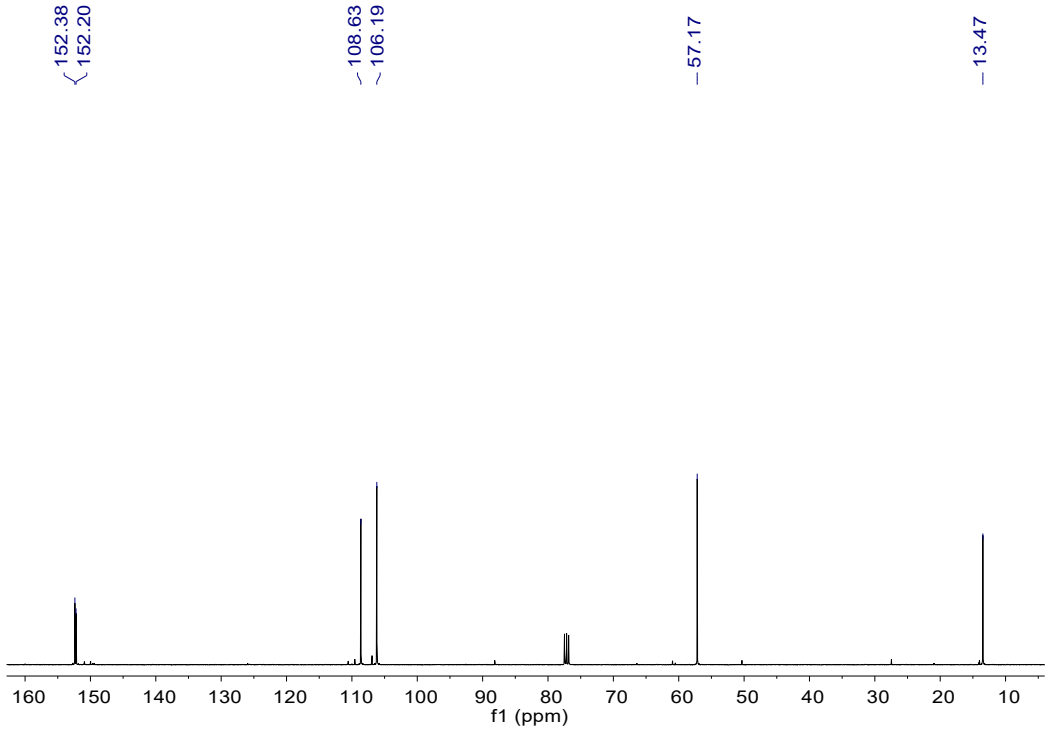

Fig. S89 ^{13}C{^{1}H} NMR spectrum of **b37**. ^{13}C{^{1}H} NMR (100 MHz, $CDCl_3$, 298 k, ppm): δ = 13.47, 57.17, 106.19, 108.63, 152.20, 152.38.

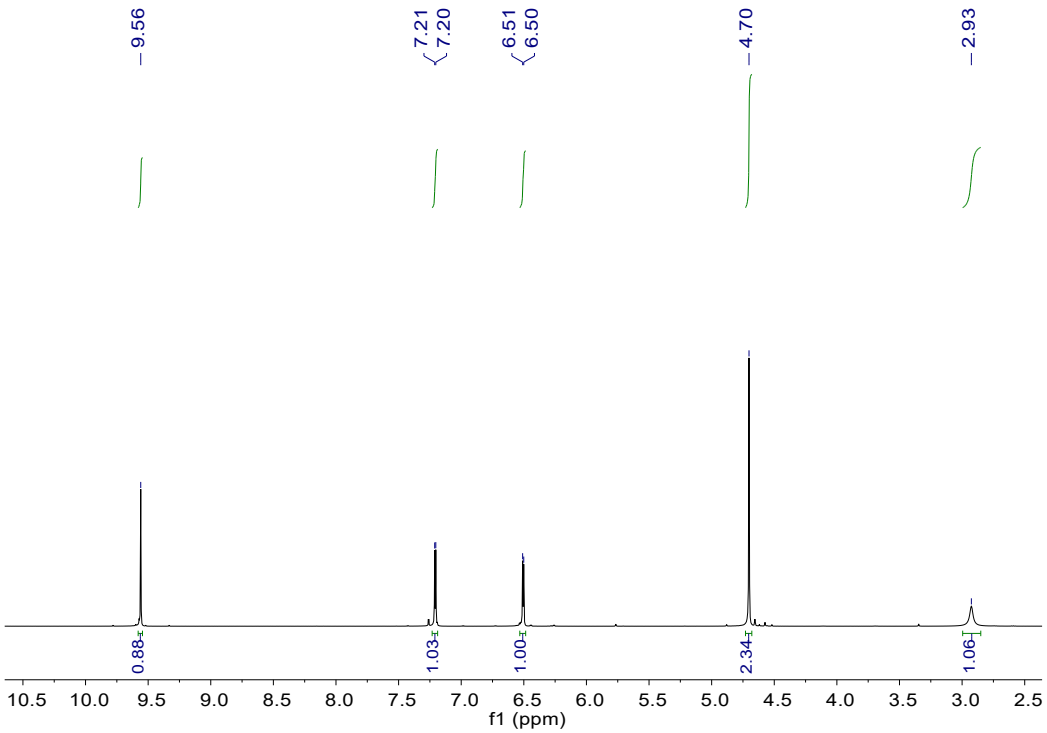

Fig. S90 ^{1}H NMR spectrum of **b38**.[17] ^{1}H NMR (400 MHz, $CDCl_3$, 298 k, ppm): δ = 2.93 (br, 1 H), 4.70 (s, 2 H), 5.50 (d, J_{HH} = 3.2 Hz, 1 H), 7.20 (d, J_{HH} = 3.6 Hz, 1 H), 9.56 (s, 1 H).

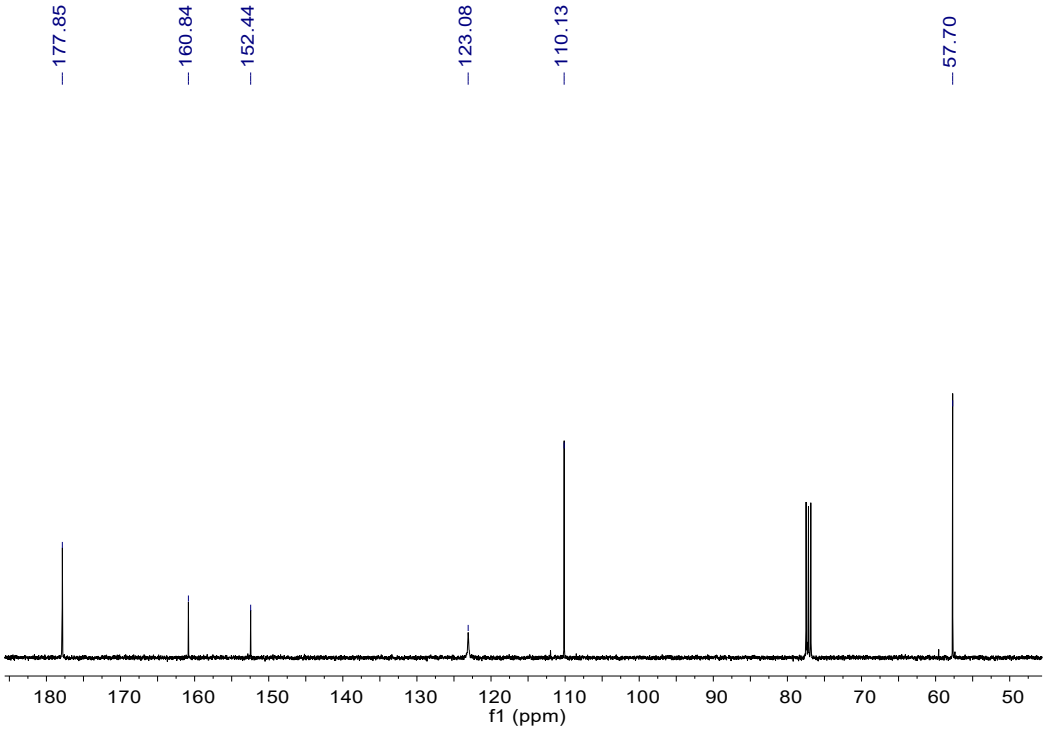

Fig. S91 ^{13}C{^{1}H} NMR spectrum of **b38**. ^{13}C{^{1}H} NMR (100 MHz, $CDCl_3$, 298 k, ppm): δ = 57.70, 110.13, 123.08, 152.44, 160.84, 177.85.

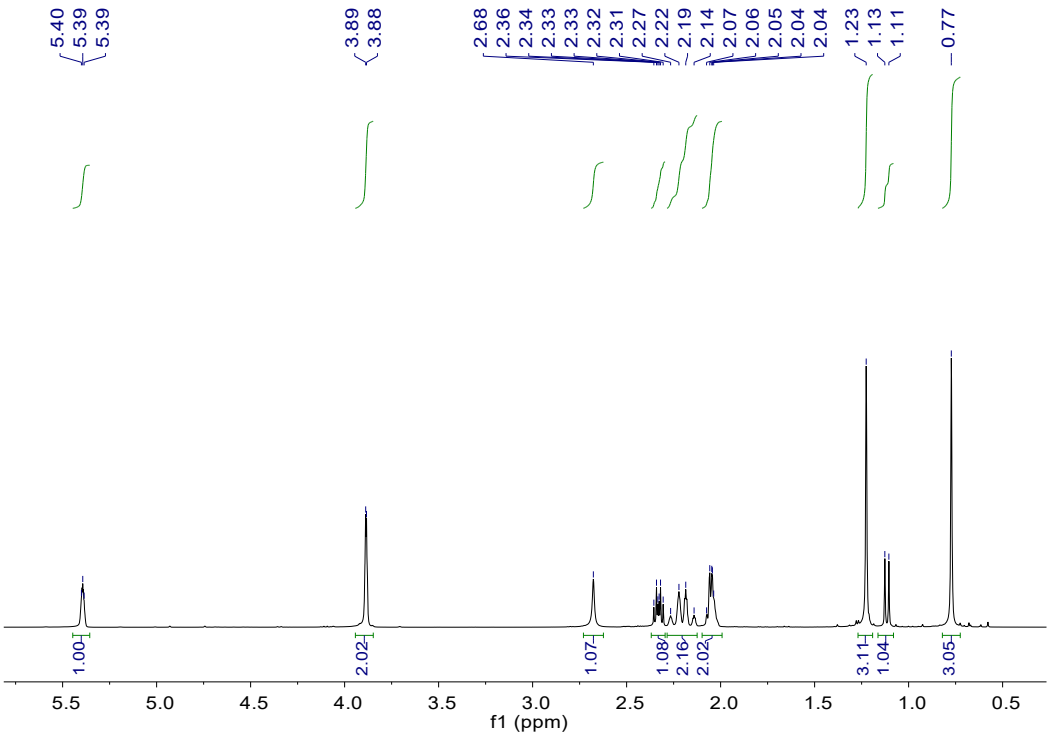

Fig. S92 ^{1}H NMR spectrum of **b39**.[18] ^{1}H NMR (400 MHz, $CDCl_3$, 298 k, ppm): δ = 0.77 (s, 3 H), 1.12 (d, J_{HH} = 8.8 Hz, 1 H), 1.23 (s, 3 H), 2.04-2.07 (m, 2 H), 2.14-2.17 (m, 2 H), 2.31-2.36 (m, 1 H), 2.68 (s, 1 H), 3.88 (d, J_{HH} = 1.6 Hz, 2 H), 5.39 (t, J_{HH} = 2.8 Hz, 1 H).

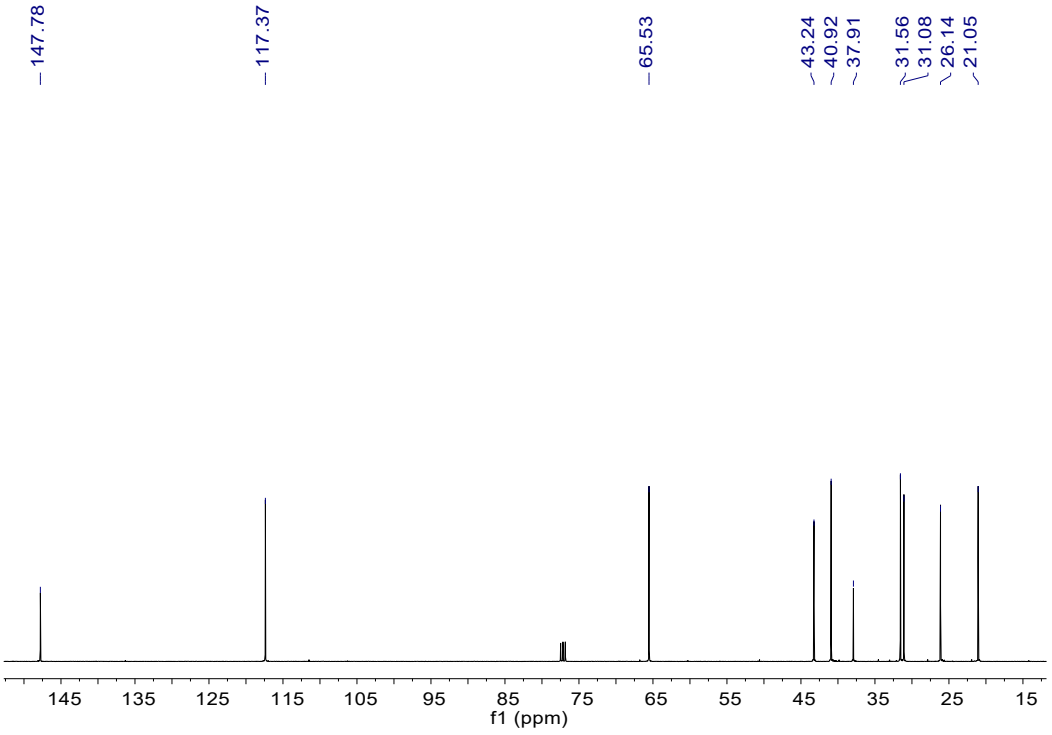

Fig. S93 ^{13}C{^{1}H} NMR spectrum of **b39**. ^{13}C{^{1}H} NMR (100 MHz, $CDCl_3$, 298 k, ppm): δ = 21.05, 26.14, 31.08, 31.56, 37.91, 40.92, 43.24, 65.53, 117.37, 147.78.

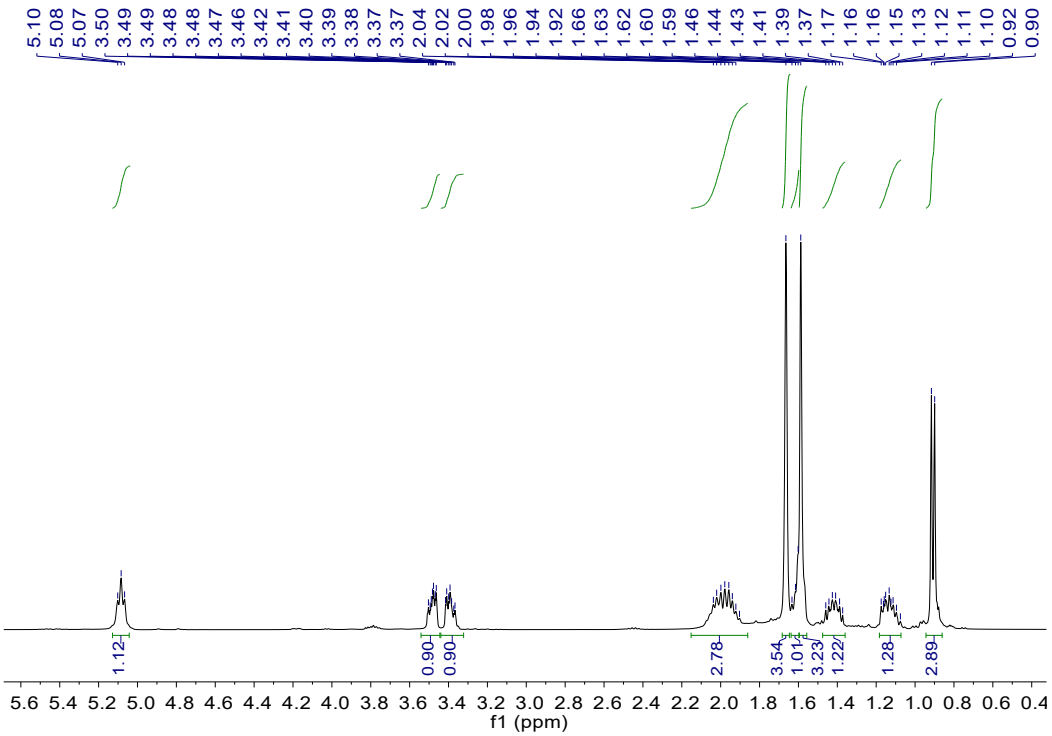

Fig. S94 ^{1}H NMR spectrum of **b40**.[19] ^{1}H NMR (400 MHz, $CDCl_3$, 298 k, ppm): δ = 0.91 (d, J_{HH} = 6.8 Hz, 3 H), 1.08-1.17 (m, 1 H), 1.37-1.46 (m, 1 H), 1.59 (s ,3 H), 1.60-1.63 (m, 1 H), 1.66 (s ,3 H), 1.90-2.04 (m, 3 H), 3.37-3.42 (m, 1 H), 3.46-3.50 (m, 1 H), 5.08 (t, J_{HH} = 7.2 Hz, 1 H).

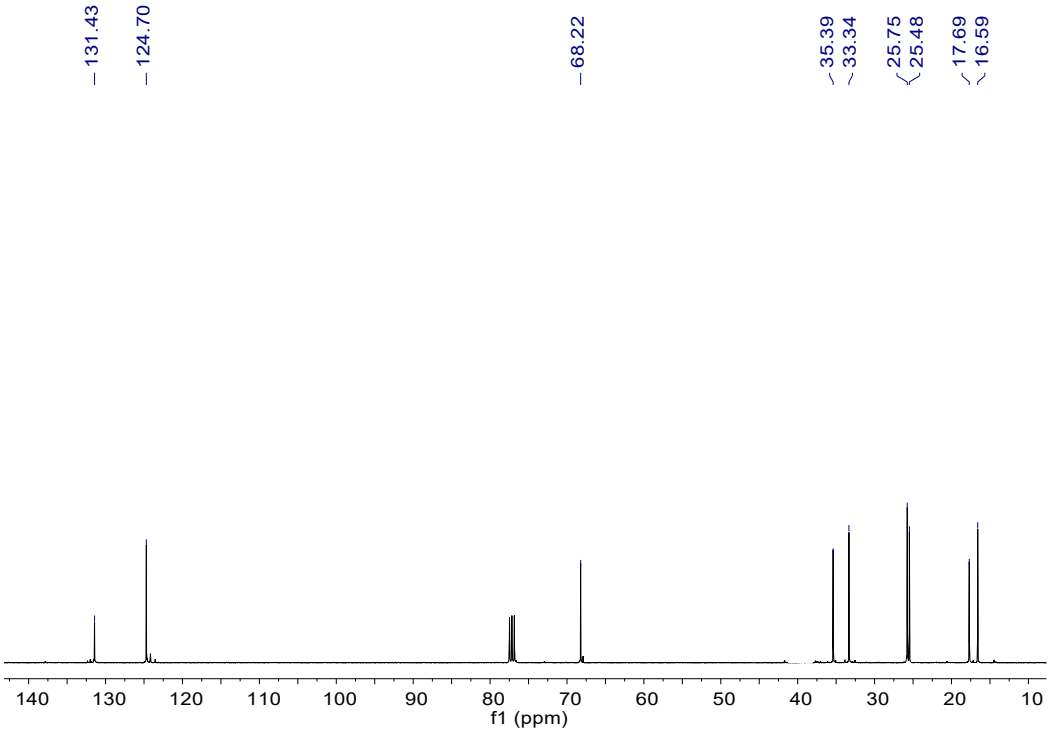

Fig. S95 ^{13}C{^{1}H} NMR spectrum of **b40**. ^{13}C{^{1}H} NMR (100 MHz, $CDCl_3$, 298 k, ppm): δ = 16.59, 17.69, 25.48, 25.75, 33.34, 35.39, 68.22, 124.70, 131.43.

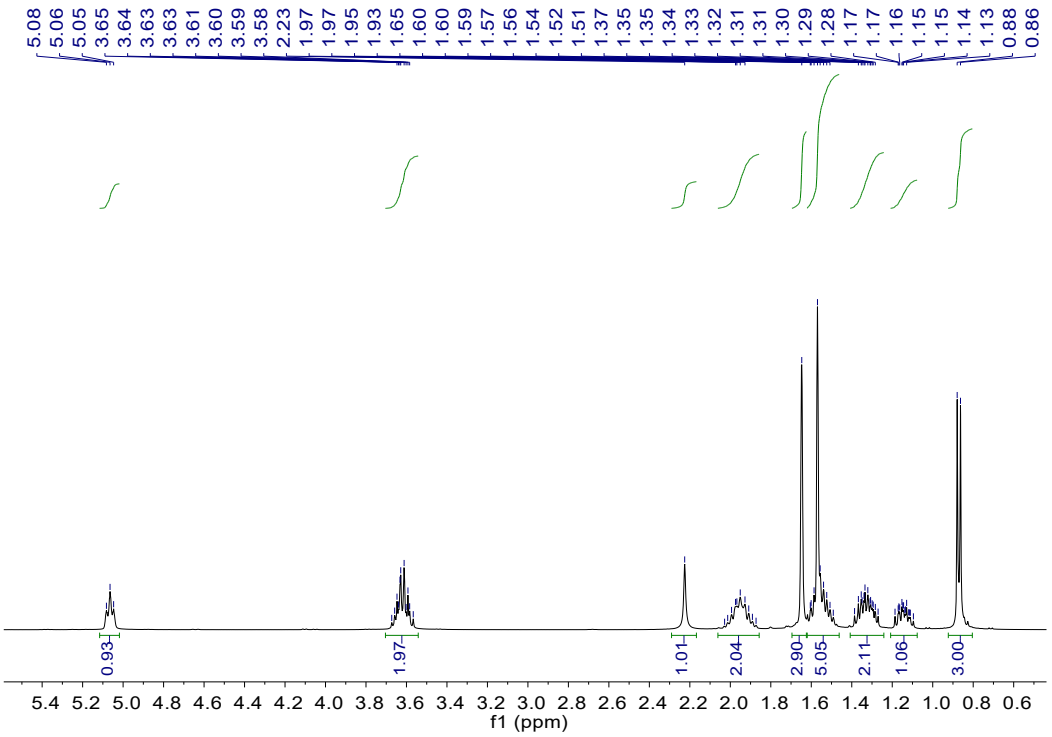

Fig. S96 ^{1}H NMR spectrum of **b41**.[20] ^{1}H NMR (400 MHz, $CDCl_3$, 298 k, ppm): δ = 0.87 (d, J_{HH} = 6.4 Hz, 3 H), 1.10-1.19 (m, 1 H), 1.27-1.39 (m, 2 H), 1.49-1.60 (m, 5 H), 1.65 (s, 3 H), 1.87-2.03 (m, 2 H), 2.23 (s, 1 H), 3.57-3.67 (m, 2 H), 5.06 (t, J_{HH} = 6.8 Hz, 1 H).

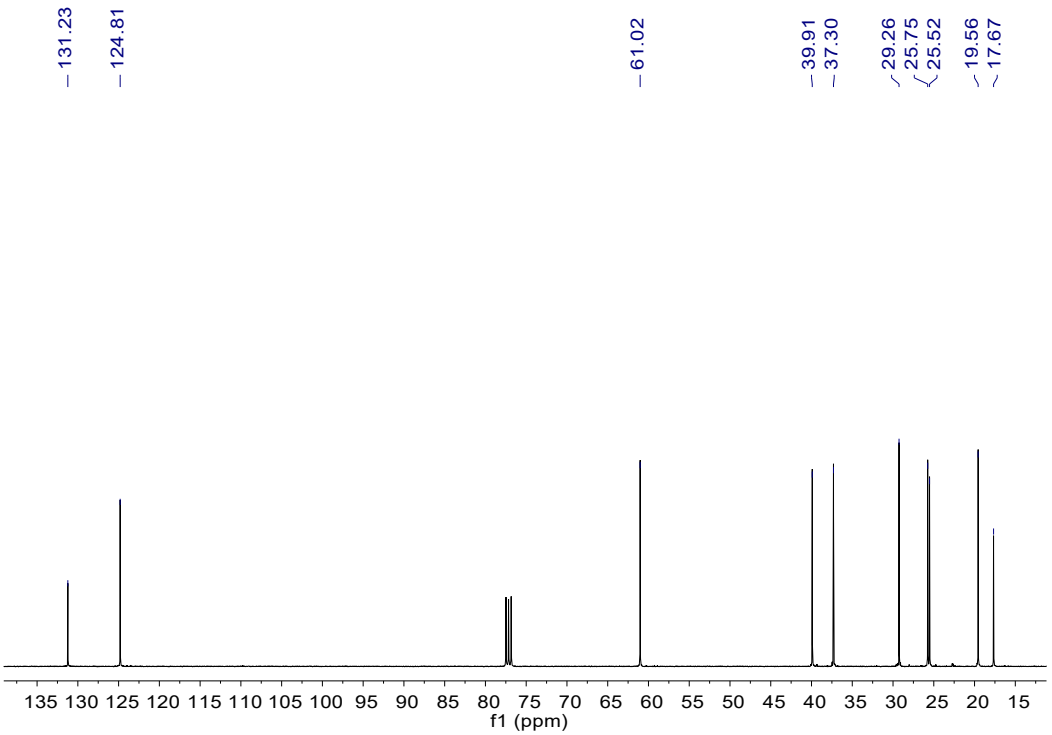

Fig. S97 ^{13}C{^{1}H} NMR spectrum of **b41**. ^{13}C{^{1}H} NMR (100 MHz, $CDCl_3$, 298 k, ppm): δ = 17.67, 19.56, 25.52, 25.75, 29.26, 37.30, 39.91, 61.02, 124.81, 131.23.

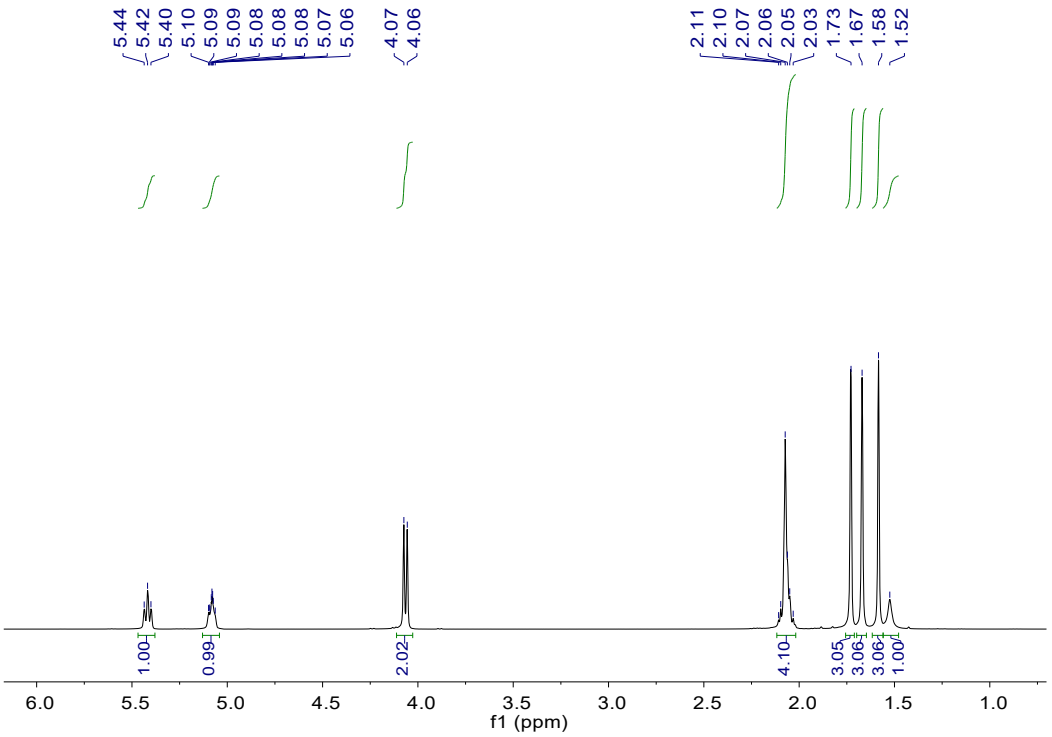

Fig. S98 ^{1}H NMR spectrum of **b42**.[20] ^{1}H NMR (400 MHz, $CDCl_3$, 298 k, ppm): δ = 1.52 (br, 1 H), 1.58 (s, 3 H), 1.67 (s, 3 H), 1.73 (s, 3 H), 2.03-2.11 (m, 4 H), 4.07 (d, J_{HH} = 7.2 Hz, 2 H), 5.06-5.10 (m, 1 H), 5.42 (t, J_{HH} = 6.4 Hz, 1 H).

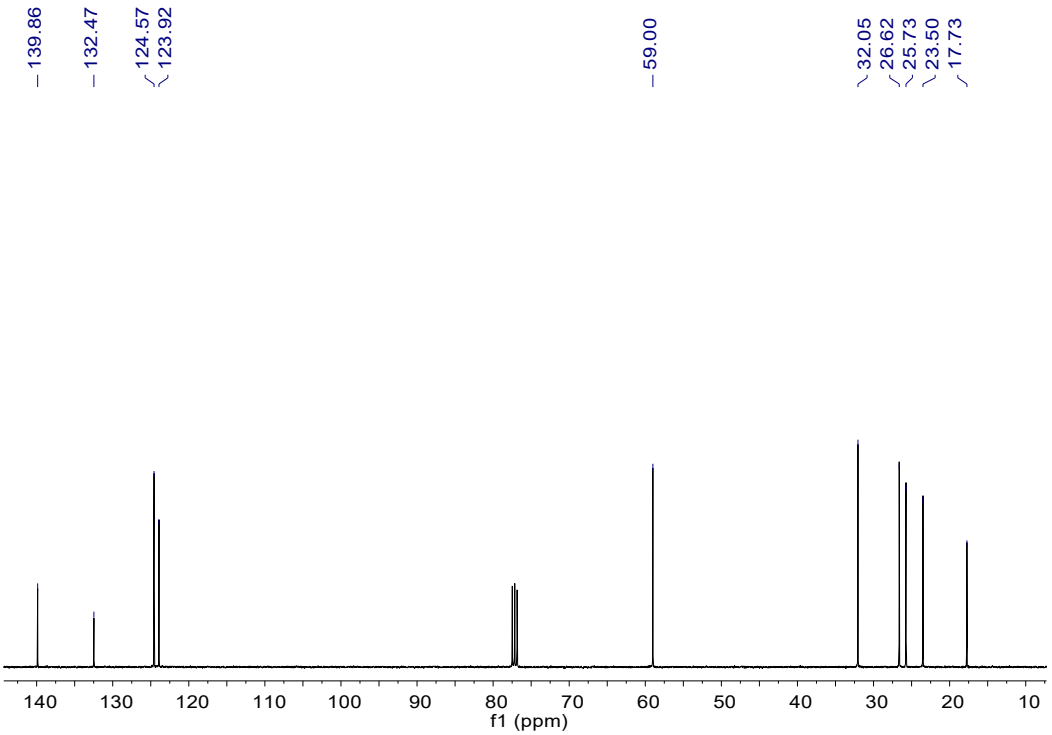

Fig. S99 ^{13}C{^{1}H} NMR spectrum of **b42**. ^{13}C{^{1}H} NMR (100 MHz, $CDCl_3$, 298 k, ppm): δ = 17.73, 23.50, 25.73, 26.62, 32.05, 59.00, 123.92, 124.57, 132.47, 139.86.

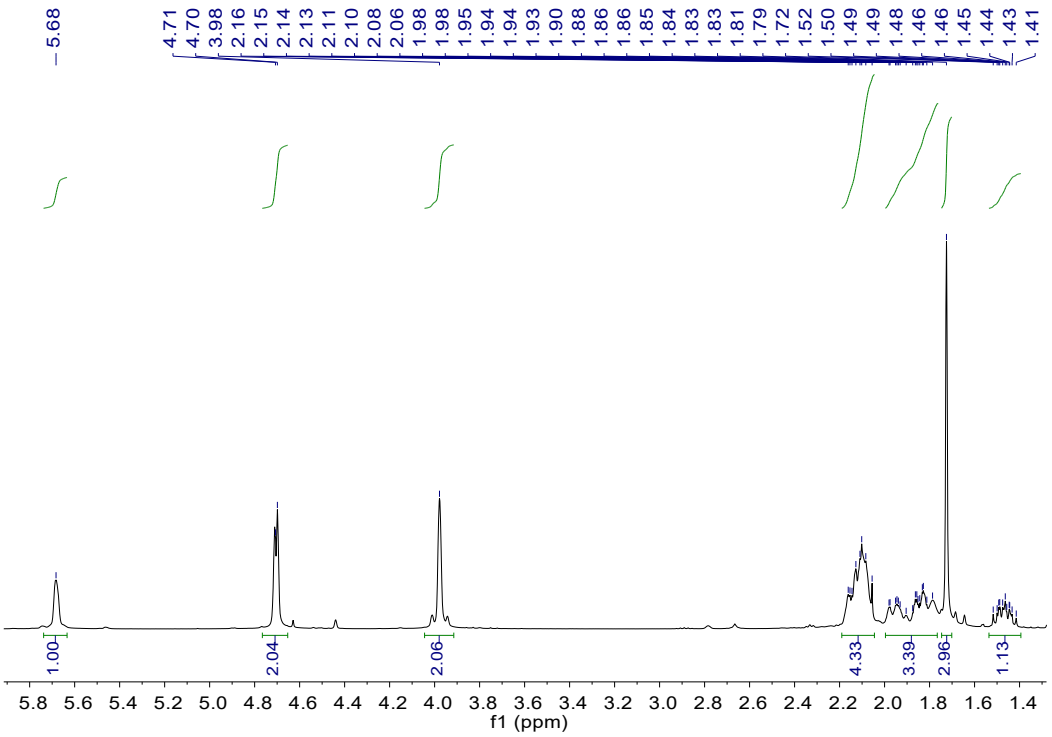

Fig. S100 ^{1}H NMR spectrum of **b43**.[21] ^{1}H NMR (400 MHz, $CDCl_3$, 298 k, ppm): δ = 1.41-1.52 (m, 1 H), 1.72 (s, 3 H), 1.79-1.98 (m, 3 H), 2.06-2.16 (m, 4 H), 3.98 (s, 2 H), 4.71 (d, J_{HH} = 4.8 Hz, 2 H), 5.68 (s ,1 H).

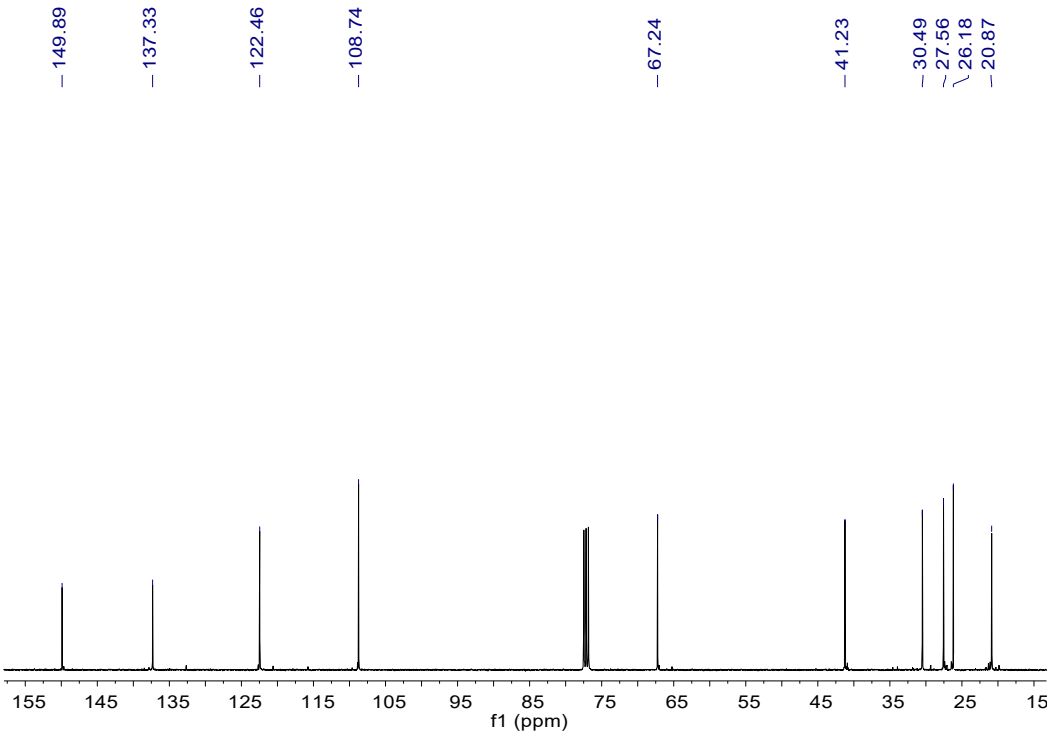

Fig. S101 ^{13}C{^{1}H} NMR spectrum of **b43**. ^{13}C{^{1}H} NMR (100 MHz, $CDCl_3$, 298 k, ppm): δ = 20.87, 26.18, 27.56, 30.49, 41.23, 67.24, 108.74, 122.46, 137.33, 149.89.

V. GC spectra

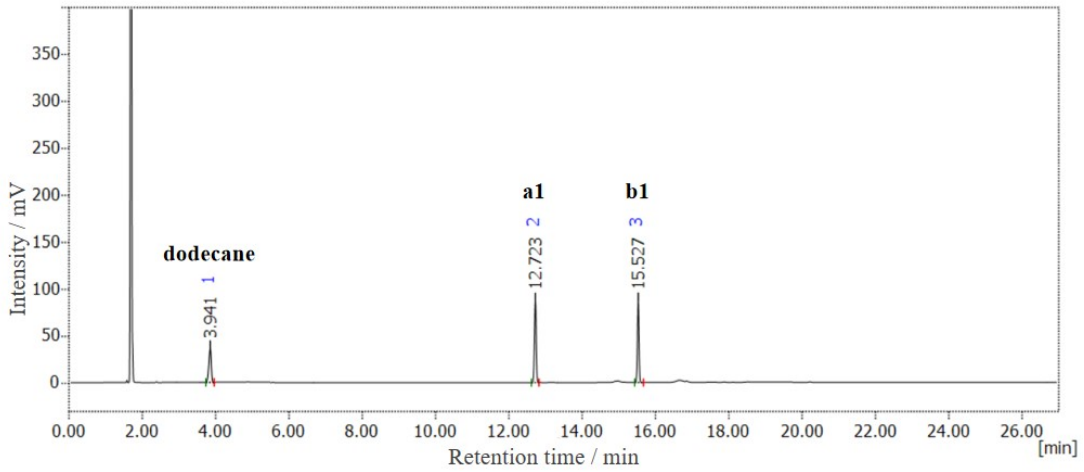

Fig. S102 GC analysis result for catalytic hydrogenation of **a1** by **2**.

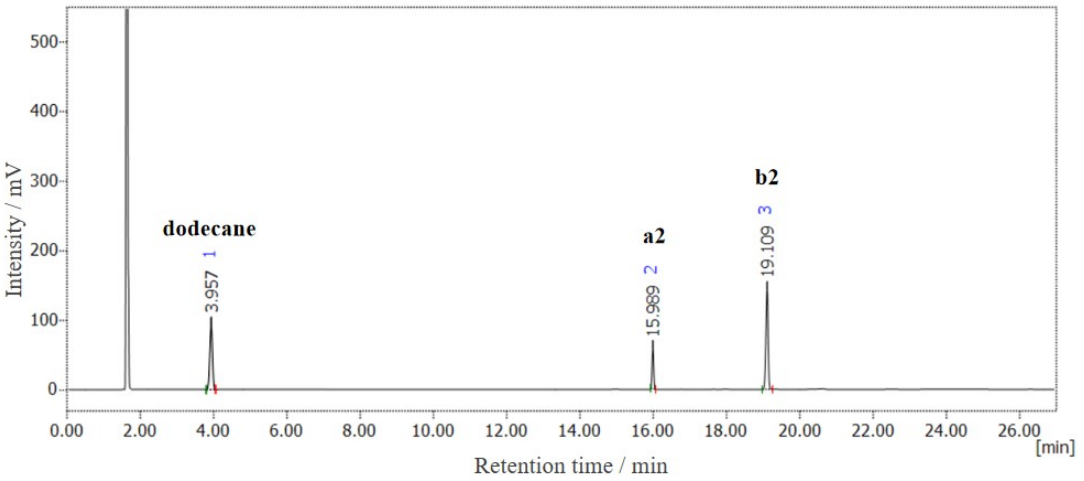

Fig. S103 GC analysis result for catalytic hydrogenation of **a2** by **2**.

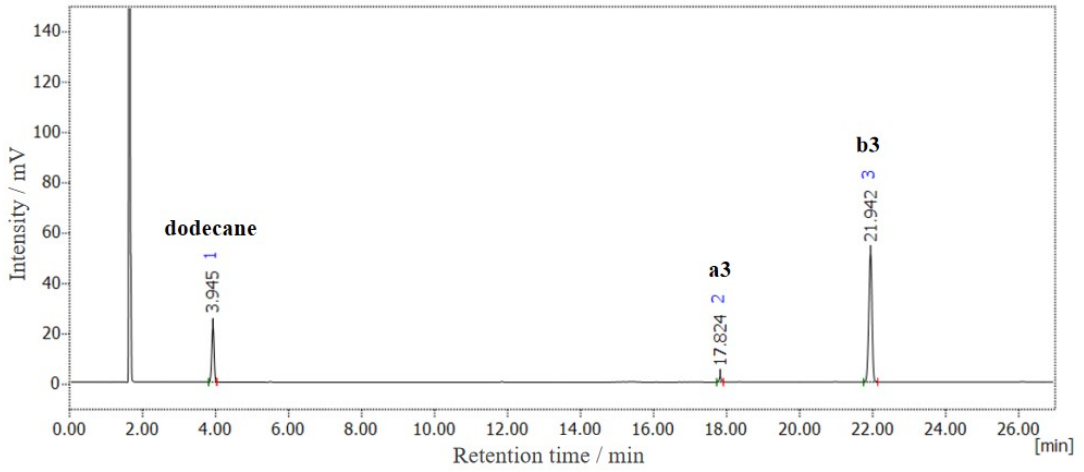

Fig. S104 GC analysis result for catalytic hydrogenation of **a3** by **2**.

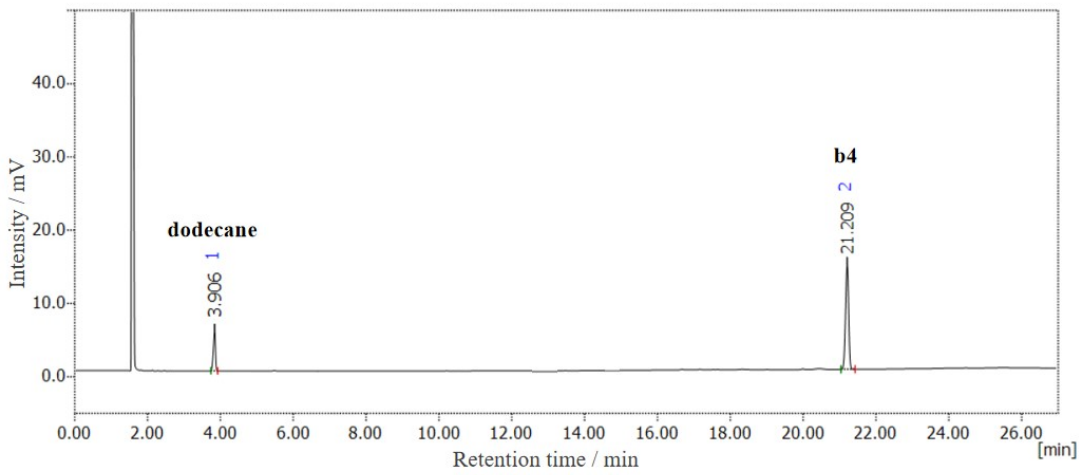

Fig. S105 GC analysis result for catalytic hydrogenation of **a4** by **2**.

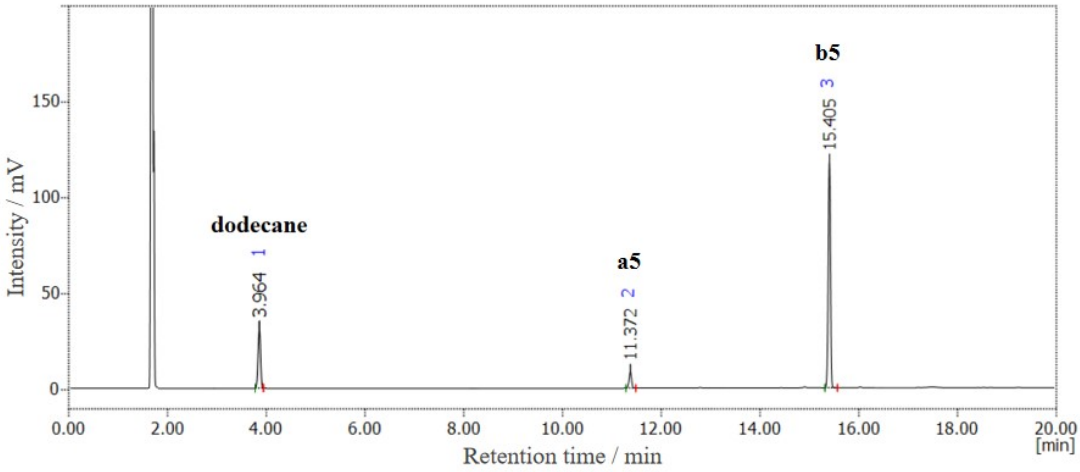

Fig. S106 GC analysis result for catalytic hydrogenation of **a5** by **2**.

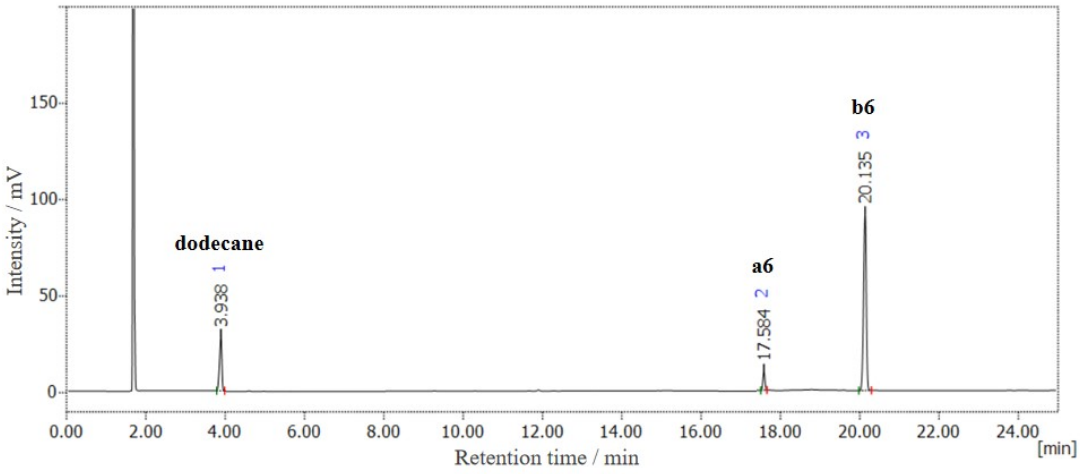

Fig. S107 GC analysis result for catalytic hydrogenation of **a6** by **2**.

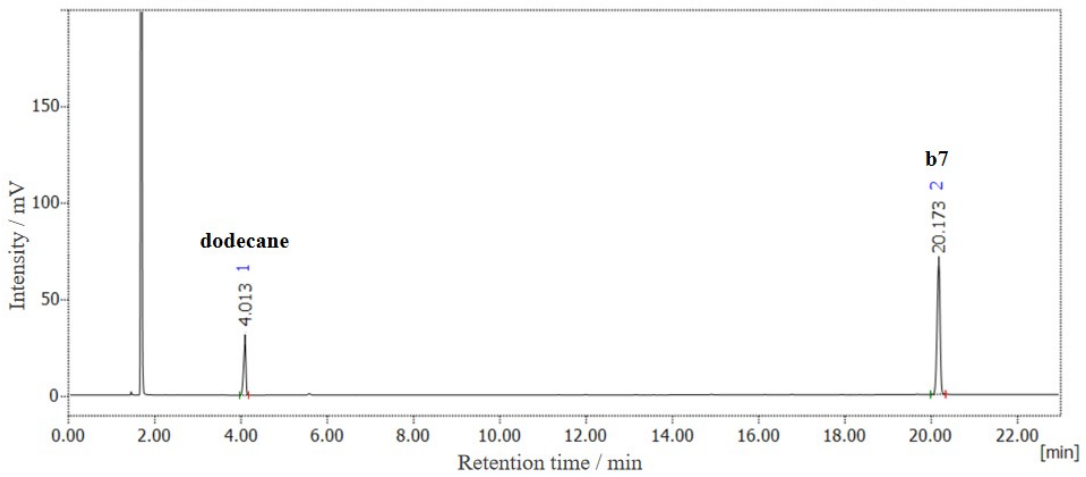

Fig. S108 GC analysis result for catalytic hydrogenation of **a7** by **2**.

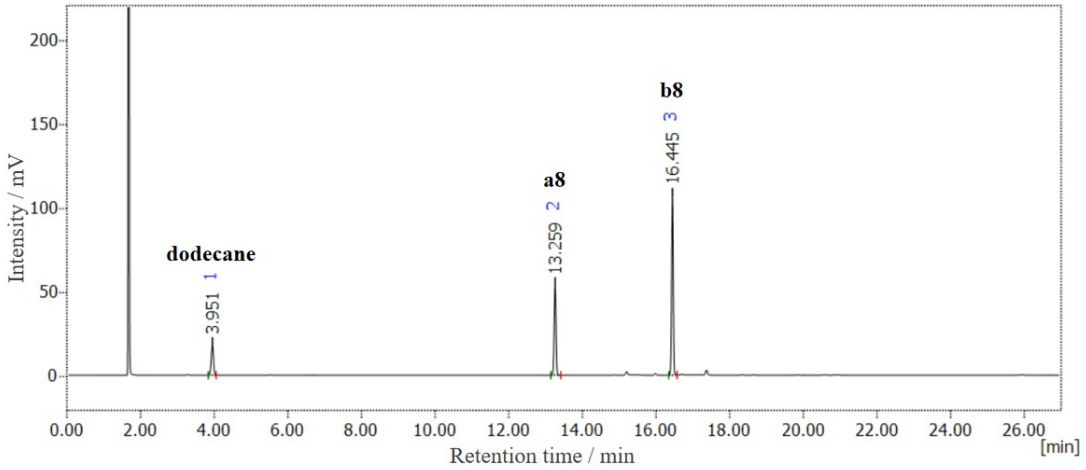

Fig. S109 GC analysis result for catalytic hydrogenation of **a8** by **2**.

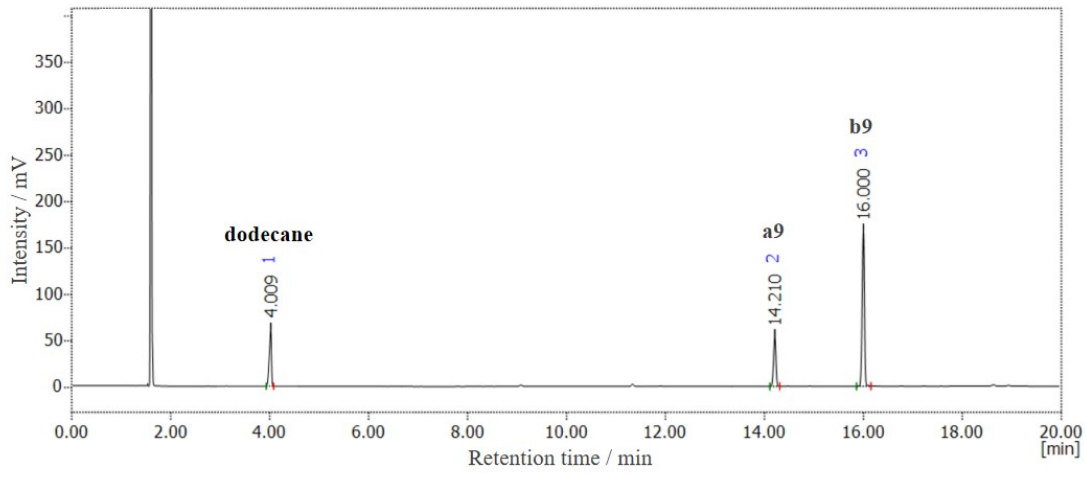

Fig. S110 GC analysis result for catalytic hydrogenation of **a9** by **2**.

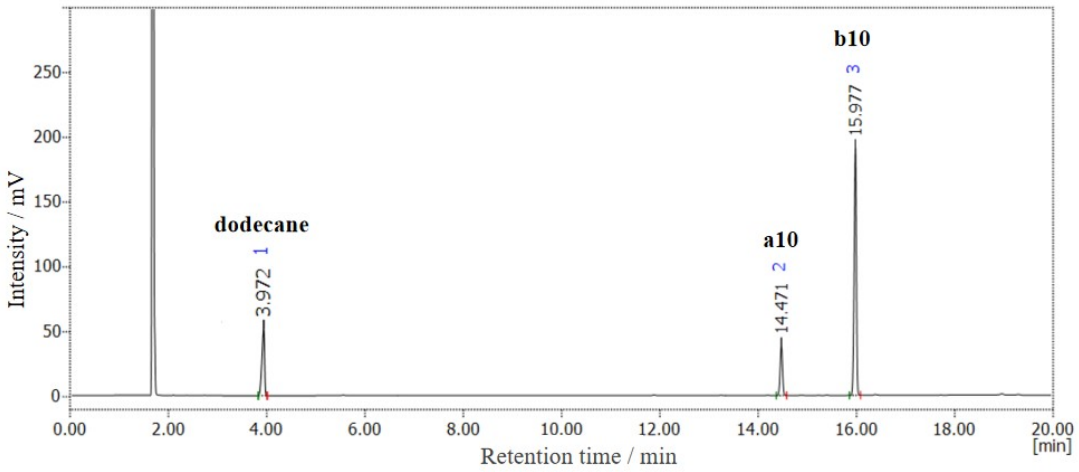

Fig. S111 GC analysis result for catalytic hydrogenation of **a10** by **2**.

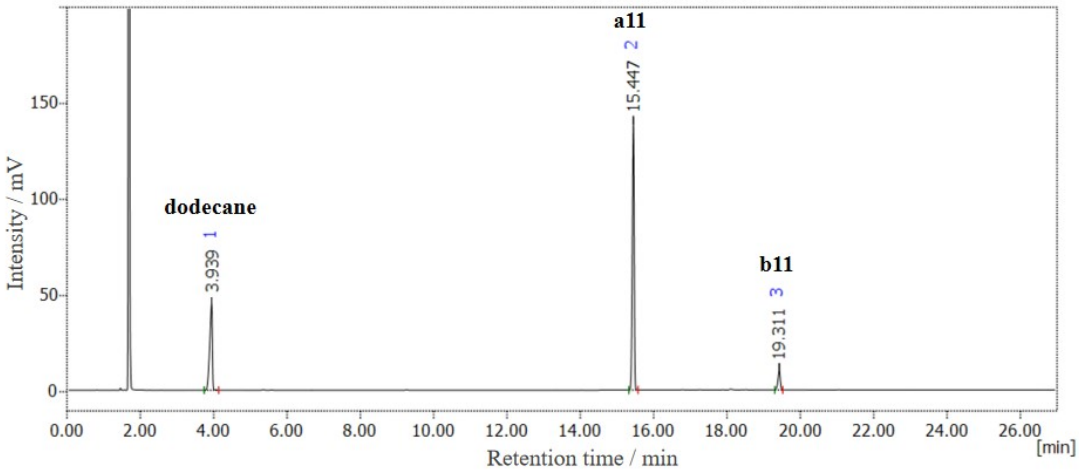

Fig. S112 GC analysis result for catalytic hydrogenation of **a11** by **2**.

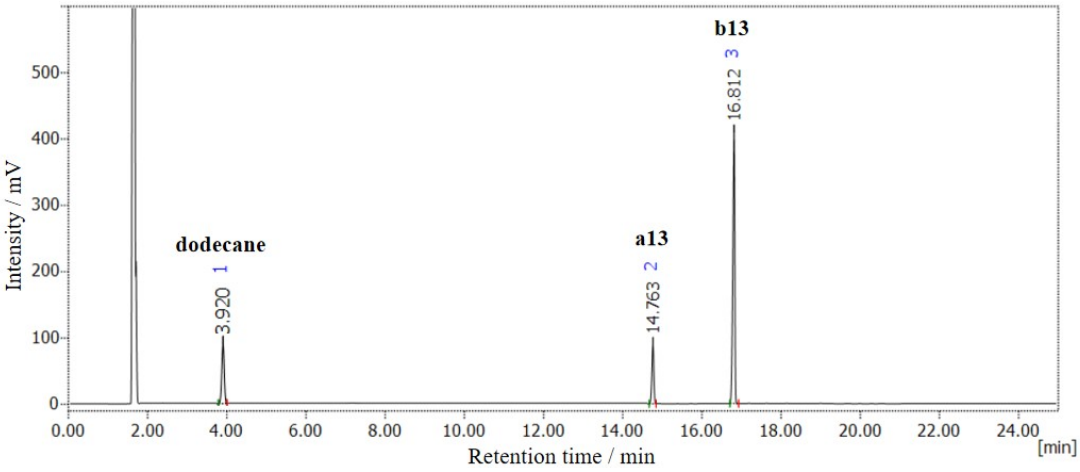

Fig. S113 GC analysis result for catalytic hydrogenation of **a13** by **2**.

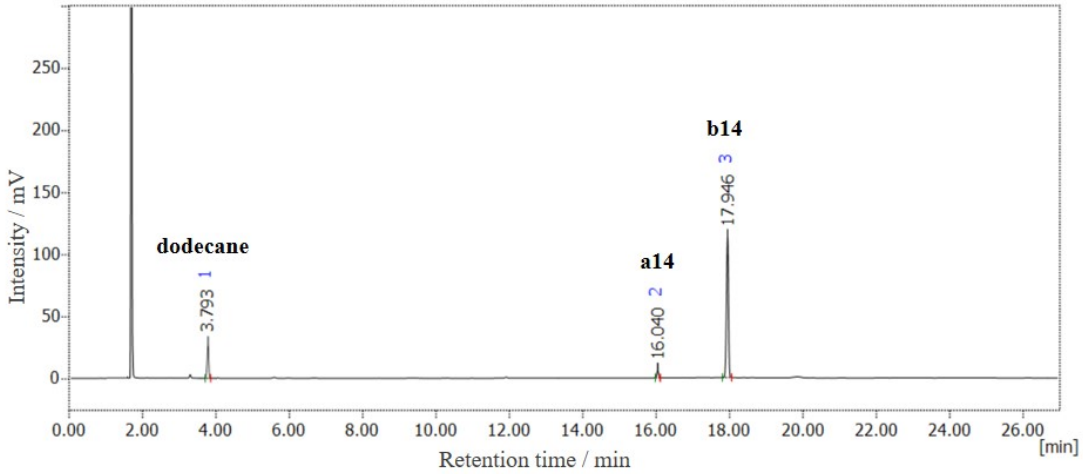

Fig. S114 GC analysis result for catalytic hydrogenation of **a14** by **2**.

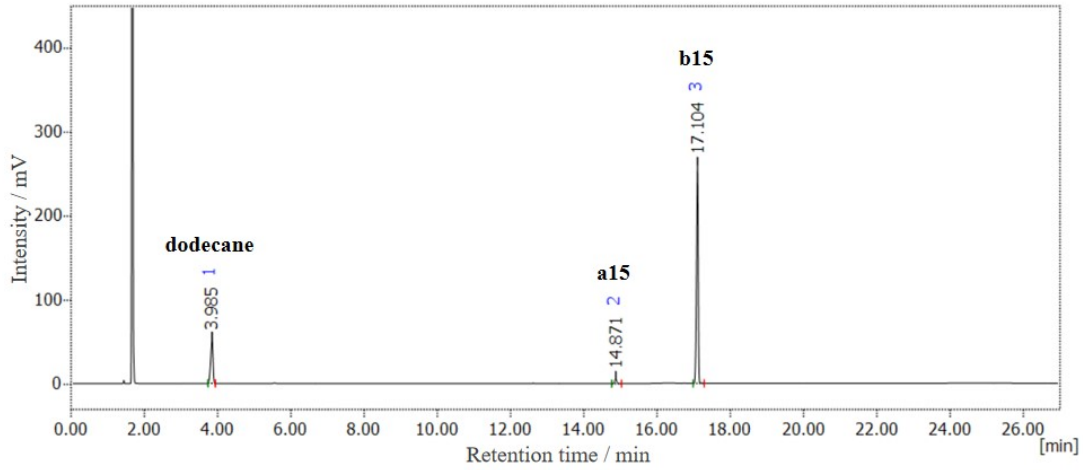

Fig. S115 GC analysis result for catalytic hydrogenation of **a15** by **2**.

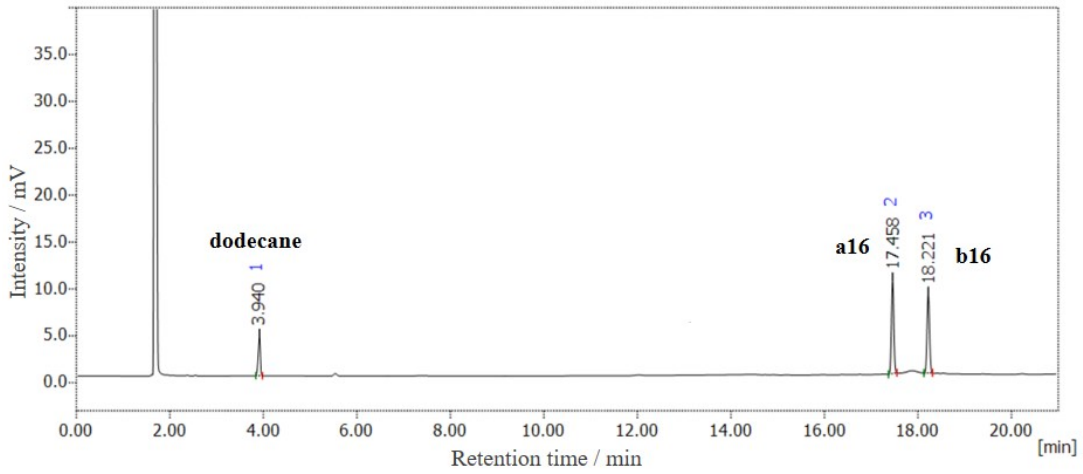

Fig. S116 GC analysis result for catalytic hydrogenation of **a16** by **2**.

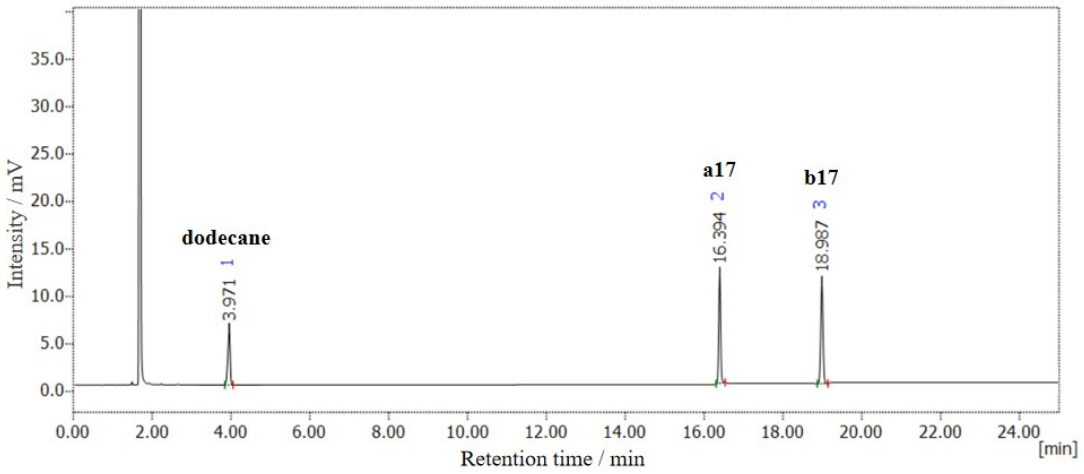

Fig. S117 GC analysis result for catalytic hydrogenation of **a17** by **2**.

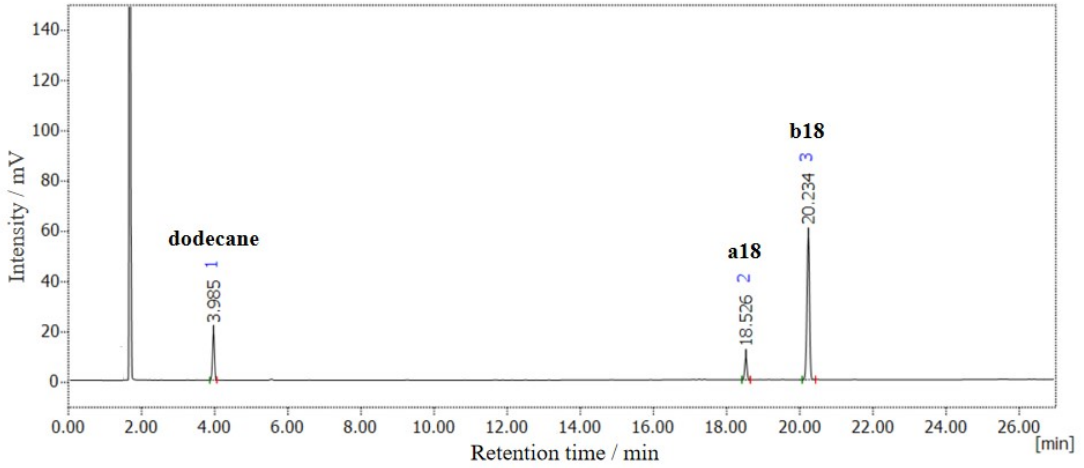

Fig. S118 GC analysis result for catalytic hydrogenation of **a18** by **2**.

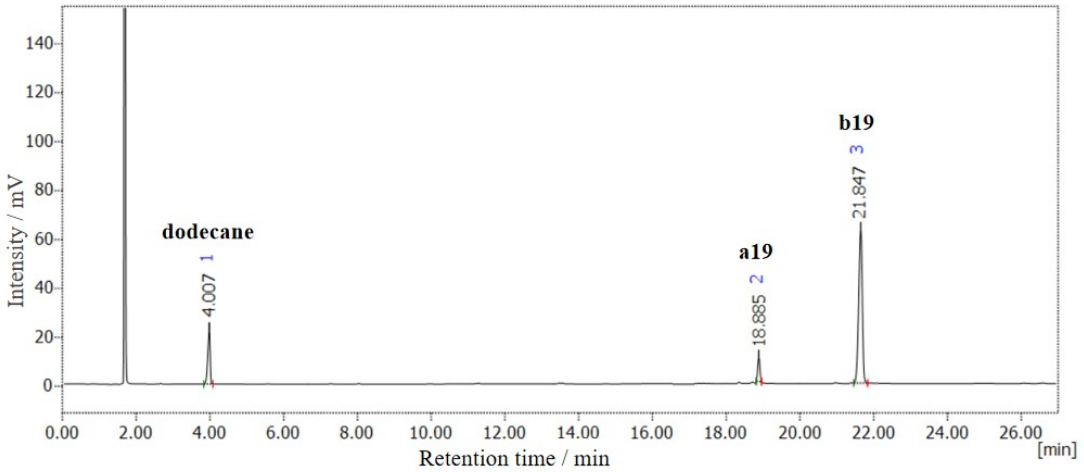

Fig. S119 GC analysis result for catalytic hydrogenation of **a19** by **2**.

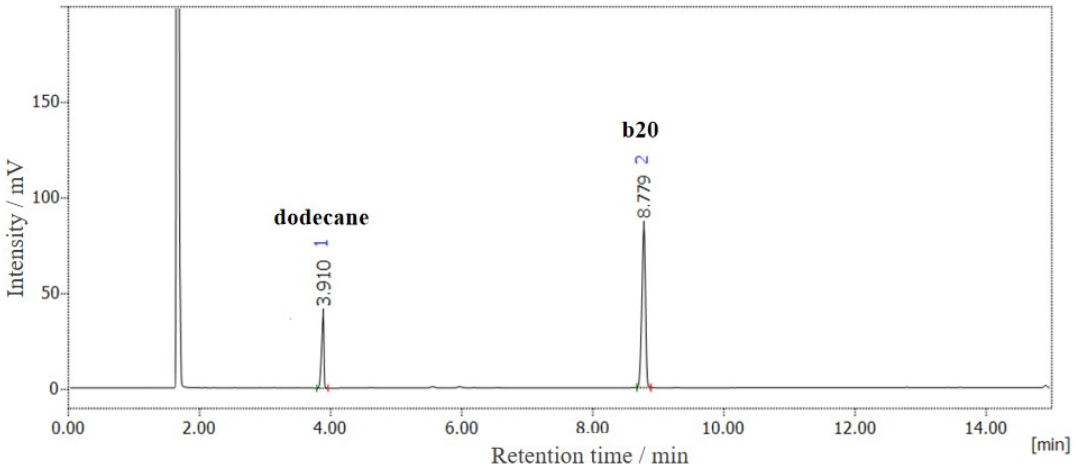

Fig. S120 GC analysis result for catalytic hydrogenation of **a20** by **2**.

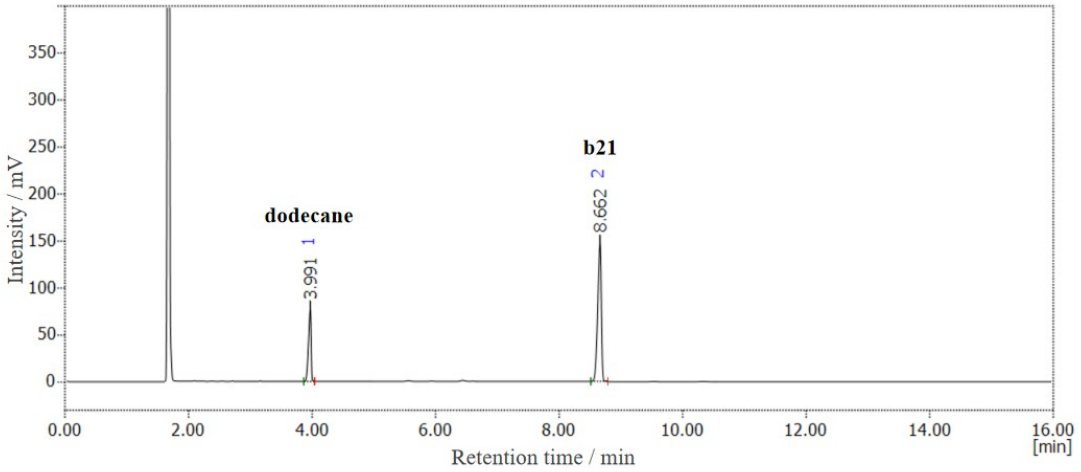

Fig. S121 GC analysis result for catalytic hydrogenation of **a21** by **2**.

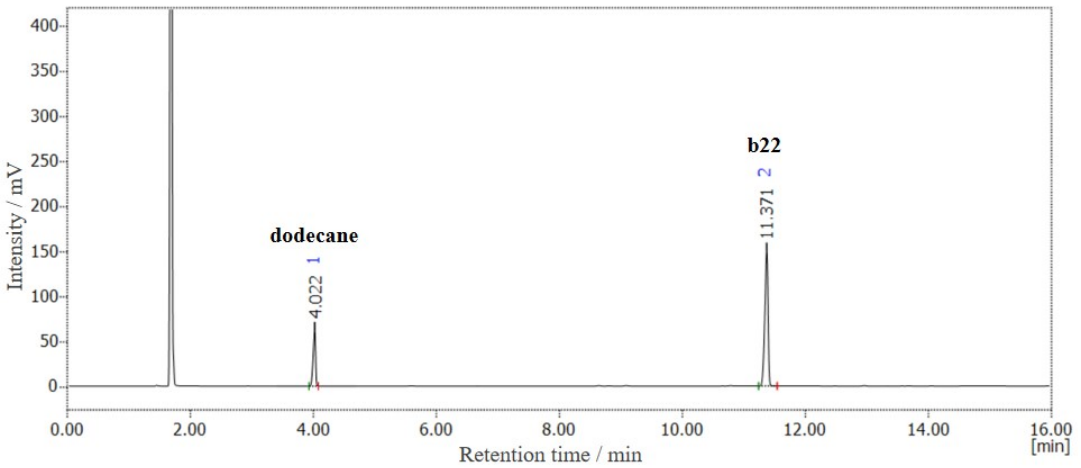

Fig. S122 GC analysis result for catalytic hydrogenation of **a22** by **2**.

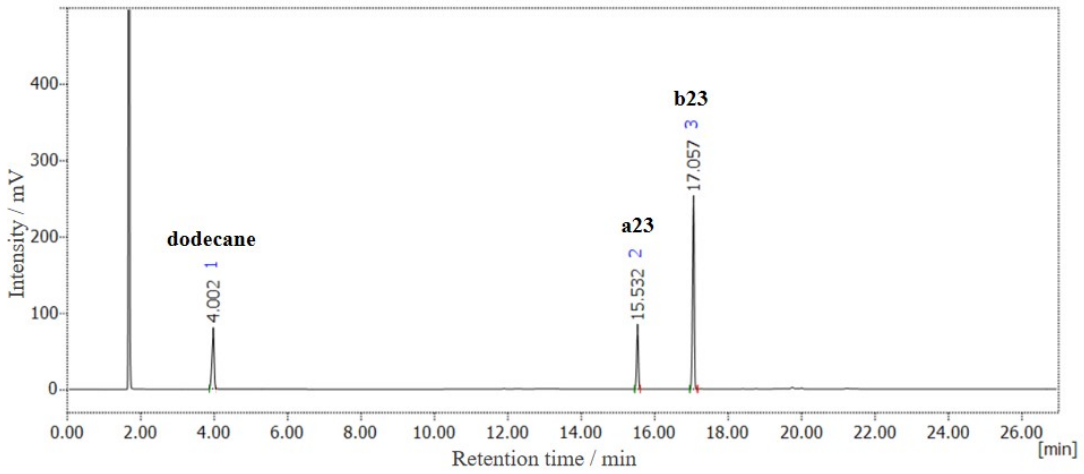

Fig. S123 GC analysis result for catalytic hydrogenation of **a23** by **2**.

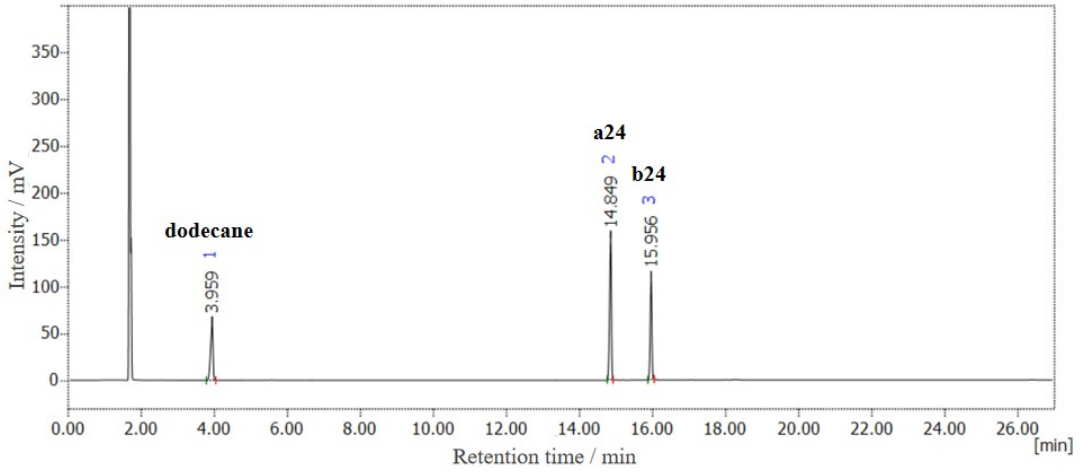

Fig. S124 GC analysis result for catalytic hydrogenation of **a24** by **2**.

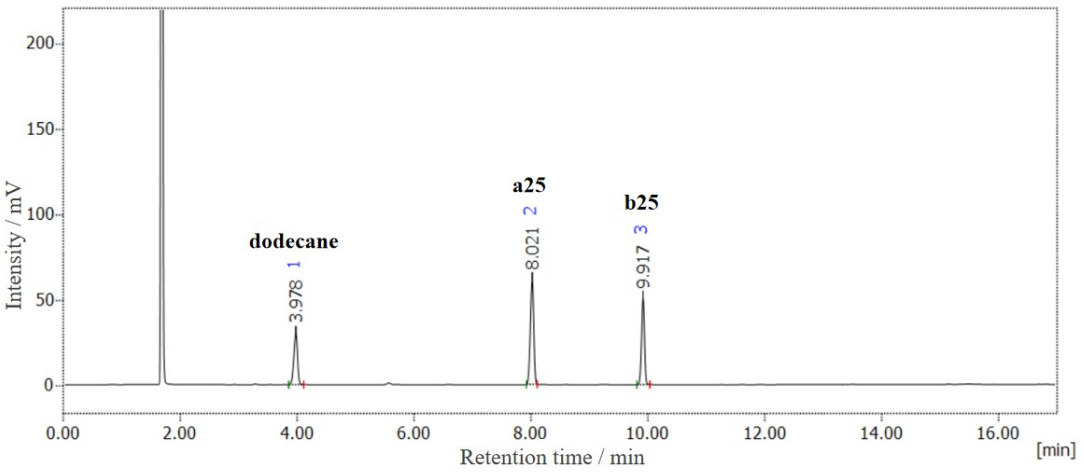

Fig. S125 GC analysis result for catalytic hydrogenation of **a25** by **2**.

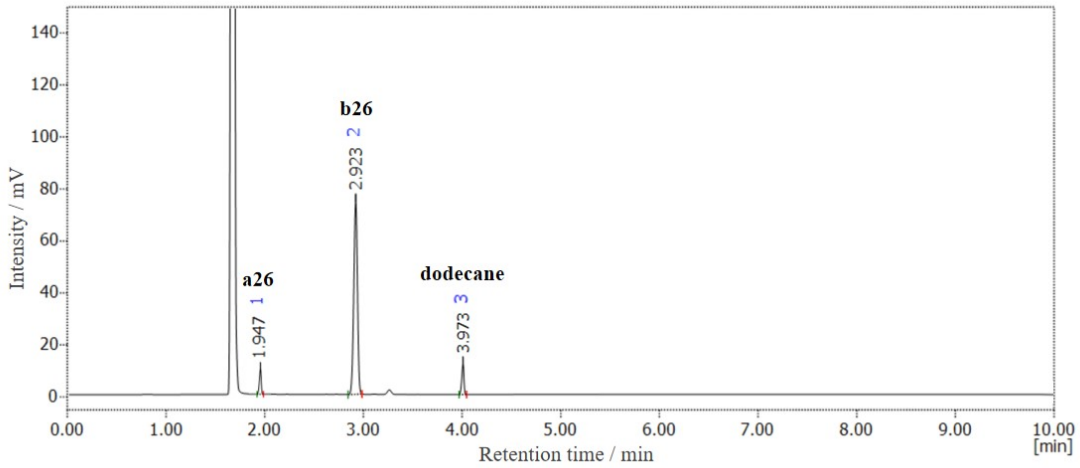

Fig. S126 GC analysis result for catalytic hydrogenation of **a26** by **2**.

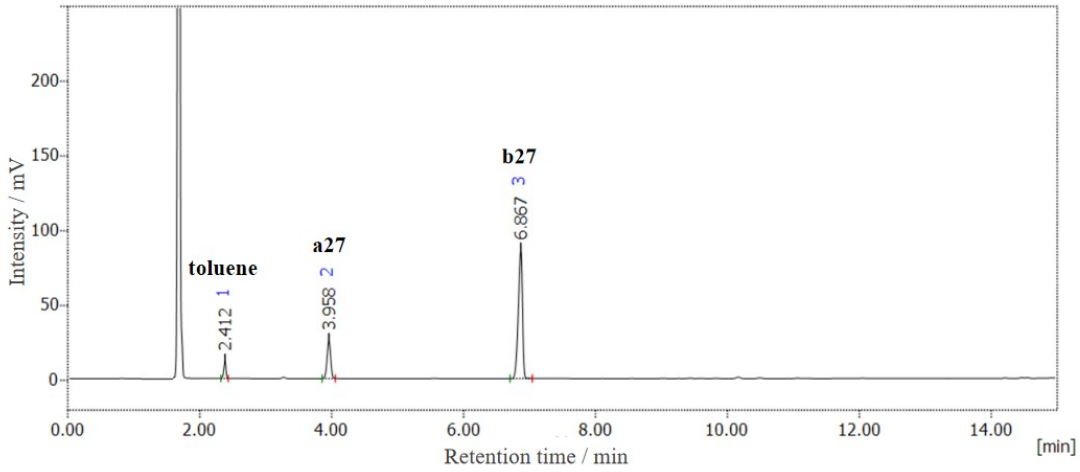

Fig. S127 GC analysis result for catalytic hydrogenation of **a27** by **2**.

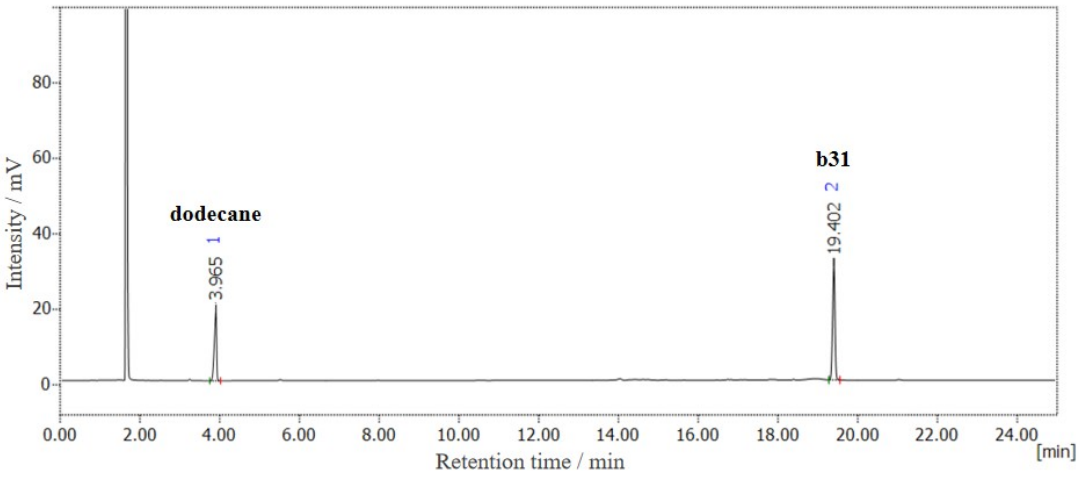

Fig. S128 GC analysis result for catalytic hydrogenation of **a31** by **2**.

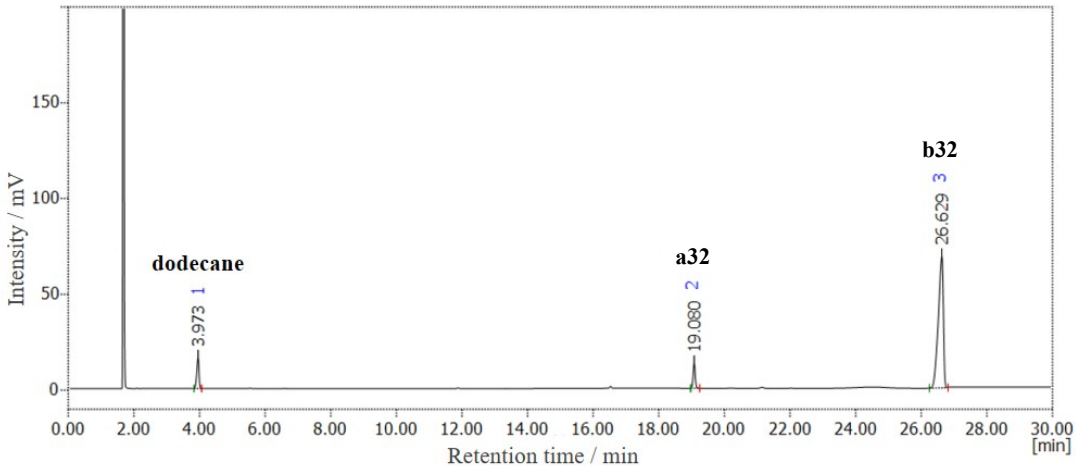

Fig. S129 GC analysis result for catalytic hydrogenation of **a32** by **2**.

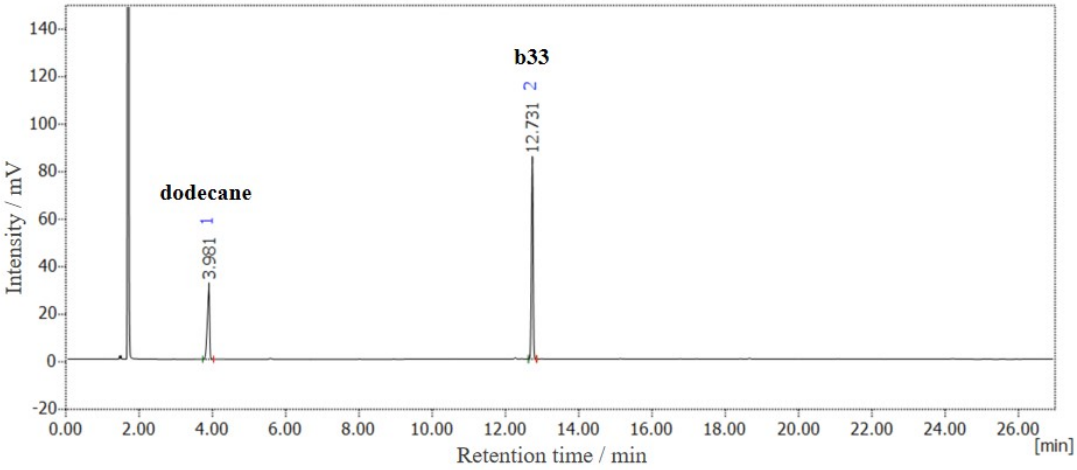

Fig. S130 GC analysis result for catalytic hydrogenation of **a33** by **2**.

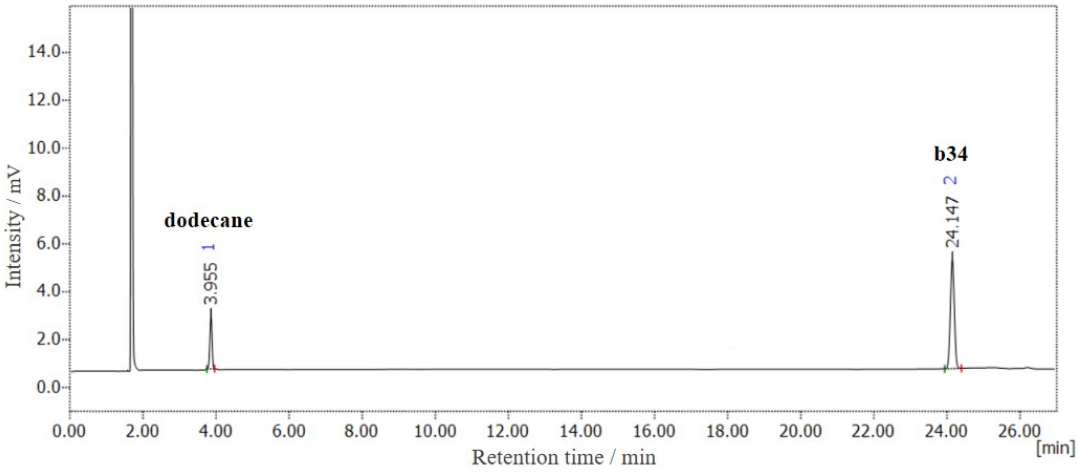

Fig. S131 GC analysis result for catalytic hydrogenation of **a34** by **2**.

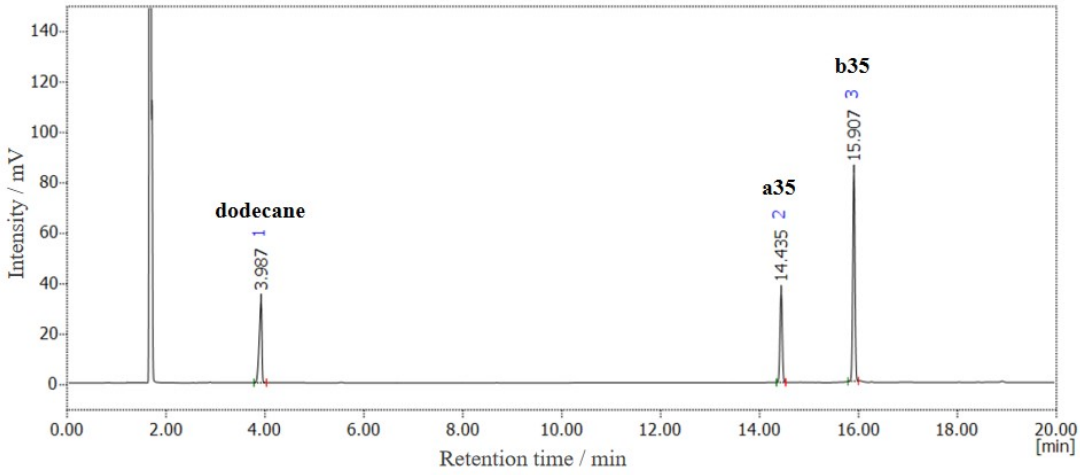

Fig. S132 GC analysis result for catalytic hydrogenation of **a35** by **2**.

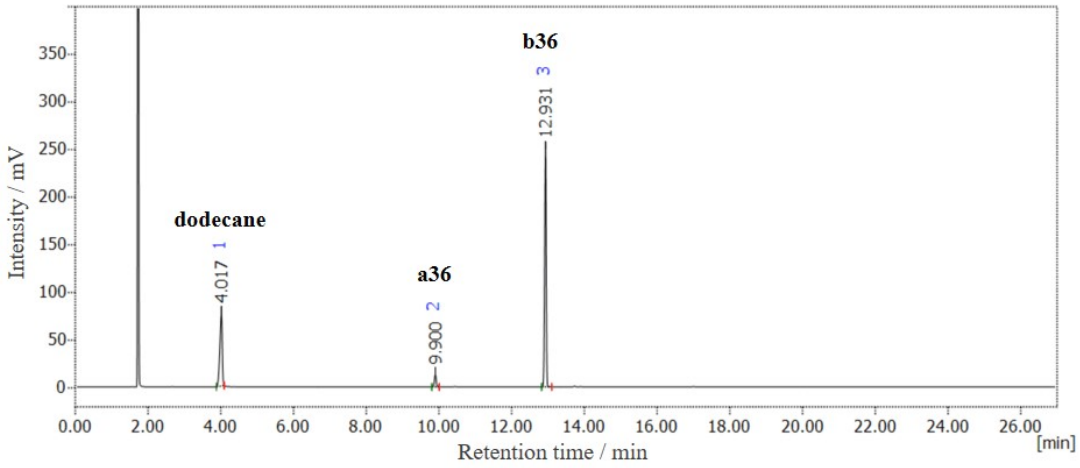

Fig. S133 GC analysis result for catalytic hydrogenation of **a36** by **2**.

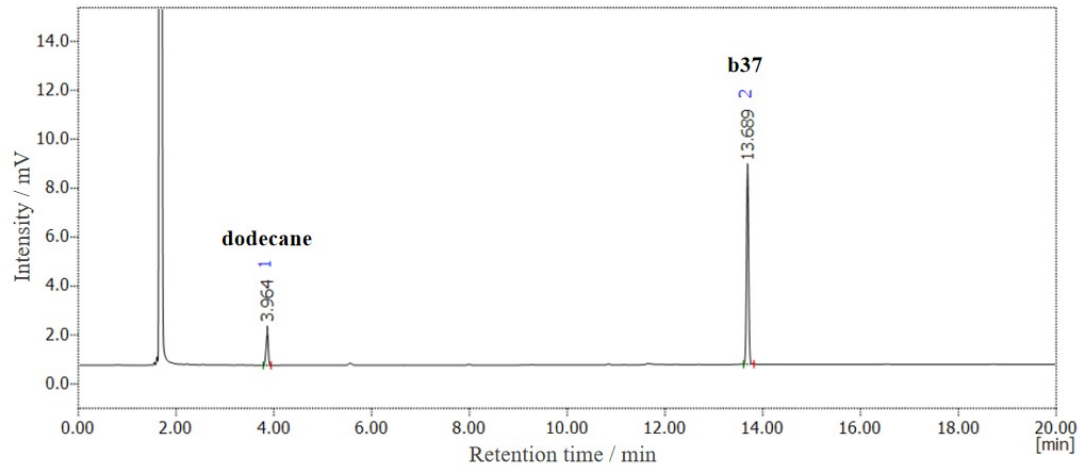

Fig. S134 GC analysis result for catalytic hydrogenation of **a37** by **2**.

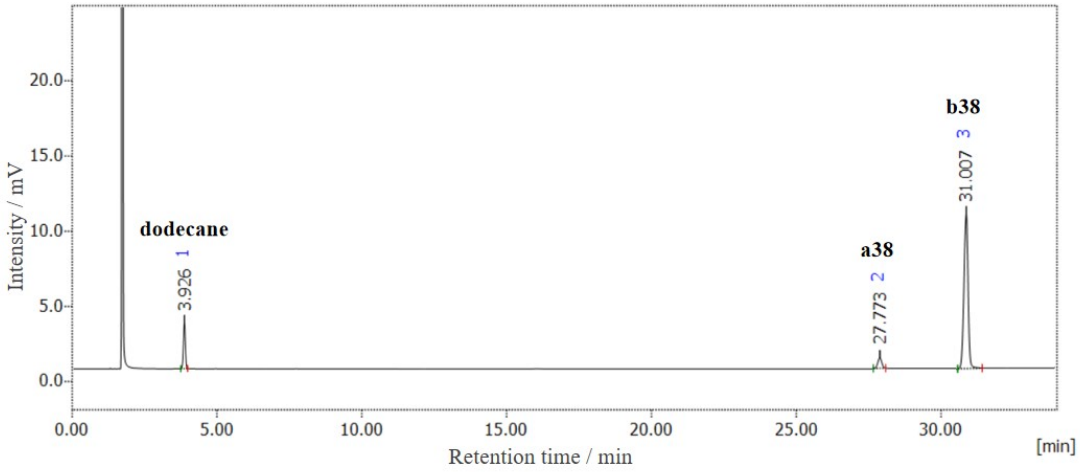

Fig. S135 GC analysis result for catalytic hydrogenation of **a38** by **2**.

VI. References

[1] M. Hingst; M. Tepper; O. Stelzer, *Eur. J. Inorg. Chem.* 1998, *1998*, 73-82.

[2] Y. Li; S. Yu; X. Wu; J. Xiao; W. Shen; Z. Dong; J. Gao, *J. Am. Chem. Soc.* 2014, *136*, 4031-4039.

[3] O. V. Dolomanov; L. J. Bourhis; R. J. Gildea; J. A. K. Howard; H. Puschmann, *J. Appl. Crystallogr.* 2009, *42*, 339–341.

[4] G. M. Sheldrick, *Acta Crystallogr.* 2015, *A71*, 3–8.

[5] G. M. Sheldrick, *Acta Crystallogr.* 2015, *C71*, 3–8.

[6] D. Wei; T. Roisnel; C. Darcel; E. Clot; J.-B. Sortais, *Chemcatchem* 2017, *9*, 80-83.

[7] R. Wang; Y. Yue; J. Qi; S. Liu; A. Song; S. Zhuo; L. Xing, *J. Catal.* 2021, *399*, 1-7.

[8] L. Zhang; Y. Tang; Z. Han; K. Ding, *Angew. Chem. Int. Ed.* 2019, *58*, 4973 –4977.

[9] F. Kallmeier; T. Irrgang; T. Dietel; R. Kempe, *Angew. Chem. Int. Ed.* 2015, *55*, 11806 – 11809.

[10] Y. Zhang; K. Lee; S. Kim; S. Choi; A. I. Gopalan; Z. Yuan, *Electrophoresis* 2004, *25*, 2711–2719.

[11] S. P. Pajk; Z. Qi; S. J. Sujansky; J. S. Bandar, *Chem. Sci.* 2022, *13*, 11427-11432.

[12] K. Herasymchuk; R. Raza; P. Saunders; N. Merbouh, *J. Chem. Educ.* 2021, *98*, 3319−3325.

[13] P. Puylaert; R. van Heck; Y. Fan; A. Spannenberg; W. Baumann; M. Beller; J. Medlock; W. Bonrath; L. Lefort; S. Hinze; J. G. de Vries, *Chem. – Eur. J.* 2017, *23*, 8473-8481.

[14] C. Li; W. Lu; B. Lu; W. Li; X. Xie; Z. Zhang, *J. Org. Chem.* 2019, *84*, 16086-16094.

[15] S. G. Davies; G. Darren Smyth, *J. Chem. Soc., Perkin Trans*. 1 1996, *20*, 2467-2477.

[16] L. Zhang; Z. Lu; A. R. Rander; T. J. Williams, *Chem. Commun.* 2023, *59*, 8107-8110.

[17] S. S. Gholap; A. A. Dakhil; P. Chakraborty; H. Li; I. Dutta; P. K. Das; K. Huang, *Chem. Commun.* 2021, *57*, 11815-11818.

[18] L. H. R. Passos; V. Martínez-Agramunt; D. G. Gusev; E. Peris; E. N. dos Santos, *ChemCatChem* 2023, *15*, e202300394.

[19] T. Mizugaki; Y. Kanayama; K. Ebitani; K. Kaneda, *J. Org. Chem*. 1998, *63*, 2378-2381.

[20] Y. Duan; Y. Zeng; Z. Cui; J Wen; X. Zhang, *J. Catal.* 2023, *417*, 109-115.

[21] R. Wang; Y. Yue; J. Qi; S. Liu; A. Song; S. Zhuo; L. Xing, *J. Catal.* 2021, *399*, 1-7.